New Riboflavin-Conjugated Biopolymers *via* Click Chemistry:

synthesis, characterization and nanotechnological applications

Giuliana Manzi

2016

Tutor: Dr. Pietro Matricardi
Co-Tutor: Dr. Ir. Tina Vermonden

This thesis was submitted to “Sapienza” University of Rome for the degree of
Doctor of Philosophy in Pharmaceutical Sciences,
Faculty of Pharmacy and Medicine.

The last 18 months of this PhD were spent at Department of Pharmaceutics,
Utrecht Institute for Pharmaceutical Sciences (UIPS),
Utrecht University, Utrecht, The Netherlands.

Everything in this book
may be all wrong.
But if so,
it's all right!

Table of contents

Chapter 1

General Introduction

1.1 Nanotechnology in Drug Delivery

Nanotechnology represents not just one specific area, but a vast variety of disciplines controlling the shape and size at the nano-meter scale. One of the important areas of nanotechnology is “nanomedicine,” which refers to highly specific medical intervention at the molecular scale, for the diagnosis, prevention and treatment of diseases and/or disorders.[1]
There is increasing optimism that performances in this field, such as the development of Nano Drug Delivery Systems (NDDS) that will bring significant advances in the diagnosis and treatment of disease, with the challenges to maximize therapeutic activity and to minimize undesirable side effects.
If your drug use consists of an occasional aspirin, you may not see the need for serious work on drug delivery. However, if you were diabetic, having to inject insulin several times a day, or a cancer patient experiencing debilitating side effects from your treatment, the benefits of improved drug delivery could change your life.[2]

Richard Feynman introduced the concept of nanotechnology as an important field for future scientific researches, during a lecture on December 1959 titled ‘‘There’s plenty of room at the bottom’’, concluding that nano-robots placed in the body may cure it at the molecular level.[3]
Then, since emerging in the early 1970s, micro- and nano-scale intelligent and responsive delivery systems (designed to perform functions like detection, isolation and/or release of therapeutic agent) have attracted increasing attention: [4,5] nanotechnology has finally entered in the field of drug delivery.
With nanotechnology, scientists are acquiring abilities to understand and manipulate materials at the scale of atoms and molecules, with having the following key properties: the increased surface area and quantum effects.[6,7]
Advantages of such nanostructures are relative to the ability to protect drugs, to delivery poorly-water soluble drugs, to increase their oral bioavailability due to their specialized uptake mechanisms and due to the ability to remain in the blood circulation for a long time (meaning a controlled release of the incorporate drug).
Moreover, one of the most conspicuous achievements in the drug delivery field was the development of stimuli-sensitive delivery systems (SDDS), for which the rapid transitions of the physicochemical property of polymer systems are stimulus-dependent. This stimulus includes physical (temperature, mechanical stress, ultrasound, electricity, light), chemical (pH, ionic strength), or biological (enzymes, biomolecules) signals.
These new SDDS have shown further advantages compared to conventional drug delivery systems: for the conventional DDS, the controlled release systems are based on the predetermined drug release rate independently of the environmental condition at the time of application. On the other hand, for the SDDS the release may be defined “on-demand”, allowing the drug carrier to

liberate a therapeutic drug only when is required, in response to a specific stimulation.[8]

Basic prerequisites for design of new materials for appropriate carriers as drug delivery systems, involve knowledge on drug incorporation and release, formulation stability and shelf life, biocompatibility, biodistribution, targeting and functionality.

In this respect, would be optimal develop biodegradable nanocarriers with life span limited as long as therapeutic effect is needed.[9] Micelles, solid lipids nanoparticles, dendrimers, polymers, silicon or carbon materials and magnetic nanoparticles and nanohydrogels are some examples of nanosystems that have been tested as drug delivery systems. Furthermore, polymer-protein conjugates, polymer-drug conjugates, polymeric micelles and polymeric drugs, are often classified as NDDSs as well.[10]

Use of smart drug delivery systems is a promising approach for developing intelligent therapeutic systems.

References

(1) NIH Roadmap Initiatives: http://nihroadmap.nih.gov/initiatives.asp

(2) http://www.understandingnano.com/nanotechnology-drug delivery.html

(3) “There’s a Plenty of Room at the Bottom”, Richard P. Feynman (Dec. 1959)

(4) J.Z. Hilt, A. Khademhosseini, R. Langer, N.A. Peppas, Hydrogels in biology and medicine: from molecular principles to bionanotechnology. *Adv. Mater.,* **2006**, 18: 1345–1360

(5) M. Caldorera-Moore, N.A. Peppas, Micro- and nanotechnologies for intelligent and responsive biomaterial-based medical systems. *Advanced Drug Delivery Reviews*, **2009**, 61: 1391–1401

(6) J. Safari, Z. Zarnegar, Advanced drug delivery systems: Nanotechnology of health design A review. *Journal of Saudi Chemical Society*, **2014**, 18: 85–99

(7) D. Duggal, Role of Nanotechnology in New Drug Delivery system. *Int. J. Drug Dev. & Res.,* **2011**, 3: 4-8

(8) M. O. Emeje, I. C. Obidike, E. I. Akpabio and S. I. Ofoefule, Nanotechnology in Drug Delivery. Chapter from the book *Recent Advances in Novel Drug Carrier Systems*

(9) W. H. De Jong, P. J. A. Borm, Drug delivery and nanoparticles: Applications and hazards. *Int. J. Nanomedicine*, **2008**, 3: 133–149

(10) B. Rogers, J. Adams, S. Pennatur, Nanotechnology: The Whole Story. CRC Press, **2013**

1.2 Nanohydrogels (NHs) as Drug Delivery Systems

Even though nanomedicine is a relative new branch of science, many type of nanocarriers for drug delivery have been already developed over the past 30 years. Among these, in our opinion, nanogels or nanohydrogels (NHs) deserve a special attention.

The term nanogels usually defines aqueous dispersions of hydrogel particles formed by physically or chemically cross-linked polymer networks of nanoscale size. The term "nanogel" (NanoGel™) was first introduced from Kabanov and Vinogradov to define cross-linked bifunctional networks of a polyion and a non-ionic polymer initially designed for delivery of antisense oligonucleotides (cross-linked polyethyleneimine (PEI) and poly(ethylene glycol) (PEG) or PEG-*cl*-PEI). [1, 2] However, prior to this, the group of Akiyoshi et al. described the phenomenon of physical cross-linking (self-assembly) of cholesterol-modified polysaccharides (e.g., pullulan, mannan, amilopectin and dextran), which resulted in formation of swollen hydrogels at nanoscale size.[3]

Nanogels or nanohydrogels (NHs) are nanoscalar 3D polymer networks, with a tendency to absorb water when placed in an aqueous environment. Their affinity to aqueous solutions, superior colloidal stability, inertness in the blood stream and the internal aqueous environment (suitable for bulky drugs incorporation) make them ideal candidates for uptake and delivery of proteins, peptides, and other biological compounds.

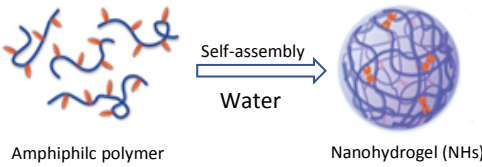

Figure 1. Molecular self-assembly of amphiphilic polymer in water, thus forming NHs.

Nanogels are superior drug delivery system than others due to their molecular size (ranging between 100- 700 nm), resulting in easy escape of renal clearance and in prolonged serum half-life period, allowing both passive and active drug targeting. Moreover, the drug release can be controlled and sustained at the target site, improving the therapeutic efficacy and reducing side effects. A typical advantage of these hydrogel nanoparticles, respect to other nanoparticles, is the possibility of obtain an elevated degree of encapsulation and offer an ideal tridimensional microenvironment for many macromolecule types, which may be encapsulated without chemical reactions: this is an important factor for preserving the drug activity. Furthermore, it is notable their ability to reach the

smallest capillary vessels, due to their tiny volume, and to penetrate the tissues either through the paracellular or the transcellular pathways. [4-7] The design and development of NHs as functional smart materials for biotechnological and biomedical applications have attracted curiosity because of their unique properties that combine the characteristics of hydrogel systems with a very small size. Due their inherent rapid swelling and de-swelling nature in response to external stimuli such as solvent composition, light, temperature, pH, pressure, magnetic and electric fields, indeed NHs may be designed to be stimuli-responsive, in order to alter the cross-linking or the swelling behavior in specific conditions. [8-11]

1.2.1 Synthesis and classification of NHs

Nanohydrogels are commonly classified into two major groups. The first classification is based on their responsive behavior, from which they can result either stimuli-responsive (swell or de-swell upon exposure to environmental changes) or non-responsive (simply swell as result of absorbing water). The second classification is based on the type of linkages present in the polymers network, resulting from the approaches used for their preparation.

Current approaches used for NHs preparation are the followings: i) physical self-assembly of interactive polymers; ii) polymerization of monomers in homogeneous phase or micro- or nano-heterogeneous environment; iii) chemical cross-linking of the polymer chains using a bi-functional cross-linking agent and iv) other synthetic techniques based on the template-assisted nanofabrication of nanogels particles.[12]

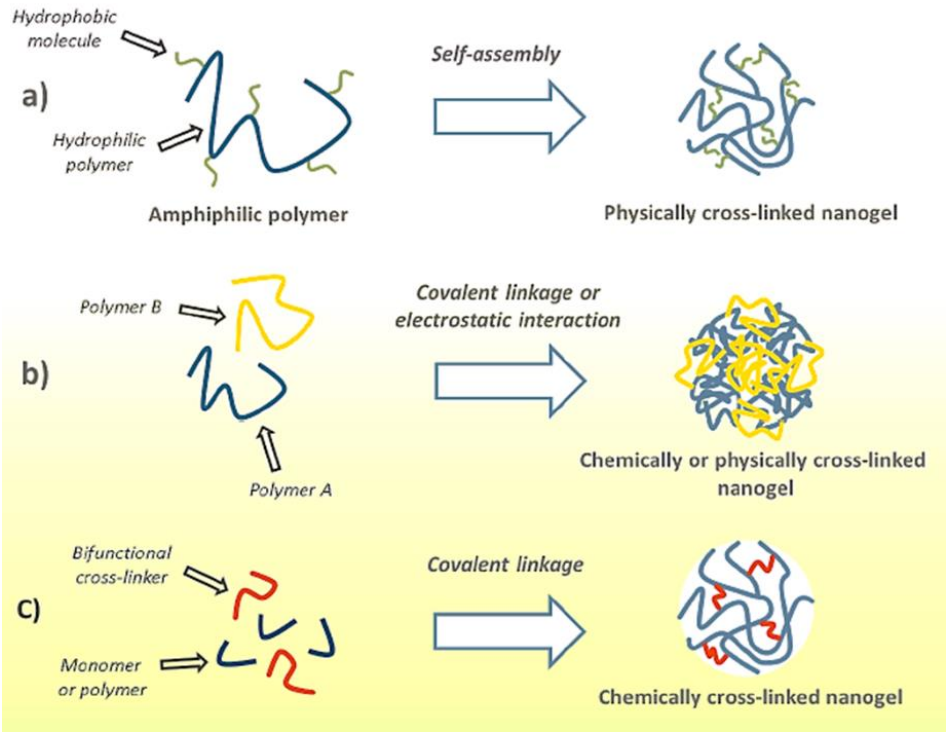

Figure 2. Typical approaches used to prepare NHs: **a)** Physically cross-linked NHs through non-covalent interactions; **b)** Chemically or physically cross-linked NHs using preformed polymers; **c)** Chemical cross-linked NHs by bi-functional cross-linker and a polymer.

An example of physical cross-linked NHs were developed from Akiyoshi et al. They prepared hydrogels nanoparticles by hydrophobic association of cholesterol-modified pullulan in presence of insulin,[13] due the advantages that physical interactions (such as van der Waals forces, hydrophobic, electrostatic interactions, or hydrogen bonding) of amphiphilic block copolymers and/or complexation of oppositely charged polymeric chains results in the formation of micro- and nanogels in only a few minutes. Moreover, self-association of hydrophilic polymers allow encapsulation of biomacromolecules while NHs are forming. The sizes of self-assembled nanogels in general are controlled by proper selection of the concentration of polymers and environmental parameters. In this respect, Yu et al. also prepared protein nanogels by temperature-induced gelation of oppositely charged proteins;[14] furthermore, in 2008, M. J. Alonso and collaborators developed the first hyaluronan-chitosan NHs, using an ionotropic gelation process.[15]

Chemical NHs are comprised of permanent chemical linkages (covalent bonds) throughout the polymer networks, instead. The properties of the resulting cross-linked NHs depend on the chemical linkages and functional groups present in the networks. Different nanogels have been synthesized using different chemical reactions strategies. Currently, various chemical cross-linking reactions have been developed, including the activating agent mediated amide bond cross-linking, quaternisation of amino groups,[16] "click" chemistry,[17]and photo-cross-linking technique.[18] These crosslinking points allow modifying entire physicochemical properties of the NHs systems.

Moreover, many studies used one of the basic procedures described above to prepare increasingly sophisticated types of nanogels.

Several polymers can be used to achieve NHs: typical natural polymers such as polysaccharides, that show a higher biocompatibility and biodegradability in comparison to synthetic polymers.[19] The most used polysaccharides used on this purpose are hyaluronan, pullulan, chitosan, alginate, dextran and mannan. On the other hand, poly(lactic-glycolic acid), poly(caprolactone), poly(*N*-isopropylacrylamide) and poly(lactic acid) represent examples of synthetic polymers capable to form NHs' networks.

1.2.2 Polysaccharide based-NHs

Nowadays, polysaccharide-based nanoparticles have been proposed for innovative DDSs due to their unique multi-functional groups in addition to their physicochemical properties, in particular their marked biocompatibility and biodegradability.[20-22]

Polysaccharides are a class of biopolymers formed of multiple monosaccharide repeating units joined together through glycosidic linkages. The multi-functional groups of the polysaccharide backbone, a wide range of molecular weights, their abundance in nature, and their varying chemical composition (which all contribute to their diversity in structure and properties), make polysaccharide the most attractive and promising biomaterial in nanomedicine investigations. [23-25] In general, hydroxyl, amino, and carboxylic acid are the reactive functional groups on polysaccharides backbone, which can be easily modified by usual synthetic methodologies.

The main methodologies for polysaccharide modifications are ester and ether formation using sugars hydroxyl group as the nucleophiles. In this respect, K. Akiyoshi and co-workers developed the first self-assembled polysaccharide NHs based on cholesterol-bearing pullulan derivative obtained by esterification,[3] or the self-assembled nanogel derived from an acid-labile cholesteryl-modified pullulan, prepared by grafting vinyl ether-cholesterol substituents onto a 100 kDa pullulan.[26]

Chemical oxidation of primary alcohols to aldehyde and carboxylic acids,[27-29] enzymatic oxidation of primary alcohols to uronic acid,[30] formation of amide bonds between saccharides carboxyl group and heteroatomic nucleophiles using coupling agents (e.g. EDC/NHS, DCC/DMAP)[31-33] and nucleophilic reactions of the amines of some polysaccharide (e.g. chitosan)[34] are further chemical modification extensively investigated.

Among the numerous techniques, polysaccharide-based NHs can be obtained through chemical or physical cross-linking, polyelectrolyte complexation and self-assembling of hydrophobic-modified polysaccharides. Compared with covalent cross-linking, the physical cross-linking shows more advantages such as mild preparation conditions and quite simpler procedures.

The functionalization of hydrophilic polysaccharides with hydrophobic molecules, based on the synthetic strategies described above, allows the formation of amphiphilic polymer chains that, upon contact with an aqueous environment, spontaneously form close nanostructures *via* intra- or intermolecular associations between hydrophobic moieties, in order to minimize the interfacial free energy. Moreover, sizes of such nanostructures can be modulate depending on the structural properties of the resulting modify-polysaccharides, the kind of functionalization strategy chosen, the degree of functionalization of the main chain, and the M_W of the polymer as well.

Based on the same considerations, naturally-derived nanohydrogels have been prepared from polysaccharide such as chitosan, hyaluronic acid, heparin, chondroitin sulfate, agarose, and alginate.
For instance, chitosan-based NHs have been developed by M. J. Alonso and collaborators; the preparation of this nano-system was based on the ability of chitosan to undergo a sol-gel transition due to the ionic interaction with poly-anions, such as tripolyphosphate (TPP).[35]

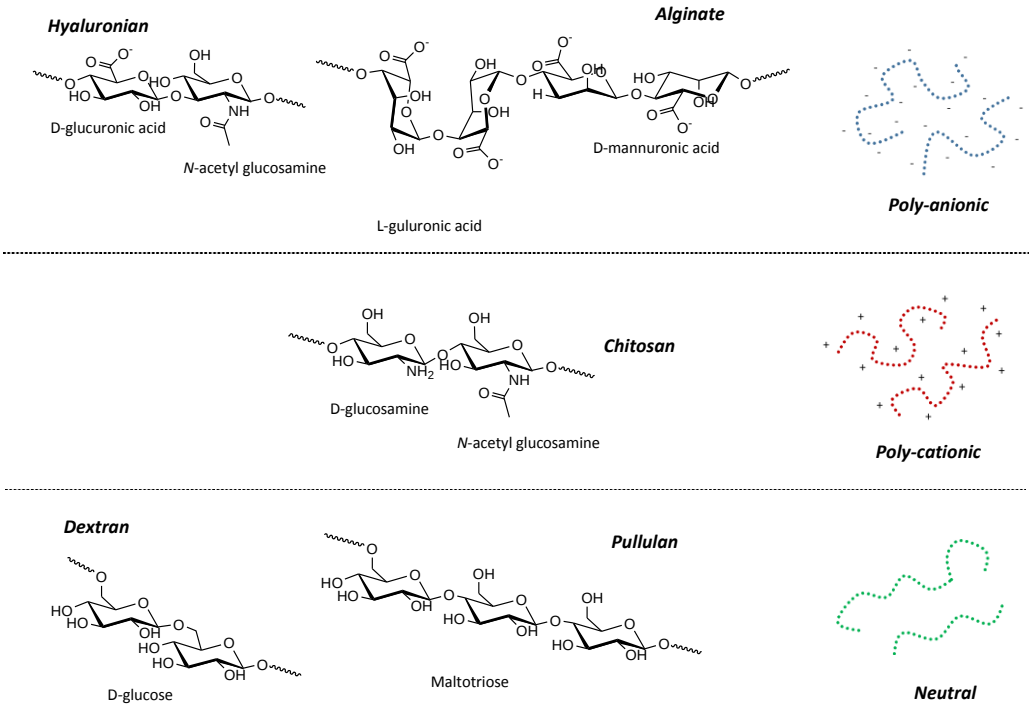

Figure 3. Chemical structures of polysaccharides typically used for NHs preparation.

Alginate was used as well from Xue et al. to develop a one-pot method for the preparation of pH-responsive doxorubicin-loaded nanogels.[36]
In recent years, our group developed two different hyaluronan based NHs, formed by self-assembly. These nano-carriers effectively showed the ability to conjugate proteins and retain their activity after the immobilization.[37,38]

1.2.2.1 Hyaluronic acid (HA) based NHs for drug delivery

Hyaluronic acid (HA), an immune-neutral polysaccharide that is ubiquitous in the human body, is strategic for many cellular and tissue functions and has been in clinical use for over three decades.[39]
HA was first isolated in 1934 from bovine vitreous humor by Meyer and Palmer.[40] The name "hyaluronic acid" was coined by them as a conjugation of two words, hyaloid (vitreous) and uronic acid (one of the two sugar molecules from which this new substance was composed). Then, Karl Meyer and his collaborators figured out the chemical structure of hyaluronic acid in the 1950s: [41] HA, or hyaluronan, is a linear hetero polysaccharide that consists of alternating units of a repeating disaccharide: β-1,4-D-glucuronic acid – β-1,3-*N*-acetyl-D-glucosamine. HA is a non-sulfated glycosaminoglycan, and is synthesized in the plasma membrane of fibroblasts and other cells by addition of sugars to the reducing end of the polymer, whereas the nonreducing-end protrudes into the pericellular space.[42]

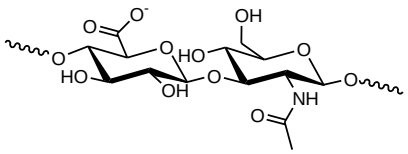

D-glucuronic acid *N*-acetyl-D-glucosamine

Figure 4. Chemical structure of HA repetitive unit

In physiological conditions, HA is in the form of sodium salt, therefore (HA^-NA^+) referred to as sodium hyaluronate. HA exists as a poly-anion *in vivo* and in this form it is highly hydrophilic and surrounded by a sphere of water molecules linked by hydrogen bonds.
Observing its chemical structure (Figure 4), it is evident that HA can be chemically modified due to its multi-functional groups such as the carboxylic acid of glucuronic acid, primary and secondary hydroxyl groups and the *N*-acetyl groups. The modifications aimed at enhance, modulate or control the therapeutic action of HA and develop new products (with alerted properties, including its hydrophobicity and biological activity).
Numerous chemical modifications have been described in the literature, which are reviewed by C.E. Schanté et al. These are performed in different solvents (to modify HA with hydrophobic molecules the organic media is necessary and, due to the poor solubility of HA in organic solvents, the tetrabutylammonium salt of HA is required[43]), target different sites on HA and yield different results in terms of modification efficacy and chain length damage. The method should be chosen

carefully, based on the starting material and final product characteristics desired.[44]

The most widely method of modification of the carboxylic group of HA is the amidation with carbodiimides.[45] Nevertheless, P. Farkas et al. showed that triazine-based reagent (in particular 4-(4,6-dimethoxy-1,3,5- triazin-2-yl)-4-methylmorpholinium (DMTMM)), was a more efficient as activator of carboxylic groups than carbodiimides, leading to higher functionalization degree of the products, and higher degree of purity.[46, 47]

Laurent, Hellsing, and Gelotte were the first to report HA crosslinking in the far 1964,[48] based on the observation that divinyl sulfone (DVS) reacts readily with HA in aqueous alkaline solutions at room temperature, i.e., about 20° C., thereby providing cross-linked HA gels. Today, the hydroxyl groups are commonly modified by etherification, esterification and cross-linking by using divinyl sulfone or epoxides. Modifications of the *N*-acetyl groups are usually performed after deacetylation. Bellini and Topai patented the amidation of HA by reaction of an acid with the deacetylated amino-group of HA.[49]

Moreover, a nearly recent methodology to prepare HA derivatives is composed by orthogonal chemistry in a simple one-step reaction based on Huisgen cycloaddition, which is a "click"-type reaction, highly selective, and free from side reactions and by-products.[50-52]

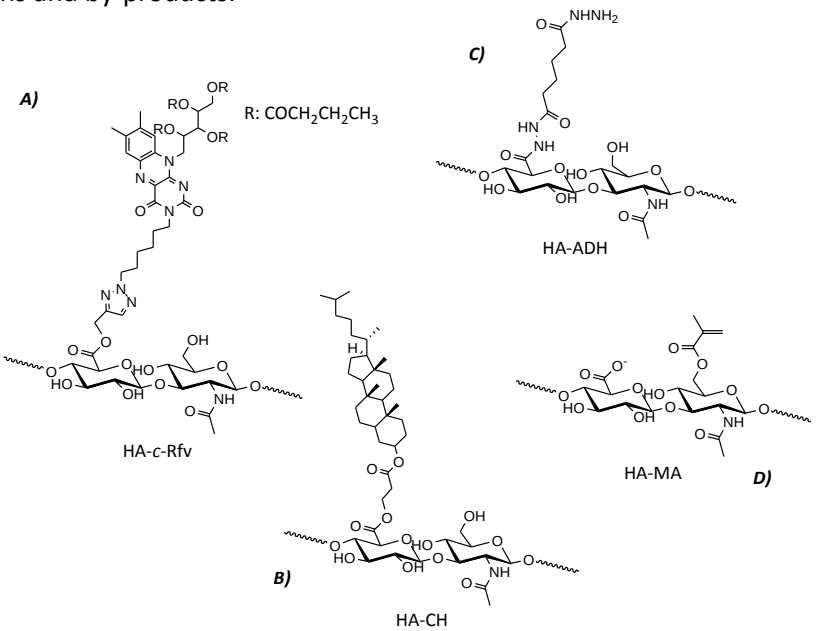

Figure 5. Examples of chemical modifications of HA: **A)** Huisgen cycloaddition ("click"-type reaction) of azid-dervative of Riboflavin tetrabutyrate and alkyl-derivative of HA (HA-c-Rfv); **B)** esterification of the carboxylic group of HA with a bromide derivative of Cholesterol (HA-CH); **C)** HA amidation with adipic dihydrazide by with EDC/NHS and EDC/HOBt (HA-ADH); **D)** etherification of HA hydroxyl group with methacrylic anhydride (HA-MA).

The resulting HA derivatives can be classified in to two primary categories: the "monolithic" that is the terminally modified forms of HA that cannot form new chemical bonds, and the "living" derivatives that can form new covalent bonds, allowing consecutive cross-linking or attachment of therapeutic drugs/polypeptides to HA.[53, 54]

Overall, the so evidenced versatility in HA macromer synthesis and processing of the materials has transitioned into materials with a range of properties useful in applications such as tissue engineering and drug delivery. Nowadays numerous researchers investigated the application of HA based nanogels in DDS. First, the arrangement of HA polymeric chains in these 3D soft nanomatrices reduce the HA clearance from the blood, thus the reduction of the degradation of HA by hyaluronidase due the modification of the chemical structure of the polymer chains. Moreover, it has been demonstrate that HA based nanoparticles can efficiently accumulate in cancer tissues (whereas native HA is quickly cleared from the body).[55, 56] This might result from the increased circulation time and EPR effect as well as tumor selective binding of HA to CD44 receptor. The binding of HA with CD44 receptors, provides not only a targeting to certain tumor cells, but also allows HA to diffuse through the cell membrane and enter into the intracellular microenvironment.[57] This peculiarity marks the extremely useful strategy to deliver certain drugs intracellularly by HA-based nanogels (for instance drugs that would not otherwise pass through the cell membrane, due to their physico-chemical properties).

Additionally, HA demonstrated the ability to interact with several proteins inside the body.[58] This evidence gave the idea to develop useful HA-based nanocarriers to conjugate proteins, challenging the preservation of their activity and increment of their stability and availability in human tissues.[59]

In general, the production of nanostructured materials from hyaluronic acid can fit many properties of nano-scale drug delivery systems for specific applications: solubility (inherent hydrophilicity of HA), biodistribution (targeting to cancer cells), biocompatibility (electrical charge), biodegradability (binding/ crosslinking density) and drug release (HA-drug spacer or physical interaction between a drug and a carrier).

On this purpose, several kinds of HA-based nano-carriers, such as HA-drug conjugates, HA-based nanocomplexes, HA-coated nucleic acid/polycation, HA-decorated nanoparticles and HA-based NHs were designed.[60]

In particular, HA-based NHs are classified by the type of crosslinks from which are formed.[56]

The most common and interesting strategy used to form such NHs is the physical crosslinking from non-covalent attractive forces between the polymer chains, which were previously partially modified with hydrophobic moieties. Based on this, hydrophobic molecules and/or hydrophobic long chains have been grafted to HA to form, in aqueous media, self-assembled NHs with internal hydrophobic

domains: 5β-cholanic acid,[61] cholesterol,[59] 2'3'4'5'-tetrabutyrilriboflavin,[38] PLGA[61] and PEG-PCL[62] are few examples of hydrophobic moieties linked to the selected polysaccharide, aiming the purpose to form smart nanocarriers. However, the HA poly-anionic nature represents a limitation in encapsulating negatively charged macromolecules such as siRNA and DNA.

Chemically cross-linked NHs are usually more stable than the physically cross-linked analogues. However, the synthetic strategies that can achieve this are normally based on phase separation, such as the inverse water-in-oil (w/o) microemulsion method,[63] or the oil-in-water type emulsion.[64] However, these techniques generally require high energy sources and hard conditions that may limit the entrapment of delicate molecules such as peptides and proteins. Moreover, the permanent cross-linkages may result in a reduced therapeutic efficacy, due the inhibition of drug release at the target site. Nevertheless, degradable linkages have been used to obtain chemically cross-linked stimuli-responsive NHs. For instance, H. S. Han and colleagues developed NHs based on an amphiphilic HA-polycaprolactone block copolymer, coupled *via* a bio reducible di-sulfide linkage (cleavable in the cytosol by glutathione (GSH)): this strategy allowed the controlled release of drugs inside the cells, increasing the HA NHs' stability in the blood circulation.[65]

HA has also the property to form nanogels *via* ionotropic gelation, which relative to the ability of polyelectrolytes to cross-link in the presence of counter ions.[66] On this purpose, Jain et al. synthesized HA coupled chitosan nanoparticles (HACTNPs) carrying 5-flurouracil (5FU) by ionotropic gelation methods, for the effective delivery of drug to the colon tumors.[67]

Nevertheless, the current limitation of the HA targeting nanocarriers is their high accumulation in the liver and spleen, because HA molecules expose the nanocarriers to the HA receptors identified in these organs.

References

(1) S. V. Vinogradov, E. V. Batrakova, A.V. Kabanov, Poly(ethylene glycol)-polyethyleneimine NanoGel(TM) particles: Novel drug delivery systems for antisense oligonucleotides. *Coll. Surf. B: Biointerfaces.,* **1999**; 16: 291–304

(2) P. Lemieux, S. V. Vinogradov, C. L. Gebhart, N. Guérin, G. Paradis, H. K. Nguyen, B. Ochietti, A. V. Kabanov, et al, Block and graft copolymers and NanoGel copolymer networks for DNA delivery into cell. *J Drug Target.*, **2000**; 8: 91-105

(3) K. Akiyoshi, S. Deguchi, N. Moriguchi, S. Yamaguchi, J. Sunamoto, Self-aggregates of hydrophobized polysaccharides in water. Formation and characteristics of nanoparticles. *Macromolecules*, **1993**, 26: 3062–3068

(4) F. Sultana, Manirujjaman, Md. Imran-Ul-Haque, M. Arafat, S. Sharmin, An Overview of Nanogel Drug Delivery System. J*. of App. Pharma. Sc.*, **2013**, 3: S95-S105

(5) S. Rigogliuso, M. A. Sabatino, G. Adamo, N. Grimaldi, C. Dispenza and G. Ghersia, Polymeric Nanogels: Nanocarriers For Drug Delivery Application. *Chem. Eng. Transactions*, **2012**, 27

(6) C. Gonçalves, P. Pereira and Mi. Gama, Self- Assembled Hydrogel Nanoparticles for Drug Delivery Applications. *Materials*, **2010**, 3: 1420-1460

(7) K. A. Wilk, K. Zieliñska, J. Pietkiewicz, J. Saczko, Loaded nanoparticles with cyanine-tipe photosensizers: preparation, characterization and encapsulation. *Chem. Eng. Transactions*, **2009**, 17: 987-992

(8) D. Schmaljohann, Thermo- and pH-responsive polymers in drug delivery. *Adv. Drug Deliv. Rev.*, **2006**, 58: 1655-1670

(9) S. Mura, J. Nicolas, P. Couvreur, Stimuli-responsive nanocarriers for drug delivery. *Nat. Mater.*, **2013**, 12: 991-1003

(10) M. Oishi, Y. Nagasaki, Stimuli-responsive smart nanogels for cancer diagnostics and therapy. *Nanomedicine*, **2010**, 5: 451-468

(11) M. Yallapu, M. Jaggi, S. C. Chauhan, Design and engineering of nanogels for cancer treatment. *Drug Discov. Today*, **2011**, 16: 457-463

(12) A. V. Kabanov and S. V. Vinogradov, Nanogels as Pharmaceutical Carriers: Finite Networks of Infinite Capabilities. *Angew. Chem. Int. Ed. Engl.*, **2009**; 48: 5418–5429

(13) K. Akiyoshi, S. Kobayashi, S. Shichibe, D. Mix, M. Baudys, S. W. Kim, J. Sunamoto, Self-assembled hydrogel nanoparticle of cholesterol-bearing pullulan

as a carrier of protein drugs: complexation and stabilization of insulin. *J Control Release*, **1998**, 54: 313-20

(14) S. Yu, P. Yao, M. Jiang, G. Zhang, Nanogels prepared by self-assembly of oppositely charged globular proteins. *Biopolymers*, **2006**, 83:148-58

(15) M. De la Fuente, B. Seijo, M. J. Alonso, Design of novel polysaccharidic nanostructures for gene delivery. *Nanotechnology*, **2008**, 19: 75-105

(16) V. Butun, A. B. Lowe, N. C Billingham et al., Synthesis of Zwitterionic Shell Cross- Linked Micelles. *J. Am. Chem. Soc.*, **1999**, 121: 4288-4289

(17) J. Zhang, Y. Zhou, Z. Zhu et al., Polyion Complex Micelles Possessing Thermoresponsive Coronas and Their Covalent Core Stabilization via "Click" Chemistry", *Macromolecules*, **2008**, 41: 1444-1454

(18) S. Yusa, M. Sugahara, T. Endo et al., Preparation and Characterization of a pH Responsive Nanogel Based on a Photo-Cross-Linked Micelle Formed From Block Copolymers with Controlled Structure. *Langmuir*, **2009**, 25: 5258-5265

(19) T. Coviello, P. Matricardi, C. Marianecci et al. Polysaccharide hydrogels for modified release formulations. *J. Control. Release*, **2007**, 119: 5-24

(20) W.H. De Jong, P.J.A. Borm, Drug delivery and nanoparticles: applications and hazards. *Int. J. Nanomedicine*, **2008**, 3: 133–149

(21) B. Kang, T. Opatz, K. Landfester, F.R. Wurm, Carbohydrate nanocarriers in biomedical applications: functionalization and construction. *Chem. Soc. Rev.,* **2015**, 44: 8301–8325

(22) Y. K. Joung, J. Y. Jang, J. H. Choi, D. K. Han, K. D. Park, Heparin-conjugated pluronic nanogels as multi-drug nanocarriers for combination chemotherapy. *Mol. Pharm.*, **2013**, 10: 685–693

(23) F. Jian, Y. Zhang, J. Wang, K. Ba, R. Mao, W. Lai, Y. Lin, Toxicity of biodegradable nanoscale preparations. *Curr. Drug Metab.*, **2012**, 13: 440–446

(24) A. Abed, N. Assoul, M. Ba, S.M. Derkaoui, P. Portes, L. Louedec, P. Flaud, I. Bataille, D. Letourneur, A. Meddahi-Pelle, Influence of polysaccharide composition on the biocompatibility of pullulan/dextran-based hydrogels. *J. Biomed. Mater. Res. Part A*, **2011**, 96: 535–542

(25) S. Rodrigues, L. Cardoso, A. da Costa, A. Grenha, Biocompatibility and stability of polysaccharide polyelectrolyte complexes aimed at respiratory delivery. *Materials*, **2015**, 8: 5268

(26) N. Morimoto, S. Hirano, H. Takahashi, S. Loethen, D. H. Thompson, and K. Akiyoshi, Self-Assembled pH-Sensitive Cholesteryl Pullulan Nanogel As a Protein Delivery Vehicle. *Biomacromolecules*, **2013**, 14: 56–63

(27) A. E. J. de Nooy, A. C. Besemer, and H. van Bekkum, Highly selective tempo mediated oxidation of primary alcohol groups in polysaccharides. *Recueil des Travaux Chimiques des PaysBas*, **1994**, 113: 165–166

(28) A. E. J. De Nooy, A. C. Besemer, and H. Van Bekkum, Highly selective nitroxyl radical-mediated oxidation of primary alcohol groups in water-soluble glucans. *Carbohydrate Research*, **1995**, 269: 89–98

(29) P. S. Chang and J. F. Robyt, Oxidation of primary alcohol groups of naturally occurring polysaccharides with 2,2,6,6- tetramethyl-1-piperidine oxoammonium ion. *J. of Carbohydrate Chem*., **1996**, 15: 819–830

(30) K. Parikka and M. Tenkanen, Oxidation of methyl α-d-galactopyranoside by galactose oxidase: products formed and optimization of reaction conditions for production of aldehyde. *Carbohydrate Research*, **2009**, 344: 14–20

(31) M. D. Cathell, J. C. Szewczyk, and C. L. Schauer, Organic modification of the polysaccharide alginate. *Mini-Reviews in Organic Chemistry*, **2010**, 7: 61–67

(32) J. S. Yang, H. B. Ren, and Y. J. Xie, Synthesis of amidic alginate derivatives and their application in microencapsulation of λ-cyhalothrin, *Biomacromolecules*, **2011**, 12: 2982–2987

(33) F. Vallee, C. M ´ uller, A. Durand et al., Synthesis and rheological properties of hydrogels based on amphiphilic alginate-amide derivatives, *Carbohydrate Research*, **2009**, 344, : 223–228

(34) M. Yalpani and L. D. Hall, Some chemical and analytical aspects of polysaccharide modifications. 3. Formation of branched-chain, soluble chitosan derivatives, *Macromolecules*, **1984**, 17: 272–281

(35) P. Calvo, C. Remunan-Lopez, J. L. Vila-Jato et al., Novel Hydrophilic Chitosan–Polyethylene Oxide Nanoparticles as Protein Carriers. *J. Appl. Polym. Sci.,* **1997**, 63: 125-132

(36) Y. Xue, X. Xia, B. Yu, X. Luo, N. Cai, S. Long, F. Yu, A green and facile method for the preparation of a pH-responsive alginate nanogel for subcellular delivery of doxorubicin. *RSC Adv.*, **2015**, 5: 73416–73423

(37) E. Montanari, S. Capece, C. Di Meo et al., Hyaluronic acid nanohydrogels as a useful tool for BSAO immobilization in the treatment of melanoma cancer cells, *Macromol. Biosci.*, **2013**, 13: 1185-1194

(38) C. Di Meo, E. Montanari, L. Manzi, C. Villani, T. Coviello, P. Matricardi, Highly versatile nanohydrogel platform based onriboflavin-polysaccharide derivatives useful in the development ofintrinsically fluorescent and cytocompatible drug carriers. *Carbohydrate Polymers,* **2015**, 115: 502–509

(39) J. W. Kuo , Practical Aspects of Hyaluronan Based Medical Products . *CRC/Taylor & Francis , Boca Raton* **2006**

(40) T. C. Laurent, J. R. Fraser, Hyaluronan. *FASEB J.,* **1992**, 6: 2397-404

(41) M. M. Rapport, B. Weissmann, A. Linker et al, Isolation of a crystalline disaccharide, hyalobiuronic acid, from hyaluronic acid. *Nature*, **1951**, 1681: 996–997

(42) J. R. Fraser, T. C. Laurent, U. B. Laurent, Hyaluronan: its nature, distribution, functions and turnover. *J Intern Med.*, **1997**, 242: 27-33

(43) F. Della Valle, A. Romeo, Esters of hyaluronic acid and their salts. *EP0216453 B1*, **1996**

(44) C. E. Schanté, G. Zuber, C. Herlin, T. F. Vandamme, Chemical modifications of hyaluronic acid for the synthesis of derivatives for a broad range of biomedical applications. *Carbohydr. Polym.*, **2011**, 85: 469–489

(45) P. Bulpitt, & D. Aeschlimann, New strategy for chemical modification of hyaluronic acid: Preparation of functionalized derivatives and their use in the formation of novel biocompatible hydrogels. *J. of Biom. Mat. Research*, **1999**, 47: 152–169

(46) P. Farkas, S. Bystriky, Efficient activation of carboxyl polysaccharides for the preparation of conjugates, *Carbohydr. Pol.*, **2007**, 68: 187-190

(47) M. Kunishima, C. Kawachi, J. Monta et al., 4-(4,6-dimethoxy-1,3,5-triazin-2-yl)-4- methylmorpholinium: An Efficient Condensing Agent. *Tetrahedron*, **1999**, 55: 13159-13170

(48) T. Laurent, K. Hellsing, & B. Gelotte, Cross-linked gels of hyaluronic acid. *Acta Chemica Scandinavia*, **1964**, 18: 274–275

(49) D. Bellini, & A. Topai, WO200001733, **2000**

(50) V. Crescenzi, L. Cornelio, C. Di Meo et al., Novel hydrogels via click chemistry: synthesis and potential biomedical applications. *Biomacromolecules,* **2007**, 8: 1844-1850

(51) C. Di Meo, L. Panza, F. Campo et al., Novel types of carborane-carrier hyaluronan derivatives via “click chemistry”. *Macromol. Biosci.,* **2008**, 8: 670-681

(52) M. Nimmo, S. C. Owen, M. S. Shoichet, Diels-Alder Click Cross-Linked Hyaluronic Acid Hydrogels for Tissue Engineering. *Biomacromolecules*, **2011**, 12: 824-830

(53) D. P. Glenn, K. Jing-wen, Chemically-modified HA for therapy and regenerative medicine. *Curr. Pharm. Biotechnol.,* **2008**, 9: 242–245

(54) J. A. Burdick, G. D. Prestwich, Hyaluronic acid hydrogels for biomedical applications. *Adv. Mater*., **2011**, 23: H41–H56 (Deerfield Beach, Fla.)

(55) K. Y. Choi, H. Chung, K. H. Min, H. Y. Yoon, K. Kim, J. H. Park, I. C. Kwon, S. Y. Jeong, Self-assembled hyaluronic acid nanoparticles for active tumor targeting. *Biomaterials*, **2010**, 31: 106-14

(56) D. A. Ossipov, Nanostructured hyaluronic acid-based materials for active delivery to cancer. *Expert Opin Drug Deliv.*, **2010**, 7 :681-703

(57) R. Racine, M. E. Mummert, Hyaluronan Endocytosis: Mechanisms of Uptake and Biological Functions. *InTech*, **2012**, 14

(58) A. J. Day, G. D. Prestwich, Hyaluronan-binding proteins: tying up the giant. *J. Biol. Chem.,* **2002**, 277: 4585-4588

(59) E. Montanari, S. Capece, C. Di Meo et al., Hyaluronic acid nanohydrogels as a useful tool for BSAO immobilization in the treatment of melanoma cancer cells, *Macromol. Biosci.,* **2013**, 13: 1185-1194

(60) K. Y. Choi, G. Saravanakumar, J. H. Park et al., Hyaluronic acid-based nanocarriers for intracellular targeting: Interfacial interactions with proteins in cancer. *Colloid Surf. Biointerfaces*, **2012**, 99: 82-94

(61) K. Y Choi, K. H. Min, H. Y. Yoon et al., PEGylation of hyaluronic acid nanoparticles improves tumor targetability *in vivo*. *Biomaterials*, **2011**, 32: 1880-1889

(61) H. Lee H, C. H. Ahn, T. G. Park, Poly [lactic-co-(glycolic acid)]-grafted hyaluronic acid copolymer micelle nanoparticles for target-specific delivery of doxorubicin. *Macromol. Biosci.*, **2009**, 9: 336-42

(62) A. K. Yadav, P. Mishra, S. Jain et al., Preparation and characterization of HA-PEG-PCL intelligent core-corona nanoparticles for delivery of doxorubicin. *J. Drug Target.*, **2008**, 16: 464-78

(63) Y. H. Yun, D. J. Goetz, P. Yellen, W. Chen, Hyaluronan microspheres for sustained gene delivery and site-specific targeting. *Biomaterials*, **2004**, 25: 147-57

(64) A. Kumar, B. Sahoo, A. Montpetit, et al. Development of hyaluronic acid-Fe_2O_3 hybrid magnetic nanoparticles for targeted delivery of peptides. *Nanomedicine*, **2007**, 3: 132-7

(65) H. S. Han, T. Thambi, K. Y. Choi et al., Bioreducible Shell-Cross-Linked Hyaluronic Acid Nanoparticles for Tumor-Targeted Drug Delivery. *Biomacromolecules*, **2015**, 16: 447-456

(66) P. Patil, D. Chavanke, M. Wagh, A review on ionotropic gelation method: novel approach for controlled gastroretentive gelispheres. *Int J Pharm Pharm Sci*, **2012**, 4: 27–32

(67) A. Jain, S. K. Jain, *In vitro* and cell uptake studies for targeting of ligand-anchored nanoparticles for colon tumors. *Eur. J. Pharm. Sci.*, **2008,** 35: 404–416

1.3 Polymeric micelles as Drug Delivery Systems

Though much progress has been made in drug delivery systems, the design of a suitable carrier for the delivery of hydrophobic drugs is still a major challenge for researchers. Recently, colloidal carrier systems have been receiving much attention in the field of drug targeting because of their high loading capacity for drugs as well as their unique disposition characteristics in the body. Amongst these carrier systems, micellar particles consisting of amphiphilic molecules is an effective way of delivery drugs to their targets.

Micelles are self-assembling nanosized colloidal particles with a hydrophobic core and hydrophilic shell and are currently successfully used as pharmaceutical carriers and they have demonstrated a series of attractive properties as drug carriers.[1] Among the micelle-forming compounds, amphiphilic copolymers (i.e. polymers consisting of hydrophobic and hydrophilic blocks) are gaining increasing attention.

Block copolymers with amphiphilic character have large solubility differences between the segments. If the length of a hydrophilic block is too high, copolymers exist in water as unimers (individual molecules), while molecules with a very long hydrophobic block form structures with non-micellar morphology, such as rods and lamellae.[2] When the block-copolymers consist of a good hydrophobicity/hydrophilicity balance, together with their molecular weight, the length of the hydrophobic block, and chemical characteristics of the blocks (in terms of their chemical nature), is known that they assemble, in an aqueous media, into polymeric micelles with a mesoscopic size range.[3-7] Generally, these micelles have a fairly narrow size distribution and are characterized by the core–shell architecture, where hydrophobic segments constitute the inner core surrounded by a barrier of hydrophilic segments. The hydrophobic part provides an environment for the encapsulation of hydrophobic drugs, protein or DNA through physical or chemical binding modes. The hydrophilic part of the polymeric micelles is important due to its brush like architecture, which allows the hydrophilic part to protect the hydrophobic part from the biological invasion, such as the minimization of plasmatic protein adsorption (i.e., meaning an increasing of the renal clearance).[8]

Polymeric micelles belong to a group of association or amphiphilic colloids, which form spontaneously under certain concentration called the critical micelle concentration (CMC). At concentrations lower than the specific CMC, in an aqueous medium such amphiphilic molecules exist separately. Moreover, as their concentration is increased, aggregation takes place within a rather narrow concentration interval.[1]

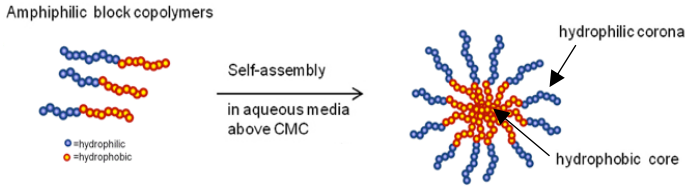

Figure 6. Formation of polymeric micelles by self-assembly of amphiphilic block copolymers in water above their CMC.

The process of micelle formation involves the decrease of free energy in the system: while micelles are forming, the hydrophobic fragments are separated from the aqueous environment and hydrogen bonds are simultaneous re-established in the water network. Additionally, at same time, the Van der Waals bonds between hydrophobic blocks in the core of the formed micelles result in energy gain.[9, 10]

The use of micelles as drug carriers provide a set of clear advantages: increased water solubility of poorly-water soluble drugs and its improved bioavailability, reduction of toxicity and other adverse effects, enhanced permeability across the physiological barriers, and substantial and favorable changes in drug biodistribution. Moreover, the use of micellar particles with specific shell properties can also enhance blood circulation time.[3]

Recently, interest has been raised in the application of these block copolymer micelles as novel systems in the field of drug targeting because of the high drug-loading capacity of the inner core as well as of the unique disposition characteristics in the body.[11, 12]

1.3.1 Synthesis and Classification of Polymeric Micelles

Block copolymer micelles can be classified according to the type of intermolecular forces driving the separation of the core segment from the aqueous media. Based on this, in the past few decades, at least three main categories were identified: amphiphilic micelles formed by hydrophobic interactions, polyion complex micelles (PICM) resulting from electrostatic interactions, and micelles stemming from metal complexation.[13-15]

In the drug delivery field, most amphiphilic copolymers employed to form micelles by self-assembly of non-polar and hydrophobic interactions, generally contain either a polyester or a poly(amino acid) derivative as the hydrophobic segment. Poly(lactic acid) (PLA),[16-18] poly(ε-caprolactone) (PCL),[19-21] and poly(glycolic acid)[22,23] are all biocompatible and biodegradable polyesters commonly used for micelle preparation aimed for biomedical application in humans. Many amphiphilic micelle-forming unimers include poly(ethylene glycol) (PEG) blocks as hydrophilic corona-forming blocks.[24] This polymer is inexpensive, has a low toxicity, and serves as an efficient steric protector of various biologically active macromolecules[25-29]and particulate delivery systems.[30-32] Moreover, numerous studies have confirmed its ability to reduce mononuclear phagocytic system (MPS) uptake of micellar delivery systems.[33]

The self-assembly of polyion complex micelles (PICM), proceeds through the neutralization and segregation of oppositely charged polyions in a way that combines features of amphiphilic micelles and interpolyelectrolyte complexes, instead. On this purpose, K. Kataoka and his collaborators prepared lactose conjugated polyion complex micelles that at physiological pH may be considered good candidates for incorporation of polyanionic plasmid DNA.[34]

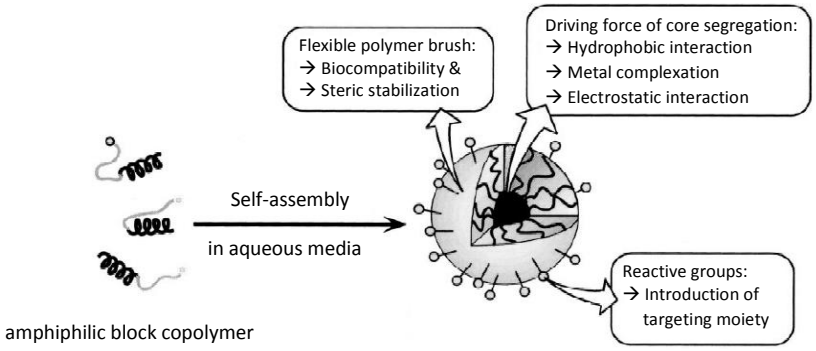

Figure 7. Characteristics of polymeric micelles that are relevant for drug delivery.

To better predict and control the properties of a micellar system, the utilized copolymer has to be well-defined, in terms of the nature of the polymer and the most appropriate polymerization reaction used. In general, micelle-forming amphiphilic copolymers can be either block copolymers (di, tri, or tetra) or graft copolymers, resulting in different final shapes/forms .[35]

Currently, a few commonly applied strategies of drug-loading procedures have been reported to form micelles . The first one is mostly employed for moderately hydrophobic copolymers, such as poloxamers, based on the direct dissolution of the block copolymer along with the drug in an aqueous solvent. Different strategies are used with amphiphilic copolymers that are not readily soluble in water and for which an organic solvent is used. In this case, the mechanism of micelle formation depends on the solvent-removal procedure: dialysis against water, for water miscible solvents; or solution-casting method for the non-water miscible ones.[36] On this respect, interestingly was the preparation of nanoparticles by nanoprecipitation of methacrylic acid copolymer (Eudragit L 100-55) with poly(vinyl alcohol) as a surfactant from which it was evidenced that the mean particle size was clearly dependent on the compatibility of the solvent with water.[37]

Among the multiple block copolymers already designed , recently, block copolymers containing thermosensitive elements have been used for the design and synthesis of smart drug-loaded polymer micelles, which dissociate in response to the range of environmental changes (i.e. change in temperature).[41-46]

1.3.2 Thermosensitive Micelles

For ideal drug targeting, the drug should be released only after the polymeric micelles accumulate at the targeted tissue, by some trigger such as changes in pH, presence of specific enzymes, etc. or by an external effect including temperature, light, ultrasound or magnetic field. The result of stimulation by either physiological or external trigger is the destabilization of micelles, termed as 'stimuli-sensitivity' of the micelles.[38] Depending on the stimulus applied varying responses may be observed including disruption of the structure, changes in shape, volume, permeation rates, hydration state, swelling/collapsing, or conformational changes.

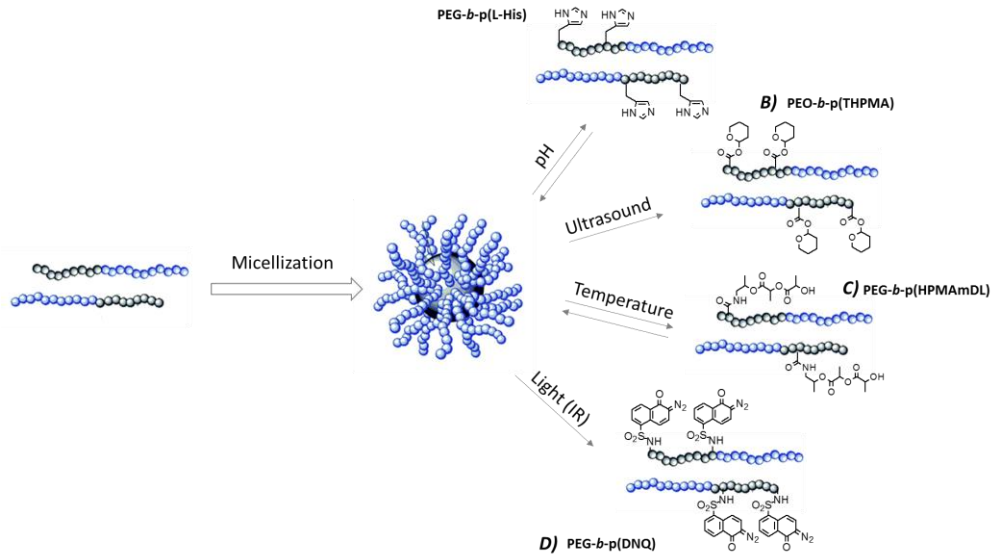

Figure 8. Examples of stimuli-sensitive polymeric micelle destabilization. **A)** poly(L-histidine)–poly(ethylene glycol) (PEG-*b*-p(L-His)) diblock copolymer based pH-sensitive micelle;[70] **B)** high-frequency ultrasound-responsive poly(ethylene oxide) and poly(2-tetrahydropyranyl methacrylate) (PEO-*b*-p(THPMA)) block copolymer based micelle;[71] **C)** block copolymer of poly(N-(2-hydroxypropyl) methacrylamide lactate) and poly(ethylene glycol) (PEG-*b*-pHPMAmDL) thermosensitive and biodegradable polymeric micelles;[72] **D)** synthetic micelle sensitive to IR light of poly(ethylene glycol) as the hydrophilic component and 2-diazo-1,2-naphthoquinone as the hydrophobic component (PEG-*b*-pDNQ).[73]

An important class of stimuli-responsive micelles are those comprising polymers with thermosensitive behavior. Thermoresponsive polymers are a class of “smart” materials that have the ability to respond to a change in temperature: a property that makes them useful materials in a wide range of applications. In particular, the nanocarriers accumulate in the required sites through either passive or active targeting, and when they reach the maximum accumulation, the carried drugs are released in a rapid manner, in response to changes in the environmental temperature, i.e. by hypo- or hyperthermia.[39-41]

Guilet and collaborators were the first to investigate, in 1985, the influence of temperature on flocculation process of this kind of polymers. They observed that certain temperature-sensitive polymers are effective flocculants below their transition temperature only.[42] However, other researchers found temperature-responsive polymers to act as flocculants above their transition temperature as well. Aqueous solutions of thermoresponsive polymers can exhibit two main types of phenomena: a lower critical solution temperature (LCST) or an upper critical solution temperature (UCST). LCST and UCST are the respective critical temperature values *below* and *above* which the polymer and solvent are completely miscible.[43]

The explanation of these phenomena is based on what phase dispositions are energetically (free energy) more favorable. Specifically, the main driving force is the entropy of water molecules, which is higher when the polymer is not dissolved .[44] It is remarkable that LCST is an entropically driven effect, while UCST is an enthalpically driven effect.[45]

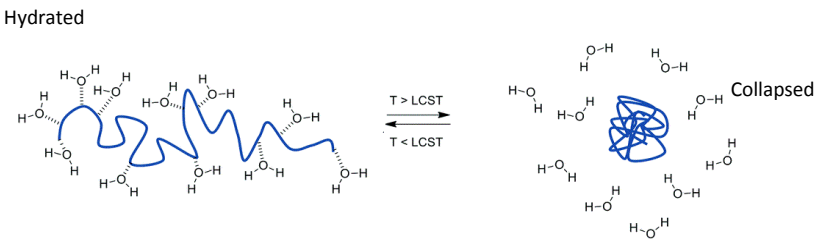

Figure 9. LCST behavior of thermosensitive polymers. Below the LCST, the polymer is water-soluble and in expanded state, above their LCST the hydrogen bonds between the polymer chains and the molecules of water are disrupted, and the polymer collapsed.

Well-known thermosensitive polymers are poly(*N*-isopropylacrylamide) (pNIPAAm) and Pluronics (PEG-*b*-PPO-*b*-PEG), a triblock copolymer of polypropylene oxide [PPO] middle block flanked by polyethylene glycol [PEG] blocks, applied in controlled drug delivery due to its properties of temperature responsive micellization and gelation.[46] Other polymers with thermoresponsive properties include poly(*N*,*N*-diethylacrylamide) (PDEAAm) with an LCST over the range of 25 to 32 °C and poly(*N*-vinlycaprolactam) (PVCL) with an LCST between 25 and 35 °C.[47,48]

San Miguel et al. synthesized ABA triblock copolymers of poly[2-(dimethylamino)ethyl methacrylate] (PDMAEMA, with an LCST of around 50 °C) as block A, and PVCL as block B, and demonstrated the formation of thermoresponsive micelles with sustained drug release *in vitro*.[49]

Moreover, poly(ethylene glycol) (PEG), also called poly(ethylene oxide) (PEO) has shown thermosensitive properties, with LCST values around 85 °C.[50,51]

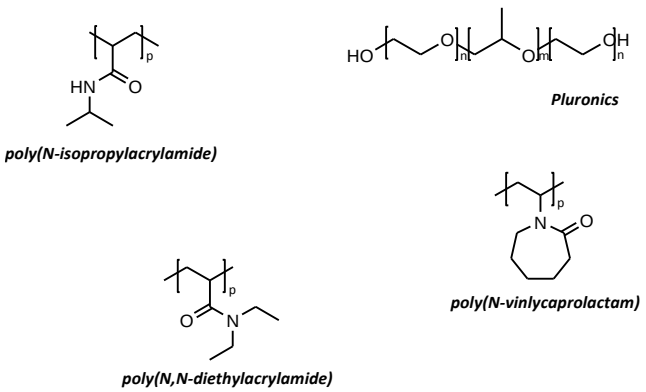

Figure 10. Chemical structures of thermosensitive polymers commonly used for micelle preparation.

It should be noted that the LCST is affected by the hydrophobiticy of the side groups. Specifically, the LCST of a polymer is often also dependent on molecular weight and architecture.[52,53]

1.3.2.1 Thermosensitive Polymeric Micelles based on poly(*N*-isopropylacrylamide) p(NIPAAm)

One of the most extensively investigated thermosensitive polymers is pNIPAAm. This polymer has an LCST of 32°C in aqueous environment, which means that it is water-soluble below this temperature and water-insoluble above this temperature. pNIPAAm is the most widely used thermosensitive polymer because of its phase transition temperature near physiological temperature. In 1998, Chung et al. showed the effect of linking different moieties to the terminal end of a pNIPAAm, concluding that the LCST dramatically change depending on the nature of the end moieties.[54] More specifically, hydrophilic end-groups raised the LCST and the inverse was noticed when hydrophobic moieties were used. Moreover, as result of these LCST changes, micelles formed from those copolymers, may have the pNIPAAm block either as hydrophilic shell or as hydrophobic core. For this purpose, Leroux and collaborators prepared polymeric micelles based on poly(*N*-isopropylacryamide-*co*-methacrylic acid-*co*- octadecyl acrylate) (p(NIPAAm-*co*-MAA-*co*-ODA)) random copolymer with NIPAAm and MAA segments constructing the shell and ODA segments forming the core. The incorporation of a small amount of hydrophilic MAA units to the polymer chains increased the LCST of the resulting copolymer to 37°C. Moreover, due the MMA units copolymerized in the polymer backbone, the resulting amphiphilic polymer showed also pH-sensitive characteristics.[55]

T. Okano and other groups prepared other micelles with thermosensitive outer shell type, which were composed of thermosensitive p(NIPAAm) blocks as the outer hydrophilic shell and hydrophobic poly(butylmethacrylate) (PBMA)[56] or poly(D,L-lactide) (PLA)[57] as the drug-incorporated inner core.

On the other hand, pNIPAAm-*b*-PEG is the most studied polymer to prepare micelles with pNIPAAm as core-forming segments. In this case, the highly hydrated hydrophilic PEG chain is used for the stabilization of dispersions. Below the LCST of pNIPAAm block, pNIPAAm-*b*-PEG is highly soluble in aqueous solution, while above the LCST, the thermo-sensitive pNIPAAm block precipitates, and the block copolymers self-assemble into polymeric micelles with a pNIPAAm core and a hydrophilic PEG shell.[58] For example, Tenhu and co-workers studied the aggregation of pNIPAAm-*b*-PEG in water by fluorescence spectroscopy and light scattering.[59]

Hennink et al. developed degradable copolymers of poly(NIPAAm-*co*-poly(*N*-(2-hydroxypropyl) methacrylamide-lactate) polymerized with PEG. In this case, due the higher hydrophilicity of the PEG block, the p(NIPAAm-*co*-HPMAm-lactate) block constituted the inner hydrophobic core of the obtained micelle. Moreover, in this work, the cleavage of the lactate moiety *in vitro* or *in vivo* causes an increase in the polymer LCST and ultimately destabilization of the micelles, releasing any encapsulated drug.[60]

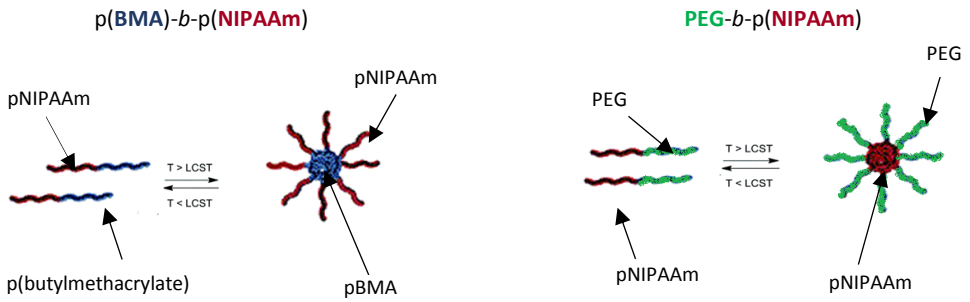

Figure 11. pNIPAAm based micelle with pNIPAAm as hydrophilic shell (p(PBA)-*b*-p(NIPAAm) or as hydrophobic core (PEG-*b*-p(NIPAAm).

The formation of micelles in solution is a reversible and dynamic process: the resulting dissociation can lead to premature release of a loaded drug. Crosslinking of the polymer chains can overcome this once micellization has occurred; this reaction can be done in the core or in the shell of micelles.

Redox-sensitive core crosslinked pNIPAM based micelles were reported by Narain et al. The resulting micelles exhibited reversible swelling behavior within a temperature range of 28-32 °C.[61]

Wei et al. produced a number of shell crosslinked hybrid micelles using inorganic ferric-based crosslinks and pNIPAAm thermoresponsive groups. They found drug release to be sustained for around 100 hours followed by a slow leveling-off of the release rate.[62,63] However, chemical conjugation methods are not always feasible, due the toxicity of some crosslinking agents and due some side reactions that can happen during the process that might affect the therapeutic properties of conjugated drugs. Alternatively, physical interactions, such as π–π stacking,[64,67] hydrogen bonding[68] or stereocomplex formation[69] have been investigated to improve the thermodynamic and kinetic stability of such polymeric micelles.

References

(1) V. P. Torchilin, Micellar Nanocarriers: Pharmaceutical Perspectives. *Pharmaceutical Research*, **2007**, 24

(2) L. Zhang and A. Eisenberg. Multiple morphologies of crew-cut aggregates of polystyrene-b-poly(acrylic acid) block copolymers. *Science,* **1995***,* 268: 1728-1731

(3) V. P. Torchilin. Structure and design of polymeric surfactant-based drug delivery systems. *J. Control. Release*, **2001**, 73:137-172

(4) M. Moffitt, K. Khougaz, A. Eisenberg, Micellization of ionic block copolymers. *Acc. Chem. Res.,* **1996**, 29: 95–102

(5) Z. Tuzar, P. Kratochvil, Block and graft copolymer micelles in solution. *Adv. Colloid Interface Sci*., **1976**, 6: 201–232

(6) P. Munk, K. Prochazka, Z. Tuzar, S.E. Webber, Exploiting polymer micelle technology. *CHEMTECH*, **1998**, 28: 20–28

(7) M. R. Talingting, P. Munk, S. E. Webber, Z. Tuzar, Onion-type micelles from polystyrene-block–poly(2-vinylpyridine) and poly(2-vinylpyridine)-block–poly(ethylene oxide). *Macromolecules*, **1999**, 32: 1593–1601

(8) Z. Ahmad, A. Shah M. Siddiq and H.-B. Kraatz, Polymeric micelles as drug delivery vehicles. *RSC Adv.*, **2014**, 4: 17028–17038

(9) M. Jones and J. Leroux. Polymeric micelles: a new generation of colloidal drug carriers. *Eur. J. Pharm. Biopharm.,* **1999***,* 48: 101-111

(10) A. Martin (ed.), *Physical Pharmacy*. Lippinkott, Williams and Wilkins, Philadelphia, **1993**

(11) G.S. Kwon, K. Kataoka, Block copolymer micelles as long-circulating drug vehicles. *Adv. Drug Deliv. Rev*., **1995**, 16: 295–309

(12) K. Kataoka, A. Harada, Y. Nagasaki, Block copolymer micelles for drug delivery: design, characterization and biological significance. *Advanced Drug Delivery Reviews,* **2001**, 47: 113–131

(13) Y. Nishiyama, Y. Kato, Y. Sugiyama, K. Kataoka, Cisplatin loaded polymer–metal complex micelle with time-modulated decaying property as a novel drug delivery system. *Pharm. Res.*, **2001**, 18: 1035– 1041

(14) N. Nishiyama, S. Okazaki, H. Cabral, M. Miyamoto, Y. Kato, Y. Sugiyama, K. Nishio, Y. Matsumura, K. Kataoka, Novel cisplatin-incorporated polymeric micelles can eradicate solid tumors in mice. *Cancer Res.,* **2003**, 63: 8977–8983

(15) J. Wang, A. de Keizer, R. Fokkink, Y. Yan, M. A. Cohen Stuart and J. van der Gucht, Complex Coacervate Core Micelles from Iron-Based Coordination Polymers. *J. Phys. Chem. B*, **2010**, 114: 8313–8319

(16) S. Tanodekaew, R. Pannu, F. Heatley, D. Attwood, C. Booth, Association and surface properties of diblock copolymers of ethylene oxide and DL-lactide in aqueous solution. *Macrom. Chem. and Phy.*, 1997, 198: 927–944

(17) C. Garofalo, G. Capuano, R. Sottile, R. Tallerico, R. Adami, E. Reverchon, E. Carbone, L. Izzo, and D. Pappalardo, Different Insight into Amphiphilic PEG-PLA Copolymers: Influence of Macromolecular Architecture on the Micelle Formation and Cellular Uptake. *Biomacromolecules*, **2014**, 15: 403−415

(18) Y. Li, X. R. Qi, Y. Maitani, T. Nagai, PEG-PLA diblock copolymer micelle-like nanoparticles as all-trans-retinoic acid carrier: *in vitro* and *in vivo* characterizations. *Nanotechnology,* **2009**, 20: 55-106

(19) J. Zhao, Y. Wang, L. Luan, Star-shaped polycaprolactone-polyethyleneglycol copolymer micelle-like nanoparticles for picropodophyllin delivery. *J Biomed Nanotechnol.*, **2014,** 10: 1627-34

(20) S. C. Owena, D. P.Y. Chana, M. S. Shoichet, Polymeric micelle stability. *Nano Today*, **2012**, 7: 53—65

(21) C. S. Brazel, J. B. Bennett, A. L. Glover, J. A. Nikles, M. Everts, J. N. Glasgow and D. E. Nikles, Design of Poly(ethylene glycol)-Polycaprolactone Diblock Micelles with RGD Targeting Ligands and Embedded Iron Oxide Nanoparticles for Thermally-activated Release. *MRS Proceedings*, **2012**, 1416: 05-31

(22) H. S. Yoo, T. G. Park, Biodegradable polymeric micelles composed of doxorubicin conjugated PLGA–PEG block copolymer. *J. of Controlled Release*, **2001**, 70, 63–70

(23) G. Ruana, S.-S. Feng, Preparation and characterization of poly(lactic acid)–poly(ethylene glycol)–poly(lactic acid) (PLA–PEG–PLA) microspheres for controlled release of paclitaxel. *Biomaterials*, **2003**, 24: 5037–5044

(24) G. S. Kwon. Polymeric micelles for delivery of poorly water soluble compounds. *Crit. Rev. Ther. Drug Carr. Syst.,* **2003***,* 20: 357-403

(25) T. Morcol, P. Nagappan, L. Nerenbaum, A. Mitchell, and S. J. Bell. Calcium phosphate-PEG-insulin-casein (CAPIC) particles as oral delivery systems for insulin. *Int. J. Pharm*., **2004**, 277: 91-97 67

(26) A. Abuchowski, T. Esvan, N. C. Palczuk, J. R. McCoy, and F. F. Davis. Treatment of l5178y tumor-bearing bdf1 mice with a nonimmunogenic 1-glutaminase-1-asparaginase. *Cancer Treat. Rep.*, **1979**, 63: 1127-1132

(27) J. M. Harris, N. E. Martin, and M. Modi. Pegylation: a novel process for modifying pharmacokinetics. *Clin. Pharmacokinet.*, **2001**, 40: 539-551

(28) M. J. Roberts, M. D. Bentley, and J. M. Harris. Chemistry for peptide and protein pegylation. *Adv. Drug Deliv. Rev.*, **2002**, 54: 459-476

(29) F. M. Veronese and J. M. Harris. Introduction and overview of peptide and protein pegylation. Adv. *Drug Deliv. Rev*., **2002**, 54: 453-456

(30) A. L. Klibanov, K. Maruyama, V. P. Torchilin, and L. Huang. Amphipathic polyethyleneglycols effectively prolong the circulation time of liposomes. *FEBS Lett*., **1990**, 268: 235-237

(31) P. Calvo, B. Gouritin, I. Brigger, C. Lasmezas, J. Deslys, A. Williams, J. P. Andreux, D. Dormont, and P. Couvreur. Pegylated polycyanoacrylate nanoparticles as vector for drug delivery in prion diseases. *J. Neurosci. Methods*, **2001**, 111: 151-155

(32) S. M. Moghimi. Chemical camouflage of nanospheres with a poorly reactive surface: towards development of stealth and target-specific nanocarriers. *Biochim. Biophys. Acta*, 2002, 1590: 131-139

(33) G. Kwon, S. Suwa, M. Yokoyama, T. Okano, Y. Sakurai, K. Kataoka, Enhanced tumor accumulation and prolonged circulation times of micelle-forming poly (ethylene oxide-aspartate) block copolymer-adriamycin conjugates. *J. of Controlled Release*, **1994,** 29: 17-23

(34) D. Wakebayashi, N. Nishiyama, Y. Yamasaki, K. Itaka, N. Kanayama, A. Harada, Y. Nagasaki, K. Kataoka, Lactoseconjugated polyion complex micelles incorporating plasmid DNA as a targetable gene vector system: their preparation and gene transfecting efficiency against cultured HepG2 cells. *J. Control. Release*, **2004**, 95: 653– 664

(35) C. Allen, D. Maysinger, A. Eisenberg, Nano-engineering block copolymer aggregates for drug delivery, *Colloids Surf.*, **1999**, 16: 3 –27

(36) G.`ve Gaucher, M.-H. Dufresne, V. P. Sant, N. Kang, D. Maysinger, J.-Ch. Leroux, Block copolymer micelles: preparation, characterization and application in drug delivery. *J. of Controlled Release*, **2005**, 109: 169–188

(37) S. Galindo-Rodriguez, E. Allemann, H. Fessi, E. Doelker, Physicochemical Parameters Associated with Nanoparticle Formation in the Salting-Out,

Emulsification-Diffusion, and Nanoprecipitation Methods. *Pharm. Res*., **2004**, 21: 1428–1439

(38) Zhang Y, Jiang M. New approaches to stimuli responsive polymeric micelles and hollow spheres. *Front Chem,* **2006**; 4: 364-68

(39) P. Shao, B. Wang, Y. Wang, J. Li, and Y. Zhang, The Application of Thermosensitive Nanocarriers in Controlled Drug Delivery. *J. of Nanomaterials,* **2011**

(40) M. A. Ward and T. K. Georgiou, Thermoresponsive Polymers for Biomedical Applications. *Polymers* **2011**, 3: 1215-1242

(41) M. Talelli and W. E. Hennink, Thermosensitive polymeric micelles for targeted drug delivery. *Nanomedicine*, **2011**, 6: 1245–1255

(42) J.E. Guillet, M. Heskins, D.G. Murray, U. S. Patent 4, 536, 294, **1985**

(43) J. Kost and R. Langer, Responsive polymeric delivery systems. *Ad. Drug Delivery Rev*, **2001**, 46: 125–148

(44) N. T. Southall, K. A. Dill, A. D. J. Haymet, A view of the hydrophobic effect. *J. Phys. Chem. B,* **2002**, 106: 521-533

(45) C. Vasile, A. K. Kulshreshtha, *Handbook of Polymer Blends and Composites*; Rapra Technology Ltd.: Shawbury, UK, **2003**

(46) C. He, S. W. Kim, and D. S. Lee, In situ gelling stimulisensitive block copolymer hydrogels for drug delivery. *J. of Controlled Release*, **2008**, 127: 189–207

(47) H. Vihola, A. Laukkanen, H. Tenhu, J. Hirvonen, Drug release characteristics of physically cross-linked thermosensitive poly(*N*-vinylcaprolactam) hydrogel particles. *J. Pharm. Sci.,* **2008**, 97: 4783-4793

(48) H. Vihola, A. K. Marttila, J. S. Pakkanen, M. Andersson, A. Laukkanen, A. M. Kaukonen, H. Tenhu, J. Hirvonen, Cell-polymer interactions of fluorescent polystyrene latex particles coated with thermosensitive poly(*N*-isopropylacrylamide) and poly(*N*-vinylcaprolactam) or grafted with poly(ethylene oxide)-macromonomer. *Int. J. Pharm.*, **2007**, 343: 238-246

(49) V. San Miguel, A. J. Limer, D. M. Haddleton, F. Catalina, C. Peinado, Biodegradable and thermoresponsive micelles of triblock copolymers based on 2-(*N*,*N*-dimethylamino)ethyl methacrylate and ε-caprolactone for controlled drug delivery. *Eur. Polym. J*., **2008**, 44: 3853-3863

(50) Z. B. Hu, T. Cai, C. L. Chi, Thermoresponsive oligo(ethylene glycol)-methacrylate-based polymers and microgels. *Soft Matter*, **2010**, 6: 2115-2123

(51) C. R. Becer, S. Hahn, M. W. M. Fijten, H. M. L. Thijs, R. Hoogenboom, U. S. Schubert, Libraries of methacrylic acid and oligo(ethylene glycol) methacrylate copolymers with LCST behavior. *J. Polym. Sci. Part A,* **2008**, 46: 7138-7147

(52) W. Li, A. Zhang, A. D. Schluter, Thermoresponsive dendronized polymers with tunable lower critical solution temperatures. *Chem. Commun*., **2008,** 5523-5525

(53) W. Li, A. Zhang, K. Feldman, P. Walde, A. D. Schluter, Thermoresponsive dendronized polymers. *Macromolecules*, **2008**, 41: 3659-3667

(54) J. E. Chung, M. Yokoyama, T. Aoyagi, Y. Sakurai, T. Okano, Effect of molecular architecture of hydrophobically modified poly(*N*-isopropylacrylamide) on the formation of thermoresponsive core-shell micellar drug carriers. *J. Control. Release*, **1998**, 53: 119-130

(55) J. Taillefer, M. C. Jones, N. Brasseur,J. E. Van lier, J. C. Leroux, Preparation and characterization of pH-sensitive polymeric micelles for the delivery of photosensitizing anticancer drugs. *J Pharm Sci,* **2000**;89: 52–62

(56) J. E. Chung, M. Yokoyama, M. Yamato, T. Aoyagi, Y. Sakurai, T. Okano, Thermo-responsive drug delivery from polymeric micelles constructed using block copolymers of poly(*N*-isopropylacrylamide) and poly(butylmethacrylate). *J. of Controlled Release*, **1999**, 62: 115–127

(57) F. Kohori, K. Sakai, T. Aoyagi, M. Yokoyama, Y. Sakurai, T. Okano, Preparation and characterization of thermally responsive block copolymer micelles comprising poly(*N*-isopropylacrylamide-b-DL-lactide). *J. Control Release*, **1998**, 55: 87-98

(58) H. Wei, S.-X. Cheng, X.-Z. Zhang, R.-X. Zhuo, Thermo-sensitive polymeric micelles based on poly(*N*-isopropylacrylamide) as drug carriers. *Prog. in Pol. Sc.,* **2009**, 34: 893–910

(59) J. Virtanen, S. Holappa, H. Lemmetyinen, H. Tenhu, Aggregation in aqueous poly(*N*-isopropylacrylamide)-block-poly(ethylene oxide) solutions studied by fluorescence spectroscopy and light scattering. *Macromolecules*, **2002**; 35: 4763–4769

(60) D. Neradovic, C. F. van Nostrum, and W. E. Hennink, Thermoresponsive Polymeric Micelles with Controlled Instability Based on Hydrolytically Sensitive *N*-Isopropylacrylamide Copolymers. *Macromolecules* **2001**, 34: 7589-7591

(61) J. Xiaoze, S. Liu, and R. Narain, Degradable Thermoresponsive Core Cross-Linked Micelles: Fabrication, Surface Functionalization, and Biorecognition. *Langmuir*, **2009**, 25: 13344–13350

(62) H. Wei, C. Cheng, C. Chang, W. Q. Chen, S. Cheng, X. Z. Zhang, R. X. Zhuo, Synthesis and applications of shell cross-linked thermoresponsive hybrid micelles based on poly(*N*-isopropylacrylamide- *co*-3-(trimethoxysilyl)propyl methacrylate)-*b*-poly(methyl methacrylate). *Langmuir*, **2008**, 24: 4564-4570

(63) H. Wei, C. Y. Quan, C. Chang, X. Z. Zhang, R. X. Zhuo, Preparation of novel ferrocene-based shell cross-linked thermoresponsive hybrid micelles with antitumor efficacy. *J. Phys. Chem. B*, **2010**, 114: 5309-5314

(64) K. M. Huh,H. S. Min, S. C. Lee, H. J. Lee, S. Kim, K. Park, Doxorubicin-loaded cholic acid-polyethyleneimine micelles for targeted delivery of antitumor drugs: synthesis, characterization, and evaluation of their in vitro cytotoxicity. *J. Controlled Release* **2008**; 126: 122–129

(65) H. Engelkamp, S. Middelbeek, JM, R. *Science,* **1999**, 284: 785–788

(66) M. G. Carstens, P. H. de Jong, C. F. van Nostrum, J. Kemmink, R. Verrijk, L. G. J. de Leede, D. J. A. Crommelin, W. E. Hennink, The effect of core composition in biodegradable oligomeric micelles as taxane formulations. *Eur. J. Pharm. Biopharm*., **2008**, 68: 596–606

(67) M. G. Carstens,J. J. L. Bevernage, C. F. van Nostrum, M. J. van Steenbergen, F. M. Flesch, R. Verrijk, L. G. J. de Leede, D. J. A. Crommelin, W. E. Hennink, Photocytotoxicity of mTHPC (Temoporfin) Loaded Polymeric Micelles Mediated by Lipase Catalyzed Degradation. *Macromolecules,* **2007**, 40: 116–122

(68) B. S. Kim, S. W. Park, P. T. Hammond, *ACS Nano,* **2008**, 2: 386–392

(69) N. Kang, M. E. Perron, R. E. Prud'Homme, Y. Zhang, G. Gaucher, J. C. Leroux; Stereocomplex block copolymer micelles: core-shell nanostructures with enhanced stability. *Nano Lett*., **2005,** 5: 315–319

(70) E. S. Lee , H. J. Shin , K. Na , Y. H. Bae, P oly(L-histidine)–PEG block copolymer micelles and pH-induced destabilization. *J. of Controlled Release,* **2009**, 90: 363–374

(71) J. Wang, M. Pelletier, H. Zhang, H. Xia, and Y. Zhao, High-Frequency Ultrasound-Responsive Block Copolymer Micelle. *Langmuir,* **2009**, 25: 13201–13205

(72) O. Soga, C. F. van Nostrum, M. Fens, C. J.F. Rijcken, R. M. Schiffelers, G. Storm, W. E. Hennink, Thermosensitive and biodegradable polymeric micelles for paclitaxel delivery. *Journal of Controlled Release*, **2005**, 103: 341 – 353

(73) A. P. Goodwin, J. L. Mynar, Y. Ma, G. R. Fleming, and J. M. J. Fre´chet, Synthetic Micelle Sensitive to IR Light via a Two-Photon Process. *J. Am. Chem. Soc*. **2005**, 127: 9952-9953

1.4 "Click Chemistry" as chemistry of Nanomaterial

A close examination of nature's favorite molecules, such as nucleic acids and proteins, reveals an overall preference for making carbon-heteroatom bonds over carbon-carbon bonds. Inspired by nature, and limiting the search for new substances to those that can be generated by joining small units together through heteroatom links, Sharpless et al. defined "click chemistry" as reactions that ''*are modular, wide in scope, high yielding, create only inoffensive by-products (that can be removed without chromatography), are stereospecific, simple to perform and that require benign or easily removed solvent*''.[1]
A wide range of click chemistry reactions include cycloaddition reactions, such as the 1,3-dipolar family, and hetero Diels- Alder reactions;[2] carbonyl chemistry, such as the formation of oxime ethers, hydrazones, and aromatic heterocycles;[3, 4] nucleophilic ring-opening reactions (e.g., epoxides, aziridines, cyclic sulfates, and so forth);[1] and azide-phosphine coupling (Staudinger ligation).[5, 6]
The most popular click reaction is the 1,3-dipolar azide-alkyne cycloaddition reaction, first discovered by Hüisgen in 1963, but it did not attract much interest due to the requirements of high temperatures and pressures.[7] Rostovtsev et al. and Mendal et collaborators demonstrated that the reaction could also be carried out under mild conditions using Cu(I) as the catalyst, and with great regio-selectivity on obtain 1,4-disubstituted 1,2,3-triazole product preparing the catalyst *in situ* by reducing copper(II) salts with a reducing agent (i.e. $CuSO_4\,5H_2O$, sodium ascorbate).[8, 9]

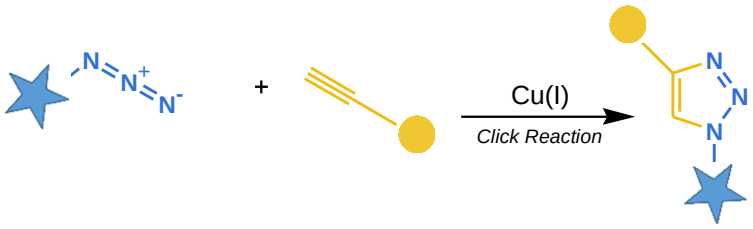

Figure 12. Copper(I)-catalyzed Azide-Alkyne Cycloaddition (CuAAC), well known as Hüisgen click chemistry reaction.

Moreover, Codelli et al. reported an alternative method to lower the activation barrier for the cycloaddition by employing intrinsically highly strained cyclic alkynes that readily and selectively react with azides, and do not need Cu(I) as catalyst of the reaction. These new 'click chemistry-Copper free' products form at ambient temperature and pressure with no apparent cytotoxicity.[10, 11]
Another widely used click chemistry reaction was reported by Staudinger and Meyer in 1919 named the 'Staudinger ligation', which forms phosphazo compounds by reacting tertiary phosphines with organic azides.[5, 6]

Even though, more click chemistry strategies have been developed.[12-16] In general, the concept of click chemistry therefore represents a highly valuable contribution to effect a 'universal' modification strategy that has the ability not only to generate novel structures, but also to simplify the covalent assembly of very chemically dissimilar molecules, such as complex carbohydrates with peptides, or chemo reporters, such as fluorescent dyes with biopolymers. This highly selective, specific chemistry has emerged as an attractive technique to conjugate easily materials for several applications. As result, numerous biomolecules including DNA, peptides, proteins, oligosaccharides and glycoconjugates have been labelled with various appendages.

Although, significant efforts have been made in formulating macromolecule based nanocarriers using the variety of synthetic click chemistry strategies above mentioned, as mild reaction conditions, high yield, simple work-up, selectivity, and specificity; due to its fulfilling of many requirements for the affixation of ligands onto i.e. polymers by pre- or post-modification processes. In this respect, Adronov et al. used click chemistry to functionalize single-walled carbon nanotubes with polystyrene, in order to increase their water solubility. The 'click reaction' was mediated by incorporation of a small alkyne bearing reactive species on to the surface of the nanotube, followed by coupling of these fragments to terminal azide bearing polystyrene chains.[17] Additionally, Goyal, Yoon, and Weck worked on development of poly(amine) dendrimer that possessed a aldehyde or azide moiety on the dendrimer surface capable of orthogonal functionalization with small molecule functional groups by click chemistry.[18]

Moreover, a wide range of polymer functionalization strategies were used to speed up the use of polymers with defined functional ligands, positioned in either the main chain or the respective side chains. For instance, Haddleton and co-workers have demonstrated the possibility to graft carbohydrates with side chain of modified polymethylacrylates (PMMA), starting from side chain-modified PMMA, which present multiple acetylenic moieties that can 'click' a number of carbohydrates (e.g., 1-azidosugars, 6-azidosugars).[19]

Surface modified nanoparticles with biomolecules by click chemistry could be applied for the targeted delivery or imaging. For instance, polycationic,[20] hydrophilic[21] and amphipilic[22] 194 β-cyclodextrin 'click cluster' had been developed via CuAAC reaction, obtaining an increasing in the serum stability of polymer repeat unit could without need grafting on large PEG chains to the polymer backbone. These copolymers formed polyplexes by complexing pDNA, and displayed a highly efficient pDNA delivery. Furthermore, fluorescent micelle with inorganic silica core with biocompatible polymer shell and a terminal unit susceptible to facile conjugations via click chemistry, were applied successfully for intracellular delivery and optical imaging which is demonstrated via *in vitro* experiments on lung cancer cells.[23]

However, clicked nanoparticles could be applied also in many other biological fields. In this respect, J. C. M. van Hest et al. developed clicked polymersome nanoreactors able to load enzyme and thus showed cellular uptake which can be applied for functional artificial organelles.[24]
Certainly, due to facility with which sequential click reactions can be performed in macromolecules, these methodologies can be extended to the design of novel nanocarriers with any desired combination of ingredients…*and nearly any conjugates you can imagine can be done by Click Chemistry.*

References

(1) H. C. Kolb, M. G. Finn and K. B. Sharpless, Click Chemistry: Diverse Chemical Function from a Few Good Reactions. *Angew Chem Int Ed Engl.,* **2001**; 40: 2004-2021

(2) K. A. Jørgensen, Catalytic asymmetric hetero-diels-alder reactions of carbonyl compounds and imines. *Angew Chem Int Ed,* **2000**; 39: 3558-3588

(3) H. Adolfsson, A. Converso, K. B. Sharpless, Comparison of amine additives most effective in the new methyltrioxorhenium catalyzed epoxidation process. *Tetrahedron Lett*, **1999**; 40: 3991-3994

(4) H. C. Kolb, M. S. Van Nieuwenhze, K. B. Sharpless, Catalytic asymmetric dihydroxylation. *Chem Rev*, **1994**; 94: 2483-2547

(5) H. Staudinger, J. Meyer, New organic compounds of phosphorus: III. Phosphinemethylene derivatives and phosphinimines [in German]. *Helv Chim Acta*, **1919**; 2: 635-646

(6) Y. G. Gololobov, I. N. Zhmurova, L. F. Kasukhin, Sixty years of Staudinger reaction. *Tetrahedron*, **1981**; 37:437-472

(7) R. Huisgen, 1,3-dipolar cycloadditions. Past and Future. *Angew Chem Int Ed*, **1963**; 2: 565-598

(8) V. V. Rostovtsev, L. G. Green, V. V. Fokin, et al. A stepwise Huisgen cycloaddition process: Copper(I)-catalyzed regioselective ‘‘ligation’’ of azides and terminal alkynes. *Angew Chem Int Ed*, **2002**; 41: 2596-2599

(9) C. W. Tornoe, C. Christensen, M. Meldal, Peptidotriazoles on solid phase: [1,2,3]-triazoles by regiospecific copper(I)- catalyzed 1,3-dipolar cycloadditions of terminal alkynes to azides. *J Org Chem*, **2002**; 67: 3057-3064

(10) J. A. Codelli, J. M. Baskin, N. J. Agard et al., Second-generation difluorinated cyclooctynes for copper-free click chemistry. *J Am Chem Soc*, **2008**; 130: 11486-11493

(11) J. M. Baskin, J. A. Prescher, S. T. Laughlin et al., Copper-free click chemistry for dynamic *in vivo* imaging. *Proc Natl Acad Sci,* **2007**; 104: 16793-16797

(12) L. Zhang, X. Chen, P. Xue, H. H. Y. Sun, I. D. Williams, K. B. Sharpless, V. V. Fokin, G. Jia, Ruthenium-Catalyzed Cycloaddition of Alkynes and Organic Azides. *J. Am. Chem. Soc.*, **2005**; 127: 15998-15999

(13) P. L. Golas, N. V. Tsarevsky, B. S. Sumerlin, K. Matyjaszewski, Catalyst Performance in “Click” Coupling Reactions of Polymers Prepared by ATRP: Ligand and Metal Effects. *Macromolecules,* **2006**; 39: 6451

(14) P. Appakkuttan, W. Dehaen, V. V. Fokin, E. van der Eyken, A Microwave-Assisted Click Chemistry Synthesis of 1,4-Disubstituted 1,2,3-Triazoles via a Copper(I)-Catalyzed Three-Component Reaction. *Org. Lett.*, **2004**; 6: 4223-4225

(15a) P. Lidstro¨m, J. Tierny, B. Wathey, J. Westman, *Tetrahedron;* **2001**, 57: 9225; (15b) C. O. Kappe, Curr. Opin., *Chem. Biol.* **2002**; 6: 314; (15c) M. Larhed, C. Moberg, A. Hallberg, *Acc. Chem. Res.* **2002**; 35: 717; (15d) C. O. Kappe, *Angew. Chem*. **2004**; 116: 6408

(16) H. A. Orgueira, D. Fokas, Y. Isome, P. Chan, C. M. Baldino, Regioselective synthesis of [1,2,3]-triazoles catalyzed by Cu(I) generated in situ fromCu(0) nanosize activated powder and amine hydrochloride salts *Tetrahedron*, **2005**; 46: 2911-2914

(17) H. Li, F. Cheng, A. M. Duft and A. Adronov, Functionalization of single-walled carbon nanotubes with well-defined polystyrene by "click" coupling. *J. Am. Chem. Soc.*, **2005**; 127: 14518-24

(18) K. Yoon, P. Goyal, M. Weck, Monofunctionalization of dendrimers with use of microwave-assisted 1,3- dipolar cycloadditions. *Organic Letters*, **2007**; 9:2051–2054

(19) V. Ladmiral, G. Mantovani, G. J. Clarkson, S. Cauet, J. L. Irwin, D. M. Haddleton, Synthesis of neoglycopolymers by a combination of "click chemistry" and living radical polymerization. *J. Am. Chem. Soc*. **2006**; 128: 4823-30

(20) S. Srinivasachari, K. M. Fichter and T. M. Reineke, Polycationic β-Cyclodextrin “Click Clusters”: Monodisperse and Versatile Scaffolds for Nucleic Acid Delivery. *J. Am. Chem. Soc.*, **2008**, 130: 4618–4627

(21) S. Srinivasachari and T. M. Reineke, Versatile supramolecular pDNA vehicles via “click polymerization” of β-cyclodextrin with oligoethyleneamines. *Biomaterials*, **2009**, 30: 928–938

(22) A. Mendez-Ardoy, M. Gomez-Garcia, C. O. Mellet, N. Sevillano, M. Dolores Giron, R. Salto, F. Santoyo-Gonzalez and J. M. Garcia Fernandez, Preorganized macromolecular gene delivery systems: amphiphilic β-cyclodextrin “click clusters”. *Org. Biomol. Chem.*, **2009**, 7: 2681–2684

(23) M. Müllner, A. Schallon, A. Walther, R. Freitag and A. H. E. Müller, Clickable, Biocompatible, and Fluorescent Hybrid Nanoparticles for Intracellular Delivery and Optical Imaging. *Biomacromolecules*, **2009**, 111: 390–396

(24) S. F. M. van Dongen, W. P. R. Verdurmen, R. J. R. W. Peters, R. J. M. Nolte, R. Brock and J. C. M. van Hest, Cellular Integration of an Enzyme-Loaded Polymersome Nanoreactor. *Angew. Chem., Int. Ed.*, **2010**, 49: 7213–7216

1.5 Riboflavin in nanotechnology

Riboflavin (Rfv), also known as vitamin B2, is a micronutrient with a key role in humans and animals health.
Historically, it was originally recognized in 1879 as a growth factor and named vitamin B2 according to the British nomenclature system. Successively, it was first isolated from egg whites in 1934 and synthesized in 1935.[1, 2]
As one of the family of B vitamins, riboflavin contributes to cellular growth, enzyme function, and energy production. It is a precursor of flavin mononucleotide (FMN) and flavin adenine dinucleotide (FAD) cofactors, and plays a key role in energy metabolism in eukaryotic cells.[3]
From a chemical point of view, Rfv is composed from a D-ribitol chain conjugated to the N10 position of an isoalloxazine moiety, which is responsible for electronic and optoelectronic properties, such as UV absorption, fluorescence, redox properties and photosensitivity.[3, 4] As a small molecule, Rfv has several functional groups that are amenable for covalent modifications,[5] even though it is insoluble in water and most of organic solvents.

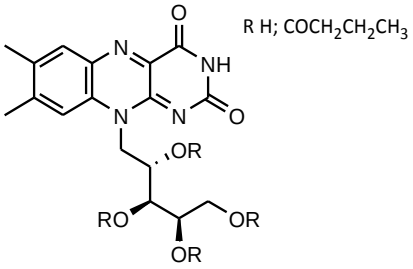

Riboflavin

Figure 13. Chemical structure of riboflavin (Rfv) and its tetrabutyrate detivative.

However, it is not synthesized *in situ*, and riboflavin intake is by food. In humans, after ingestion, three Rfv transporters (RFT) and carrier protein (RCP-Riboflavin Carrier Protein) mediate Rfv internalization.[6, 7] Moreover, overexpression of RCP was found in tumor tissues, in particular in the cases of breast,[8] prostate[9] and hepatocellular carcinoma.[10] Nevertheless, the interactions between Rfv and cancer cells is quite complex and the regulative mechanisms is not well clarified yet.
Thanks to these interesting peculiarities, a number of Rfv applications in nanotechnology have been recently investigated. In this respect, Rfv or its derivatives were utilized to decorate several nanosystems.
On this purpose, B.-C. Ye and collaborators exploit the feasibility of the synthesis of novel gold nanoclusters (AuNCs) using riboflavin as a stabilizer, due the

stronger complexing property absorbing on metal surfaces (i.e. gold, silver etc.) through the C=O and –NH group.[11] Even more, in the close 2016, F. Kiessling and co-workers evaluated the nucleotides AMP, ADP and ATP as spacers to stabilize FMN-targeted iron oxide nanoparticles.[12] Moreover, Thomas et al. conjugated Rfv to the fifth generation (G5) polyamidoamine (PAMAM) dendrimer *via* N3 nitrogen of the isoalloxazine ring (N(3)-conjugates) or primary alcohol of ribitol chain (N(10)-conjugates).[5]
In addition, our group have already developed a new nanohydrogel platform based on polysaccharides (Hyaluronan and Pullulan) modified with the hydrophobic Rfv tetrabutyrate, capable to induce self-assembling properties to the polysaccharide chains once chemically linked to such polymers.[13]
Furthermore, due to its fluorescence properties, the amount of Rfv derivatives in the nanomedicine could be easily quantified.

To date, the nano-conjugated Riboflavin systems are in the beginning of their investigation from researcher. However, use of Rfv in nanomedicine field could indeed represent a promising alternative, due to Rfv biocompatibility, low cost, versatile chemistry and specific transporter systems overexpressed in metabolically active cells.

References

(1) J. Spallholz J. The nutrients. 1. In: J. Spallholz, ed. *Nutrition: Chemistry and Biology.* Englewood Cliffs, NJ: Prentice Hill; **1989**: 65-68

(2) L. Moran, G. Scrimgeour. Coenzymes. In: L. Moran, G. Scrimgeour, R. Horton, et al, eds. *Biochemistry*. 2nd ed. Englewood Cliffs, NJ: Prentice Hall; **1994**; 8: 13-47

(3) Riboflavin. Monograph. *Altern. Med. Rev. J. Clin. Ther*., **2008**, 13: 334–340

(4) N. Beztsinna, M. Solé, N. Taib, I. Bestel, Bioengineered riboflavin in nanotechnology. *Biomaterials*, **2016**, 80: 121-133

(5) T. P. Thomas, S. K. Choi, M.-H. Li, A. Kotlyar, J. R. Baker Jr., Design of riboflavin-presenting PAMAM dendrimers as a new nanoplatform for cancer-targeted delivery. *Bioorg. Med. Chem. Lett.,* **2010***,* 20: 5191–5194

(6) Y.Yao, A. Yonezawa, H. Yoshimatsu, S. Masuda, T. Katsura, and K. I. Inui, Identification and comparative functional characterization of a new human riboflavin transporter hRFT3 expressed in the brain. *J. Nutr*., **2010**, 140: 1220–1226

(7) A. Yonezawa, and K. Inui, Novel riboflavin transporter family RFVT/SLC52 identification, nomenclature, functional characterization and genetic diseases of RFVT/SLC52. *Mol. Aspects Med*., **2013**, 34: 693–701

(8) J. Jayapaul, S. Arns, W. Lederle, T. Lammers, P. Comba, J. Gätjens, and F. Kiessling, Riboflavin carrier protein-targeted fluorescent USPIO for the assessment of vascular metabolism in tumors. *Biomaterials*, **2012**, 33: 8822–8829

(9) M. E. Mertens, J. Frese, D. A. Bölükbas, L. Hrdlicka, S. Golombek, S. Koch, P. Mela, S. Jockenhövel, F. Kiessling, and T. Lammers, FMN-coated fluorescent USPIO for cell labeling and non-invasive MR imaging in tissue engineering. *Theranostics*, **2014**, 4: 1002–1013

(10) H. Iida, M. Miki, S. Iwahana, & E. Yashima, Riboflavin-based fluorogenic sensor for chemo- and enantioselective detection of amine vapors. *Chem. Weinh. Bergstr. Ger.*, **2014**, 20: 4257–4262

(11) M. Zhang, H.-N. Le, X.-Q. Jiang, S.-M. Guo, H.-J. Yu, B.-C. Ye, A ratiometric fluorescent probe for sensitive, selective and reversible detection of copper (II) based on riboflavin-stabilized gold nanoclusters. *Talanta*, **2013**, 117: 399–404

(12) Y. Tsvetkova, N. Beztsinna, J. Jayapaul, M. Weiler, S. Arns, Y. Shi, T. Lammersa and F. Kiesslinga, Refinement of adsorptive coatings for fluorescent riboflavin-receptor-targeted iron oxide nanoparticles. *Contrast Media Mol. Imaging*, **2016**, 11: 47–54

(13) C. D. Meo, E. Montanari, L. Manzi, C. Villani, T. Coviello, P. Matricardi, Highly versatile nanohydrogel platform based onriboflavin-polysaccharide derivatives useful in the development ofintrinsically fluorescent and cytocompatible drug carriers. *Carbohydrate Polymers,* **2015**, 115: 502–509

1.6 Aim and outline of the thesis

As stated above, the development of Nano Drug Delivery Systems (NDDS) is a promising approach for developing intelligent therapeutic systems, which will bring significant advances in the diagnosis and treatment of disease, with the challenges to maximize therapeutic activity and to minimize undesirable side effects. The aim of this thesis was focused on the design of two kind of self-assembled nanocarrier for the delivery of hydrophobic drugs: Hyaluronan based nanohydrogel and pNIPAAm based micelles that both show hydrophobic internal domains and a surrounding hydrophilic shell.

To achieve such self-assembled nanostructures, amphiphilic polymers were synthesized and extensively characterized. Hyaluronan (HA) and the thermosensitive di-block copolymer of methoxy poly(ethylene glycol)-*b*-(*N*-isopropylacrylamide)-*co*-(2-azidoethyl) methacrylate (mPEG-*b*-p(NIPAAm)-*co*-AzEMA) constituted the starting polymers on which riboflavin 2',3',4',5'-tetrabutyrate (Rfv), due to its interesting chemical-physical proprieties and due to its particularly biocompatibility, was conjugated as hydrophobic moiety *via* azide-alkyne click chemistry reaction.

The HA-Prop derivatives were synthesized in order to provide the polymer of alkyne groups and make it versatile for “click” reaction. In this way, the azido-hexyl derivative of riboflavin tetrabutyrate was synthesized and covalently coupled to the propargyl derivative of hyaluronic acid by Copper(I)-catalyzed Azide-Alkyne Cycloaddition (CuAAC), due to the high efficacy and selectivity of this kind of reaction.

Sterile self-assembled NHs were obtained in one-step by thermal treatment in autoclave of the aqueous dispersion of the HA-*c*-Rfv polymers. Size and polydispersity of the obtained NHs resulted be influenced from the M_w and from the degrees of derivatization of the starting Hyaluronan.

Micellar nano-assemblies composed of thermosensitive amphiphilic block polymers were formed by heating the aqueous solutions of the resulting poly(NIPAAm) block copolymer, in order to obtain temporal control of the release of the encapsulated drugs. For this purpose, mPEG-*b*-p(NIPAAm)-*co*-AzEMA block copolymer was synthesized by free radical polymerization and subsequently, a propargyl derivative of riboflavin (Rfv-Prop) was synthesized and covalently coupled to the azide modified diblock copolymers by Copper(I)-catalyzed Azide-Alkyne Cycloaddition (CuAAC).

The nanosystems thus formed were intended to be used for the delivery of hydrophobic drugs, thus taking advantages of the lipophilic core represented by riboflavin. Moreover, the potential π-π stacking interactions between the aromatic rings of the riboflavin in the core of such nanocarriers, may bring more stable nanostructures able to provide increased loading capacity.

In **Chapter 2**
the synthesis and characterization of amphiphilic HA-*c*-Rfv derivatives are reported. The strategy used to obtain self-assembled NHs, based on the method to form and sterilize, in one step, using an autoclave, is described. The HA-*c*-Rfv NHs were loaded with hydrophobic drugs (i.e. piroxicam, dexamethasone and paclitaxel), and characterized in terms of loading efficiency, stability and physico-chemical properties.

In **Chapter 3**
the synthesis and characterization of a novel thermosensitive polymer, mPEG-*b*-p(NIPAAm)-*co*-AzEMA-Rfv, is described which forms polymeric micelles. Stability of micelles and drug loading capacity for paclitaxel (PTX) were studied. Moreover, we hypothesized that by exploiting the hydrophobic interactions and the potential π-π stacking interactions that might exist between the aromatic rings of riboflavin and the drugs molecule (containing aromatic rings as well) would affect loading and release of this drug from the micelles.

In **Chapter 4**
finally are summarized the results of the aforementioned chapters and the perspectives for the optimization of this promising Nano Drug Delivery Systems.

Chapter 2

Click Hyaluronan-Riboflavin based Nanohydrogels as Drug Delivery System

G. Manzi [a, b], N. Zoratto [a], S. Matano [a,b], T. Coviello [a], R. Sabia [a], C. Villani [a], W. E. Hennink [b], T. Vermonden [b], P. Matricardi [a], C. Di Meo [a]

[a] *Department of Drug Chemistry and Technology, ''Sapienza'' University of Rome, Rome, Italy*
[b] *Department of Pharmaceutics, Utrecht Institute for Pharmaceutical Sciences (UIPS), Utrecht University, Utrecht, The Netherlands*

ABSTRACT: Highly hydrophilic and biocompatible nanocarriers based on polysaccharide hydrogels (nanohydrogels, NHs) were shown to be promising systems for drug delivery applications. Inspired by these emerging and promising drug carriers for therapeutic applications, in this work we aimed to develop self-assembled hydrogel nanoparticles based on amphiphilic derivative of hyaluronic acid (HA). For this purpose, new HA-Riboflavin (HA-*c*-Rfv) derivatives were synthetized by "click" Copper(I)-catalyzed Azide-Alkyne Cycloaddition (CuAAC) reaction, requiring a previous HA derivatization with alkyne moieties and Riboflavin modification with azide groups. The resulting amphiphilic product was able to form nanohydrogels in aqueous environments by suitable treatments, in particular by an innovative method by using an autoclave cycle.

Various HA molecular weights (M_w) and derivatization degrees of the starting polymers have been used in order to assess the effect of different parameters on the NHs formation. The derivative HA^{220}-*c*-Rfv (M_w 220kDa, 40% of propargylic portions and 40% of Rfv moieties), was chosen as the most interesting NHs forming system; NHs were 150-200 nm in size and showed a ζ-potential in the range -40 / -50 mV, depending on the experimental conditions adopted. NHs resulted to be stable in water and at physiological pH. Moreover, by the addition of a suitable cryoprotectant, the NHs suspension can be freeze-dried and recovered by re-suspension in water.

The developed system is intended to be used for the delivery of hydrophobic drugs, such us dexamethasone, piroxicam and paclitaxel, used as model drugs. Drug encapsulations were performed by hydrating drugs film with polymers aqueous suspensions, followed by an autoclave treatment, resulting in a high encapsulation efficiency (EE%).

Moreover, the HA-propargyl backbone with 60% of propargylic portions and partially linked to Rfv, was capable to react with other molecules bearing an azide group, opening the route to a wide spectrum of functionalization opportunities: in this direction, PEG-N_3 have been tested as model molecule for the NHs.

Introduction

Hydrogels nanoparticles (also known as polymeric nanohydrogels (NHs)) have captured attention as one of the most promising nanostructured drug delivery systems, in terms of loading capacity, stability, release and targeting profile of several therapeutic and/or diagnostic agents.[1]

Such a nanoparticulate result very interesting and notable because of their unique physico-chemical properties that combine the characteristics of hydrogel systems (as the soft consistency, the high water content and the low interfacial tension with water and biological fluids) with a very small size (in the nano-scale). These unusual peculiarities make NHs more similar to living tissues than many other classes of synthetic nanosystems.[2]

Nanohydrogels prepared from natural polymers (including polysaccharides) offer several advantages and are non-toxic, generally biocompatible, and biodegradable (a must to avoid organ accumulation and other undesirable side effects). [3,4] On this purpose, a wide range of polysaccharides were already investigated such as pullulan,[5] chitosan,[6] alginate,[7] and hyaluronic acid.[8-10] They exhibit quite variable structures and properties, different reactive groups, a wide range of molecular weights and variable chemical composition. They can be easily derivatized with hydrophobic moieties to form amphiphilic polymers that spontaneously self-assemble in aqueous media, thus forming NHs.

Molecular self-assembly is defined as the autonomous organization of components into structurally well-defined aggregates, characterized by specific association of molecules through non-covalent interactions, including electrostatic and/or hydrophobic associations, in order to minimize the interfacial free energy.[11]

Inspired by these emerging and promising drug carriers for therapeutic applications, in this work we aimed to develop hydrogel nanoparticles formed by self-assembly based on an amphiphilic derivative of hyaluronic acid.

Among polysaccharides, hyaluronic acid (HA) seems to be one of the most interesting materials for the development of biocompatible drug carriers; it is one of the major components of the extracellular matrix (ECM) and is present at high concentrations in all connective tissues (cartilage, in the vitreous humor and in synovial fluids). Moreover, due to its capacity to interact with some cell receptors, HA plays an important role in cell proliferation, migration and differentiation.[12] Indeed, HA provides an active targeting to CD44 receptor, a transmembrane glycoprotein over-expressed on the surface of some cancer cells (e.g. solid tumors). In this regard, HA is a good candidate for systemic drug delivery applications. [8, 10, 13, 14]

From a chemical point of view, HA is a linear non-sulphated glycosaminoglycan composed of β-1, 4-linked disaccharide units of β-1, 3-linked D-glucuronic acid and *N*-acetyl-glucosamine. In physiological conditions, HA is in the form of a

sodium salt, therefore negatively charged and referred to as sodium hyaluronate. In these conditions, it is highly hydrophilic. HA can be modified in order to obtain materials with new physico-chemical and biological characteristics. The chemical modification of HA can be performed mainly on the two available functional sites: the carboxylic acid group and the hydroxyl groups.

Riboflavin (Rfv) (Vitamin B2) is an interesting molecule with important properties[15] such as biological activity as coenzyme for the flavoenzymes Flavin adenine dinucleotide (FAD) and Flavin mononucleotide (FMN).[16] Chemically, Riboflavin consists of an isoalloxazine ring responsible for the UV absorption, fluorescence, redox properties and photosensitivity.[15] It is widely distributed in nature and particularly biocompatible.

For this purpose, new HA derivatives were synthesized in order to provide the polymer of alkyne groups and make it versatile for "click" reaction. In this way, the azido-hexyl derivative of riboflavin tetrabutyrate was synthesized and covalently coupled to the propargyl derivative of hyaluronic acid by Copper(I)-catalyzed Azide-Alkyne Cycloaddition (CuAAC), due to the high efficacy and selectivity of this kind of reaction.[17-20]

The amphiphilic nature of the synthetized polymer hyaluronic acid-riboflavin (HA-*c*-Rfv) allowed the formation of NHs by macromolecular self-association. HA nanogels are composed of HA chains that are associated into three-dimensional soft nanomatrices. With their high water content, these HA nanogels are similar to macroscopic bulk hydrogel materials and thus belonging to soft drug delivery systems.

Different molecular weights (M_w) and different degrees of derivatization of the starting polymer have been investigated in order to study the effect of these two parameters on the NHs formation. Usually, self-assembled NHs are formed by bath-sonication in aqueous media,[8] or reverse nanoprecipitation process.[34]

In this case, NHs were formed by an innovative method based on the use of an autoclave sterilization cycle (121°C, 20 min 1.1 bar).[30] This method can thus lead, in a single step, the formation of sterile NHs. Moreover, during the same procedure, these nanoparticles can be loaded with hydrophilic and lipophilic drugs.[21] The obtained nanohydrogels were characterized in terms of size (DLS-analysis), ζ potential, and stability in different conditions.

The developed system is intended to be used for the delivery of hydrophobic drugs. The hydrophobic nature of such drugs is a serious hurdle in their efficient formulation and restricts their use in aqueous based solvents. With a view to overcome such limitations, several hydrophobic drugs-loaded nano-formulations were investigated and well described in literature.[23-28] In the present work, we described the synthesis of HA-*c*-Rfv derivative, the preparation of NHs and their loading hydrophobic drugs, having at least, one aromatic ring (such as piroxicam, dexamethasone and paclitaxel). We assumed that drug are accomodated in the lipophilic core (associated to riboflavin moieties), exploiting the hydrophobic

interactions and the π-π stacking interactions that might exist between the aromatic rings of riboflavin and the drugs molecules.[22]

Finally, surface-modification of delivery vehicles with polyethylene glycol (PEG) is usually adopted to improve the stability and *in vivo* performance of various drug and gene vectors. In addition, PEGylation has recently been shown to dramatically improve particle transport through biological barriers.[36-42]

For this purpose, on the polymers HA-*c*-Rfv with a excess of propargylic moieties still available for further conjugation, PEG-N_3 chains were coupled to NHs by azide/alkyne click reaction, in order to additionally improve such innovative and versatile nanocarriers.

2.2 Materials and Methods

2.2.1 Materials

Hyaluronan sodium salt (HANa) was provided by Contipro, Dolní Dobrouč, Czech Republic and it was modified in hyaluronan tetrabutylammonium salt (HATBA) form by using a Dowex cation exchange resin. Methoxypolyethylene glycol azide (PEG-N_3, number-average molar mass M_n = 2000 g mol^{-1}), sodium azide (NaN_3), 1,6-dibromohexane, sodium chloride (NaCl), propargyl bromide solution 80 wt. % in toluene (PropBr), anhydrous sodium sulfate (Na_2SO_4), sodium hydroxide (NaOH), ethylenediaminetetraacetic acid disodium salt dihydrate (EDTA), copper(II) sulfate ($CuSO_4$), L-ascorbic acid, potassium carbonate (K_2CO_3), potassium bromide (KBr), glycerol, dextrose, piroxicam (PIR) and dexamethasone (DEX), acetonitrile (ACN), dichloromethane (DCM), acetone, ethyl acetate, n-hexane, *N,N*-dimethylformamide (DMF), trifluoroacetic acid (TFA), ethanol (EtOH), and dimethyl sulfoxide (DMSO) were purchased from Sigma-Aldrich. Riboflavin tetrabutyrate was purchased from TCI Europe. Paclitaxel (PTX) was purchased from LC Laboratories (MA, U.S.A.). Simulated Intestinal Fluid without Enzyme (SIF) pH 7.4 buffer was prepared as following: NaH_2PO_4 H_2O 0.5243 g and Na_2HPO_4 2.2997 g in 200 ml of MilliQ water.

2.2.2 Synthesis of 2'3'4'5'- tetrabutyril-3-(6-azidohexyl) riboflavin ($RfvN_3$)

$RfvN_3$ derivative was synthesized in a two-steps synthesis. The first step provided the synthesis of 2'3'4'5'- tetrabutyril-3-(6-bromohexyl) riboflavin (RfvBr) derivative as described by C. Di Meo et al.[21] Briefly, 500 mg of 2'3'4'5'-tetrabutyrilriboflavin (0.761 mmol) were solubilized in 4.5 ml of dry DMF under N_2 atmosphere. Then 158 mg of K_2CO_3 (1.14 mmol) was added and the reaction was stirred for 45 min. Afterwards, 0.470 ml of a solution of 1,6-dibromohexane (0.74 g, 3.0 mmol) was added dropwise in 2.5 ml of DMF and the mixture was stirred for 5 h. The reaction was monitored by TLC (SiO_2, dichloromethane/ethyl acetate 4/1) and ESI-MS. The crude product was then purified first by liquid-liquid organic extraction, the product was collected in the organic phase, dried over Na_2SO_4 and the solvent was evaporated. The crude product was purified by open column chromatography (SiO_2 40-63 μm), and collected as yellow/orange fraction. (Yield ~ 50%) (Eluents: first elution n-hexane, then DCM/ethyl acetate 4/1).

^{1}H NMR ($CDCl_3$) δ (ppm) 8.04 (s, 1H), 7.57 (s, 1H), 5.70 (br s,1H), 5.47 (m, 2H), 4.91 (br s, 2H), 4.48 (d, 1H), 4.23 (dd, 1H), 4.07 (t, 2H), 3.40 (t, 2H), 2.57 (s, 3H), 2.46 (s, 3H), 2.30 (t, 2H), 2.07 (m, 1H), 1.86 (m, 3H), 1.74–1.60 (m, 10H), 1.66 (dd, 2H), 1.54–1.21 (m, 6H), 1.0 (q, 6H), 0.94 (t, 3H), 0.63 (t, 3H).

FT-IR (KBr) cm^{-1} 2964, 2936, 2874, 1745, 1663, 1550, 1158.

ESI–MS (+) m/z 821, 843 $[M + Na]^+$.

The azido-derivative of the riboflavin was synthetized by nucleophilic substitution of the terminal -Br of the RfvBr with an azido group. Briefly, 500 mg of 2'3'4'5'-tetrabutyril-3-(6-bromohexyl) riboflavin (0.61 mmol) and 198 mg of NaN_3 (3.05 mmol) were dissolved in DMF and left reacting under slow stirring for 6 hours. The reaction was monitored by ESI-MS. Then, DCM was added to the crude product and it was washed with brine for 5 times. The organic phases were dried over Na_2SO_4 and the pure product was collected as orange/red solid after solvent evaporation (Yield ~ 98%).

^{1}H NMR ($CDCl_3$) δ (ppm) 8.04 (s, 1H), 7.57 (s, 1H), 5.70 (br s,1H), 5.47 (m, 2H), 4.91 (br s, 2H), 4.48 (d, 1H), 4.23 (dd, 1H), 4.07 (t, 2H), 3.28 (t, 2H), 2.57(s, 3H), 2.46 (s, 3H), 2.30 (t, 2H), 2.07 (m, 1H), 1.74–1.60 (m, 10H), 1.66 (dd, 2H), 1.0 (q, 6H), 0.94 (t, 3H), 0.63 (t, 3H).

FT-IR (KBr) cm^{-1} 2964, 2936, 2874, 2100, 1745, 1663, 1550, 1158.

ESI–MS (+) m/z 782, 804 $[M + Na]^+$.

2.2.3 Synthesis of propargyl derivatives of Hyaluronan (HA-Prop)

HATBA was dissolved in DMSO until complete solubilization. Then, PropBr solution was added dropwise at the mixture in order to obtain the desired stoichiometric derivatization degree (mol Rfv/mol HA repeating units). The reaction was carried out for 40 h at room temperature under magnetic stirring, and purified by exhaustive dialysis against distilled water (Visking tubing, cut-off: 12-14 kDa); the final product HA-Prop was finally collected as white fluffy solid after freeze-drying (Yield ~ 90%).

^{1}H NMR (D_2O) δ (ppm) 4.78 (-CH_2C≡CH, s), 3.06 ($CH_3CH_2CH_2CH_2N^+$, t), 2.92 (-CH_2C≡C*H*, s), 1.87 (CH_3CONH-HA, s), 1.51 ($CH_3CH_2CH_2CH_2N^+$, m), 1.23 ($CH_3CH_2CH_2CH_2N^+$, m), 0.81 ($CH_3CH_2CH_2CH_2N^+$, t).

FT-IR ATR 3305, 2876, 1649, 1752, 1076

2.2.4 Hydrolysis reaction of the HA-prop derivative

HA-Prop derivative was dissolved in H_2O and NaOH 0.25 M at 40°C. Aliquots were withdrawn at different timeslots (2, 4, 6 and 20 h) and purified by dialysis against water from the propargyl alcohol formed after the cleavage of the ester bond. Next, the purified HA-Na obtained was freeze-dried and analyzed by ^{1}H NMR.

^{1}H NMR (D_2O) δ (ppm) 3.06 ($CH_3CH_2CH_2CH_2^*N^+$, t), 1.87 (CH_3^*CONH-HA, s), 1.51 ($CH_3CH_2CH_2^*CH_2N^+$, m), 1.23 ($CH_3CH_2^*CH_2CH_2N^+$, m), 0.81 ($CH_3^*CH_2CH_2CH_2N^+$, t).

2.2.5 Synthesis of HA-*c*-Rfv derivatives by *click-chemistry*

The HA-*c*-Rfv products were synthetized using HA-Prop and $RfvN_3$; the coupling was obtained by azido-alkyne "click chemistry" reaction.
HA with different M_w (57, 115, 220 and 280 kDa) were used to obtain different derivatization degree (feed propargyl percentage of 40, 60, 80 and 100%; feed riboflavin percentage of 20, 40, 50, 64 and 100 %); coupling reaction were carried out thus obtaining a set of products HA-*c*-Rfv.
In a typical reaction, the polymer HA-Prop was dissolved in a mixture of DMSO/H_2O 85/15; then, depending on the desired degree of substitution, the suitable amount of $RfvN_3$ previously dissolved in DMSO was added dropwise to the reaction mixture. $CuSO_4$ and ascorbic acid at the final concentration of 0.65 mg/ml were added to the mixture and the reaction was carried out at room temperature for 2 hours.
The products were then exhaustively dialyzed against a 10 mM EDTA solution, then against distilled water. Next, products purification was optimized by centrifugation (4000 rpm, 30 min). The products were finally collected as yellow fluffy solids after freeze-drying (Yield ~ 84-89 %).

2.2.6 HA derivatives characterization

The synthetized polymers were characterized by ^{1}H NMR (Agilent 400 MHz spectrometer), FT-IR ATR (PerkinElmer Spectrum 100 Optica FT-IR spectrometer), GPC (Viscotek 305 TDA) and UV-Vis spectroscopy (PerkinElmer LAMBDA 25 UV/Vis system).
^{1}HNMR spectra were recorded using Agilent 400 MHz spectrometer (Agilent Technologies, Santa Clara, California, US) using D_2O as solvent (solvent signal at 4.79 ppm) in order to obtain information about the derivatization degree of HA-Prop derivatives. The value of the signal of the methylene group of HA (–C=OCH_3, 1.87ppm) was normalized for 3 protons and used as reference signals. Based on this normalization, the signals of the propargylic protons (-CH_2-C≡C*H,* 2.90 ppm; -CH_2-C≡CH, 4.76 ppm) were integrated and the area under the curve, divided for

the respective numbers of protons that took place at the resonance process, gave information about the substitution degree of HA.
Molecular weight analysis and polydispersity index determination were conducted by GPC measurements. The Viscotek Triple Detector Array (TDA) incorporates RI, Light Scattering, Viscosity detectors. A universal calibration (running a single narrow standard of which all the parameters are known) was made in order calculate the detector constants and to correct for the inter-detector delay volumes, by using a Polyethylenglycol (PEO, 24 kDa) as narrow standard, and Dextran (73 kDa) as broad standard, for aqueous elutions; Pullulan (105 kDa) as narrow standard, and Dextran (73 kDa) as broad standard for DMSO elutions. Each synthesized polymer was filtered through a 0.2 μm syringe filter prior to analysis, and then injected at different concentrations (from 1 to 4 mg/ml) in order to obtain the proper dn/dc value, characteristic of each polymer. Eluents used were aqueous solution of $NaNO_3$ 0.1 M + NaN_3 0,01 % w/V for the elution of HA-TBA, and HA-Prop derivatives and DMSO for the HA-*c*-Rfv derivatives. The flow rate was 0.6 ml/min by three seral columns (TSK gel 13μm, 300x7.8, 100-1000 Å) at 35°C for the aqueous elutions; two seral columns (Phenogel 5μm, 300x7, 500 and 10^5 Å), at 60 °C for DMSO elutions. The GPC chromatograms were riealobrated by software to calculate the molecular weight (M_w), polydispersity index (PDI), intrinsic viscosity (IV), hydrodynamic radius (Rh), α and K of the Mark-Houwink equation.
The expected mass average molar mass or M_w of the polymers were calculated by the following equation:

$$Mw = \sum (MWHA\ repetitive\ unit + \%MW\ Prop + \%MW\ Rfv) * N°\ repetitve\ unts$$

FT-IR ATR spectra of the polymers were measured using a Spectrum 100 Optica FT-IR spectrometer (PerkinElmer, Waltham, Massachusetts, US) in ATR mode. A spectral resolution of 4 cm^{-1} with 64 co-added scans was used for collection of reference spectra over a spectral range of 4000–600 cm^{-1}.
UV-Vis spectra of the HA-*c*-Rfv derivatives were carried out using a LAMBDA 25 UV/Vis system (PerkinElmer, Waltham, Massachusetts, US). Bandwidth fixed at 1 nm, light source of deuterium and tungsten prealigned sources with automatic switch-over; wavelength range from 200 to 600 nm.
The calibration curve was established with $RfvN_3$ standards in a concentration range of 100-6.25 μg/ml in DMSO. Unknown samples were dissolved in DMSO at starting concentration of 1 mg/ml and diluted 5, 10 and 20 folds. Acquisition of the absorbance intensities were performed at 346 and 450 nm.

2.2.7 NHs formation and characterization

In a typical experiment, 3 mg of each derivative HA-*c*-Rfv were dispersed in 3 ml of distilled water (1 mg/ml) by overnight magnetic stirring at room temperature. The samples were then autoclaved for 20 min at 121 °C (Juno Liarre autoclave 230 Vac, 50/60 Hz, 12A, 2000 W), leading to NHs formation.[30] The recovered NHs suspensions were then analyzed in terms of size and polidispersity index (PDI) by dynamic light scattering (DLS) using Submicron Particle Sizer Autodilute Model 370 (Nicomp). The ζ-potential was measured with a DLS Malvern NanoZetaSizer apparatus (Malvern Instruments, Worcestershire, United Kingdom), equipped with a 5 mW HeNe laser (k = 632.8 nm). Normalized intensity autocorrelation functions were detected at a 90 ° angle by a logarithmic digital correlator and analyzed by Contin algorithm.
Stability studies of HA-*c*-Rfv NHs suspensions, prepared as above described, were carried out by monitoring the size and PDI values of NHs in water at 4 °C for 72 days, and at 37 °C in glycerol/Simulated Intestinal Fluids (SIF) (pH 7.4) media for 48 hours.

2.2.8 Hydrophobic model drugs loading in HA-*c*-Rfv NHs

Piroxicam (water solubility 23 μg/ml at 22 °C, logP 3.06), dexamethasone (water solubility 89 μg/ml at 25 °C, logP 1.83) and paclitaxel (water solubility 5.56 μg/ml, logP 3.54) were chosen as model drugs.[35]
In a typical preparation, a drug thin film was formed in a vial by evaporating under vacuum 0.5 ml of a drug solution in acetone (2 mg/ml). Next, a polymeric aqueous suspension (1 mg/ml, 3 ml), was added in the vial and stirred for 1 h to hydrate the drug film. The system was then autoclaved in order to form, in one-step, drug-loaded NHs.[30] The non-encapsulated drug was removed by centrifugation (3000 g, 10 min), the pellet was then dissolved in ACN or EtOH and analyzed by HPLC in order to evaluate the amount of un-loaded drug. The drug-loaded NHs dispersions were analyzed in term of size by DLS measurement while the amount of the different drugs loaded in the NHs were evaluated by isocratic HPLC chromatography, using a Eurospher II C18 (5 μm, 4.6x250 mm) column. The eluents used at flow rate 1 ml/min were: a mixture of ACN/water (50/50) + TFA 0.1% V/V for the elution of piroxicam, a mixture of ACN/water (50/50) for the elution of dexamethasone, and a mixture of ACN/water (60/40) + TFA 0.1% V/V for the elution of paclitaxel. The detection was performed by UV detector at 356 nm for piroxicam, 239 nm for dexamethasone, and 227 nm for paclitaxel. Samples of drugs in EtOH in a concentration range from 2 to 250 μg/ml were used as standards for the calibration.
Encapsulation Efficiency (EE) and Drug Loading (DL) were calculated from the HPLC analysis data, based on these equations:

$$\%EE = \frac{concentration\ of\ drug\ loaded}{concentration\ of\ drug\ added}\ x\ 100$$

$$\%DL = \frac{concentration\ of\ drug\ loaded}{concentration\ of\ drug\ loaded + polymer\ concentration}\ x\ 100$$

Stability studies of drug-loaded NHs suspensions, prepared as above described, were carried out by monitoring the size and PDI of NHs in water at 4 °C for at least 50 days.

2.2.9 Drug-loaded NHs freeze-drying

Purified drug-loaded NHs suspensions were added of a dextrose solution (10% w/V) in order to obtain a final concentration of 1% w/V of cryoprotectant. The samples were frozen in liquid nitrogen and freeze-dried. The recovered drug-loaded NHs powders were then suspended in water and their size and PDI were assessed by DLS analysis.

2.2.10 PEG-N_3 conjugation to HA-*c*-Rfv by *click chemistry* reaction and PEG-NHs formation

PEG-HA^{220}-*c*-Rfv 60-40 was synthetized starting from the derivative HA^{220}-*c*-Rfv 60-40; the coupling was carried out by using azido-alkyne click chemistry reaction. HA 220 kDa of M_w, with 60% of propargyl derivatization degree and 40% of riboflavin percentage, was dissolved in a mixture of DMSO/H_2O 85/15. Then, an excess of PEG-N_3 previously dissolved in DMSO was added dropwise at the reaction. $CuSO_4$ and ascorbic acid at the final concentration of 0.65 mg/ml were added at the mixture and the reaction was carried out in dark, at room temperature for 4 hours. The product was then exhaustively dialyzed against a 10 mM EDTA solution overnight, and next against distilled water. Finally, the product was collected as yellow fluffy solids after freeze-drying (Yield ~ 80 %).
PEGhylated NHs based on PEG-HA^{220}-*c*-Rfv derivative were formed as previously described in aqueous suspension (1 mg/ml and 2 mg/ml) and analyzed in terms of size, PDI and ζ-potential as described in 2.2.7.

^{1}H NMR (D_2O) δ (ppm) 3.57 ($CH_3OC\mathit{H_2}C\mathit{H_2}$, br, PEG), 1.88 ($C\mathit{H_3}CONH$-HA, s).

2.3 Results and Discussion

2.3.1 Synthesis of 2'3'4'5'- tetrabutyril-3-(6-azidohexyl) riboflavin ($RfvN_3$)

In the synthesis of $RfvN_3$ derivative, the first step was the preparation of the 2'3'4'5'- tetrabutyril-3-(6-bromohexyl) riboflavin (RfvBr) derivative, as described by C. Di Meo et al.[21] Next, the conversion of the 6-bromohexyl to 6-azidohexyl-riboflavin derivative was carried out by a nucleophilic substitution of the Br with an azido group, using a large excess of NaN_3, as shown in the Scheme 1.

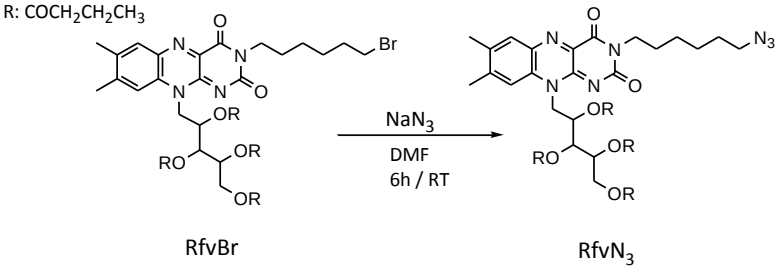

Scheme 1. Conversion of 2'3'4'5'- tetrabutyril-3-(6-bromohexyl) riboflavin (RfvBr) to 6-azidohexyl-riboflavin derivative ($RfvN_3$).

$RfvN_3$ was obtained in a high yield (~98%) and its structure was confirmed by ^1H NMR analysis (Figure 1A). The overlapped spectra of the RfvBr and the $RfvN_3$ derivative clearly show the shift from 3.4 ppm (-C*H*$_2$Br) to 3.2 ppm (-C*H*$_2$N$_3$) of the signal of the methylene group adjacent to the nucleophilic terminal substituent.
RfvBr and $RfvN_3$ were analyzed by FT-IR spectroscopy (Figure 1B). Comparing the two spectra, the strong asymmetric vibration (N≡N asymmetric stretching absorption) at 2100 cm^{-1} confirmed the chemical structure of the $RfvN_3$ derivative.

A) ***B)***

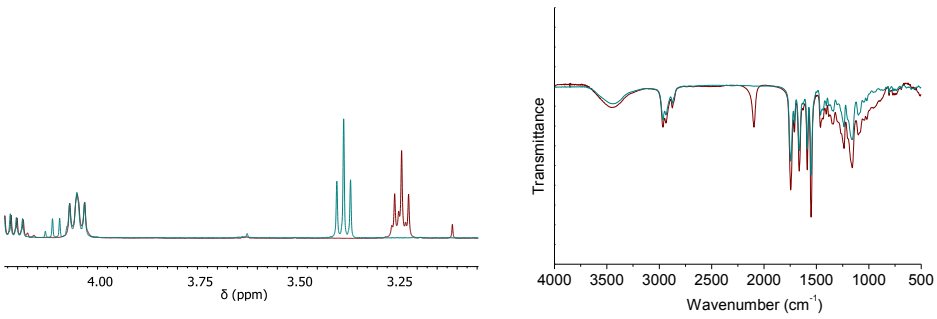

Figure 1. (A) ^1H NMR spectra in $CDCl_3$ of RfvBr (in green) and $RfvN_3$ (in red). The area of resonances of methylenes near to the nucleophilic terminal substituent is evidenced. **(B)** FT-IR spectra of RfvBr (in green) and $RfvN_3$ (in red). The asymmetric vibration at 2100 cm^{-1} is evidenced in the azido-derivative.

2.3.2 Synthesis of propargyl derivatives of hyaluronan (HA-Prop)

In this work, several coupling reactions were carried out starting from HA with different M_w (57, 115, 220 and 280 kDa), using various feed ratio, to reach the aimed substitution degrees (Table 2).
Polysaccharides can be easily derivatized with small molecules in order to modify their physico-chemical properties, and in particular, their solubility and gelling ability.[33]
In the present case, to obtain polymer chains able to couple with $RfvN_3$ via click chemistry reaction, HA carboxylic groups were esterified with alkyne moieties (Scheme 2).

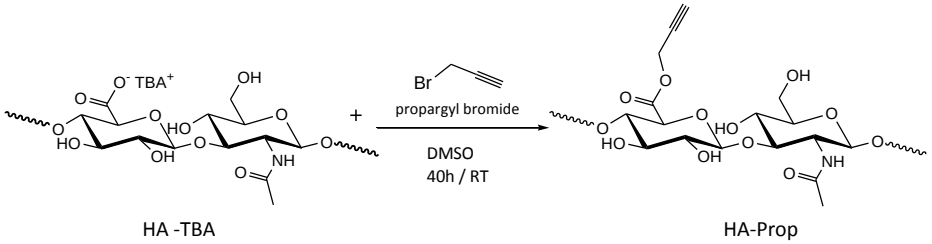

Scheme 2. Synthesis of HA-Prop ester derivative from HA TBA salt and propargyl bromide.

As well known, the nucleophilic substitution reaction needs a polar aprotic environment, avoiding water as solvent: for this reason, the tetrabutylammonium (TBA^+) salt of HA, soluble in DMSO, [22] was used as starting polymer; PropBr was used as alkyne moiety donor for esterification on the polymer carboxylic groups. The amount of the PropBr was modulated proportionally to the desired stoichiometric derivatization degree (mol PropBr/mol HA repeating units). The reaction was carried out at room temperature for 40 h, purified by extensive dialysis and the white solid product was recovered by freeze-drying in high yield (~ 90%).
Exploiting the above described synthesis, various HA-Prop substrates, with degree of substitution (DS) of Prop ranging from 40 to 80%, were prepared, using various feed ratio of Prop to HA.
HA-Prop products were analyzed by ^1H NMR spectroscopy (Figure 2) in order to evaluate the degree of functionalization.

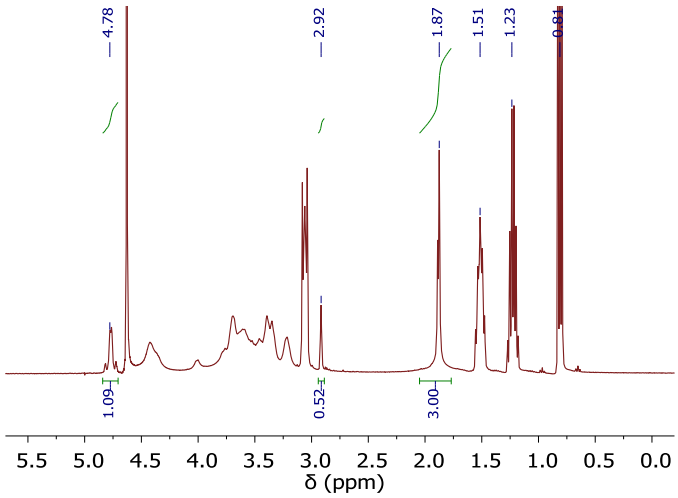

Figure 2.[1]H NMR spectra of HA-Prop 53% (57 kDa) in D_2O.

The spectra showed the signal at 1.87 ppm relative to acetamido moiety of the *N*-acetyl-D-glucosamine residue of HA, that was normalized for 3 protons and used as reference signals. The signal at 2.92 ppm is relative to the terminal proton of the alkyne portion (-$CH_2C{\equiv}C\mathit{H}$), and the signal at 4.78 ppm is related to the 2 protons of the propargyl substituent in α to the triple bond (-$C\mathit{H}_2C{\equiv}CH$). The degree of modification was determined by comparison of the integration of these signals, divided for the respective numbers of protons that took place at the resonance process. In this shown spectra (Figure 2), the resulted derivatization degree, based on this calculation, was 53% mol/mol (mol of Prop/mol HA repeating unit).

Moreover, to confirm that the HA substitution with PropBr resulted in esterification of carboxylic groups instead of the etherification of the hydroxyl groups, a typical hydrolysis of esters under mild basic conditions was carried out, since ether bond cleavage is only possible under strongly acidic or extremely basic conditions. Aliquots at different time slots (2, 4, 6 and 20 h) were analyzed by ^{1}H NMR in order to monitor and verify the ongoing status of the hydrolysis reaction by the disappearance of the signals of the propargylic portion (2.92 ppm -$CH_2C{\equiv}C\mathit{H}$, 4.78 ppm -$C\mathit{H}_2C{\equiv}CH$).

As shown in Figure 3, already after only 2h of reaction, the two signals of the alkyne portion of the starting material HA-Prop 53% (57 kDa) were not present in the spectra, indicating a complete hydrolysis of the ester.

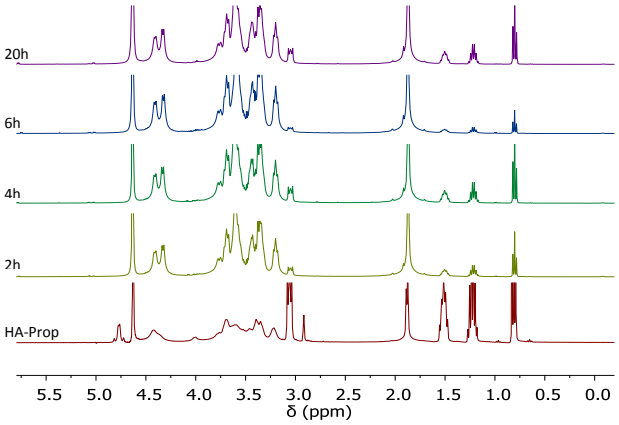

Figure 3. ^{1}H NMR spectra in D_2O, overlap of HA-Prop 53% (57 kDa) and aliquots at 2, 4, 6 and 20 h of the hydrolyzed HA-Prop.

To further confirm the above described results, infrared spectra of the polymers HA-Prop were recorded (Figure 4). The spectra showed a strong stretching absorption at 1752 cm^{-1} due to the C=O of the ester groups.

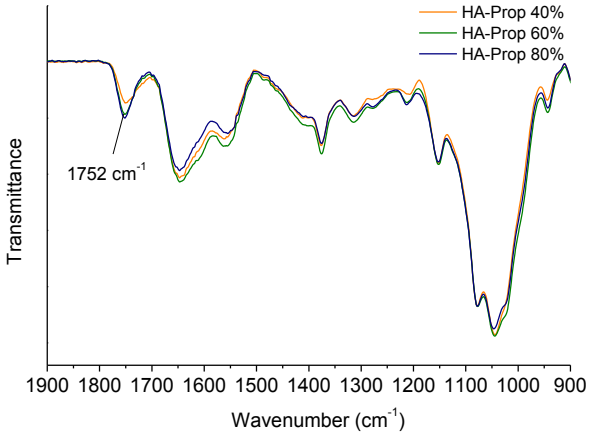

Figure 4. FT-IR spectra in of HA^{220}-Prop, overlap of different derivatization degrees: HA-Prop 40% (in orange), HA-Prop 60% (in green) and HA-Prop 80% (in blue).

In Table 2, the characteristics of the prepared HA-prop samples are summarized. It is worth noticing that, when the feed ratio was higher than 60 % mol/mol, the resulting conjugates were insoluble in water because of their hydrophobicity due to the excess amount of conjugated Prop. Since the self-assembled hydrogel nanoparticles are formed based on an appropriate balance of hydrophilicity and hydrophobicity, the water-insoluble conjugates that might have high DS (>60) were no longer investigated in this study.

2.3.3 Synthesis of Hyaluronan-Riboflavin derivative by click reaction (HA-*c*-Rfv)

The azidohexyl-riboflavin derivative was linked to HA modified chains, in order to remarkably change the water solubility of the polysaccharide.
In this work, we proposed a coupling reaction of the $RfvN_3$ derivative to the HA-Prop polymers by azide-alkyne Huisgen 1,3-dipolar cycloaddition c*lick-chemistry* reaction using $CuSO_4$/ascorbic acid as catalysts (Scheme 3).

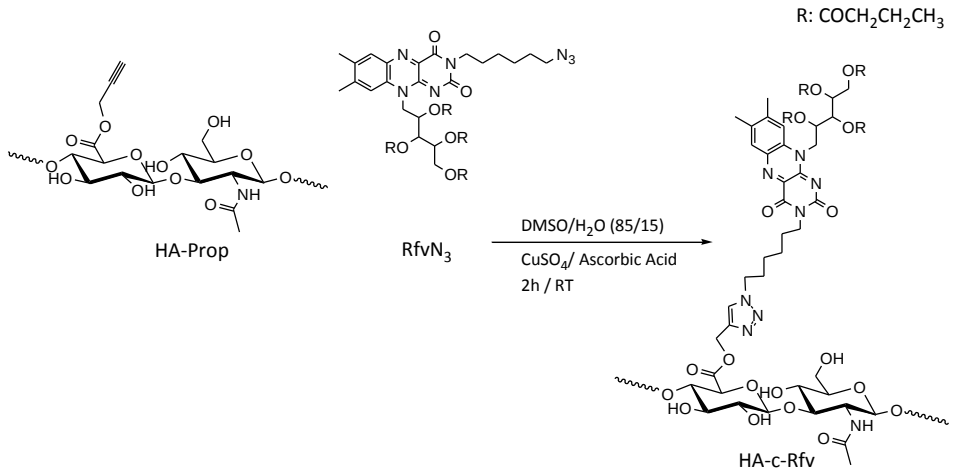

Scheme 3. Click reaction between HA-Prop polymer and $RfvN_3$.

In a typical reaction, the quantity of $RfvN_3$ was modulated proportionally to the desired stoichiometric derivatization degree (mol Rfv/mol HA repeating units). $CuSO_4$ and ascorbic acid were used as catalysts to yield Cu^+ *in situ*. Further, a dialysis against EDTA solution was used to purify the polymer, complexing the Cu^+ ions.
With the aim to purify the product from the un-coupled riboflavin still remained after the following extensive dialysis against water, a cycle of mild centrifugation (4000 rpm, 30 min) on the aqueous suspension of the polymer was performed: in this way: due to its very low water solubility, the free riboflavin tetrabutyrate was separated as pellet.
The yellow polymer obtained by freeze-drying was analyzed by FT-IR ATR in order to verify the disappearance of the azide absorption frequency at 2100 cm^{-1}, thus monitoring the outcome of the reaction and of the purification process.
FT-IR spectra reported in Figure 5A and 5B, clearly show the disappearance of the N≡N strong asymmetric stretching absorption at 2100 cm^{-1}, relative to the excess of $RfvN_3$ still remained after dialysis, together with the reduction (in terms of intensity) of the band at 1744 cm^{-1} relative to strong stretching C=O absorption of the ester bonds of the riboflavin tetrabutyrate. A very pure final polymer (HA-*c*-

Rfv) was thus obtained, concluding that the chosen purification process resulted successful.

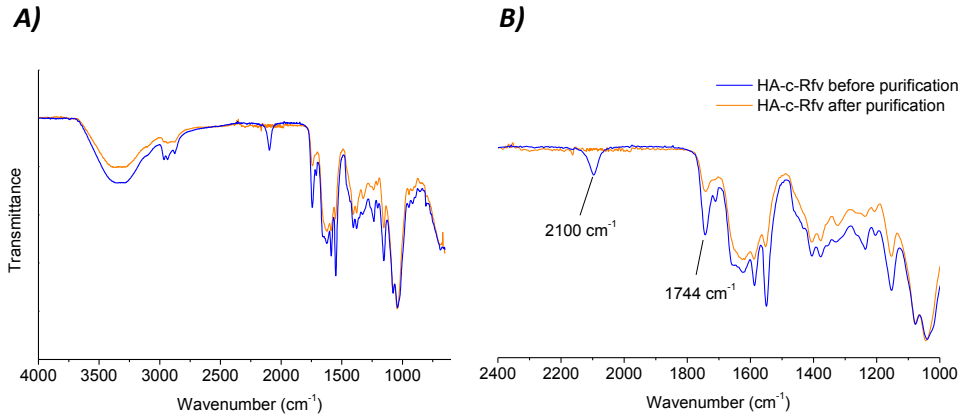

Figure 5. FTIR-ATR whole **(A)** and zoomed-in **(B)** spectra of HA-*c*-Rfv before (blue) and after (orange) purification by centrifugation.

In order to quantify the amount of $RfvN_3$ coupled to the polymers, several analyses were performed. ^1H NMR in solution and HR-MAS NMR on the swollen solid product did not allow to obtain spectra useful for the identification of the aromatic signals of riboflavin in the down field region, probably because of the rigidity of the molecule and/or the strong hydrophobic interactions.
From UV-Vis spectroscopy analysis carried out as described in 2.2.6 it was possible obtain a right quantification of the riboflavin bonded to the polymers. In particular, the analysis was performed with dual detection (at 346 and 450 nm, corresponding to the characteristic wavelengths of Rfv absorptions), and the ratio between the mol of $RfvN_3$ (related to the absorbance values obtained) and the mol of the relative HA-Prop derivative on which Rfv was coupled, was considered the derivatization degree.
In table 2 the characteristics of the prepared HA-*c*-Rfv derivatives are summarized.

2.3.4 Molecular weight characterization of HA derivatives

GPC analysis was carried out in order to collect information about the fate of the molecular weight and molecular weight distribution during the synthetic steps. In particular, in this work, GPC Viscotek 305 TDA analysis was performed. When GPC is coupled with light scattering, viscometer and concentration detectors (known as triple detection), it can measure absolute molecular weight (M_w), hydrodynamic radius (Rh) and intrinsic viscosity (IV), and generate information on macromolecular structure, conformation, aggregation and branching.
From the elution of HA^{220}-TBA, HA^{220}-Prop 40 and 60% in ionic strength buffered aqueous eluent, and of HA^{220}-*c*-Rfv 40/40 and HA^{220}-*c*-Rfv 60/40 in DMSO, information about the M_w of the synthesized polymers were obtained (Table 1).

Table 1. Summary of the GPC data of the analyzed HA derivatives in terms of molecular weight (M_w), refractive index (dn/dc), polydispersity index (PDI), intrinsic viscosity (IV), hydrodynamic radius (Rh), α and K of the Mark-Houwink equation.

	M_w expected (kDa)	M_w by GPC (kDa)	dn/dc	PDI	IV (dl/g)	Rh (nm)	α	logK
HA-TBA [a, b]	340	347	0.1024	1.6	3.81	26.4	0.838	-4.042
HA-Prop 40% [b]	296	270	0.1280	4.1	3.35	22.7	0.676	-3.105
HA-Prop 60% [b]	293	315	0.1280	4.1	3.15	22.9	0.608	-2.781
HA-*c*-Rfv 40/40 [c]	395	209	0.0389	1.3	0.54	11.8	0.701	-3.981
HA-*c*-Rfv 60/40 [c]	397	523	0.0389	1.5	0.55	15.6	0.574	-3.499

a. HA of 220 kDa, relative to the $HANa^+$ salt
b. Elution performed in aqueous solution of $NaNO_3$ 0.1 M + NaN_3 0,01 % w/V
c. Elution performed in DMSO

The first synthetic step provided the derivatization of the starting HA-TBA with a propargylic portion by an esterification of HA carboxylic groups. Looking at the M_w of the HA-Prop 40 and 60% obtained (270 and 315 kDa respectively), that resulted very close by the M_w expected (296 and 293 kDa respectively, calculated as described in 2.6), we might conclude that this synthetic step did not affect the structure and the molecular weight distribution of the starting polysaccharide.
The second synthetic step was the "click" coupling (Cu^+-catalyzed) of the azidohexyl-derivative of riboflavin on the propargylic-HA derivatives. From the elution of the resulting HA-*c*-Rfv in DMSO, no clear results in terms of M_w of the analyzed polymers were obtained (i.e. 209 kDa for the HA-*c*-Rfv 40/40 derivative, and 523 kDa for the HA-*c*-Rfv 60/40 derivative). These results let us conclude that DMSO may be not a good solvent for such derivatives, and further investigation is needed.
This hypothesis can be supported by the IV values obtained, that resulted very low for the Rfv-derivatized polymers (0.54 and 0.55 for the HA-*c*-Rfv 40/40 and HA-*c*-Rfv 60/40 respectively), suggesting a very closed disposition of the polymer chains

in DMSO. It has to be noticed that after the "click" coupling with $RfvN_3$, a purification step with EDTA is necessary to purify from the Cu^+ ions. The EDTA used in this work was the disodium salt dehydrate form, meaning that after the dialysis against EDTA solution, the less not derivatized HA-carboxylic groups were converted in Na^+ salts, resulting in an HA form less soluble in dipolar aprotic solvents such as DMSO.
The α values of the Mark-Houwink equation, reported in Table 2, decreased by derivatization of HA with Prop, suggesting that polymers become more flexible. This phenomenon can be explained by the fact that the derivatization of HA-carboxylic groups reduced the charge density along the polymer chains, thus improving the flexibility of the polymer chains.

2.3.5 Empty NHs preparation

NHs can be easily obtained from HA-*c*-Rfv derivatives. It has been demonstrated that HA derivatized with hydrophobic moieties, in aqueous media is able to spontaneously self-assemble in NHs,[21,22,29] with the aim of minimizing the interfacial free energy of the whole system. A new method to obtain NHs was tested, i.e. the autoclaving process, already used for the preparation of HA-cholesterol and gellan-cholesterol[24] sterile NHs suspensions. In this case, HA-*c*-Rfv suspended in water can be autoclaved to generate spontaneously NHs by self-assembling of the polymer chains. The high temperature seems to be able to promote the interactions between hydrophobic moieties linked to the polymer chains (inter- and intramolecular interactions as well), thus forming sterile nanoparticulate suspensions. NHs were prepared by treating the water suspension of the all the synthetized polymers HA-*c*-Rfv (1 mg/ml) for 20 min at 121°C, 1.1 bar, and characterized in terms of size by DLS analysis (Table 2).

All the synthetized polymers were characterized in terms of degree of substitution (DS) obtained with the Prop by ^1H NMR analysis, $RfvN_3$ portions by UV-Vis spectroscopy, and in terms of the ability to form self-assembled NHs by DLS measurements.

In table 2, the obtained results are summarized:

Table 2. Summary of the HA-*c*-Rfv polymers synthesized in terms of HA M_w, feed and experimental coupling of Prop (mol Prop/mol HA repeating units) and Rfv (mol Rfv/mol HA repeating units), and the relative dimensions of NHs obtained from these polymers.

HA-TBA (M_w)	%Prop		%Rfv		NHs Z_{ave} (nm)	PDI
	Feed	by NMR	Feed	by UV-Vis	by DLS	
57 kDa	64	53	excess	-	no NHs	-
	64	55	63	-	no NHs	-
	64	55	54	-	no NHs	-
115 kDa	100	93	20	-	no NHs	-
	80	60	50	-	no NHs	-
220 kDa	40	39	40	35	162 ± 10	0.20 ± 0.05
	60	56	40	39	232 ± 5	0.20 ± 0.03
	80	61	-	-	-	-
280 kDa	40	40	25	-	250 ± 30	0.40 ± 0.03
	40	40	40	-	160 ± 20	0.50 ± 0.02
	40	40	50	-	320 ± 20	0.50 ± 0.05
	60	54	25	-	230 ± 30	0.30 ± 0.13
	60	54	40	-	280 ± 20	0.50 ± 0.22
	80	-	-	-	-	-

The data summarized in Table 2 suggest that the HA derivatization with propargylic portion was always a good strategy to easily modify the polymer chains and obtain a derivative in high yield and with a good derivatization degree (related to the feed), ranging in the error of 10%. The coupling with $RfvN_3$ by click chemistry, as expected, resulted in quantitative derivatization, due to the high efficacy and selectivity of this kind of reaction.[17-20]

Moreover, we can observe that both HA M_W and the degree of functionalization with Prop and Rfv affected NHs formation and size. In particular, the HA-*c*-Rfv derivatives obtained from HATBA with M_w of 57 and 115 kDa (HA^{57}-*c*-Rfv and HA^{115}-*c*-Rfv, respectively), did not form NHs: in general, the physical self-assembly of amphiphilic polymers depends on the hydrophobicity/hydrophilicity balance of the portions of the polymers, as well as their M_w and chemical characteristics of the hydrophobic portions. Based on these considerations, it can be concluded that these polymers with relatively low M_w, even after derivatization, had a residual high hydrophilic character portion not balanced by the hydrophobic contribution of Rfv, resulting in water-soluble polymers. On the other hand, the HA^{220}-*c*-Rfv and HA^{280}-*c*-Rfv derivatives (obtained from HATBA with M_w of 220 kDa and 280, respectively), were able to form NHs with good dimensions and PDI, except for those with a Prop DS of 80% that resulted already water-insoluble; however, the

NHs obtained with the HA^{280}-*c*-Rfv derivatives presented higher PDI than those formed with HA^{220}-*c*-Rfv.
For this reason, the HA^{220}-*c*-Rfv derivatives were chosen for further investigations as NHs constituents for drug delivery applications.

2.3.6 Stability studies and drug-loaded NHs preparation

Empty NHs obtained from the selected HA^{220}-*c*-Rfv 40/40 derivative showed a size of 162 ± 10 nm, a PDI of 0.20 ± 0.05 and a ζ-potential of about −50 mV.
The stability of the HA^{220}-*c*-Rfv 40/40 suspensions was investigated in water at 4°C and NHs were stable for more than two months, whereas at 37°C in glycerol/Simulated Intestinal Fluids (SIF) (pH 7.4) media, NHs resulted stable for 48 h, at least (Figure 6).

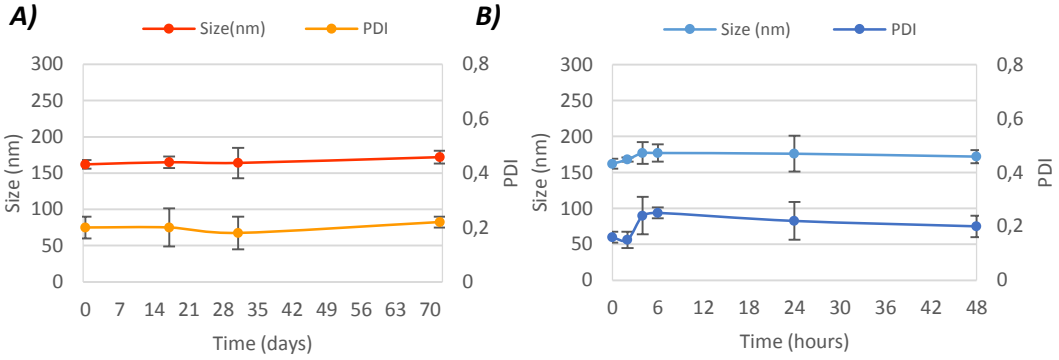

Figure 6. Average dimensions of empty HA^{220}-c-Rfv 40/40 NHs as a function of time at 1 mg/ml (A) in water at 4°C, (B) in glycerol/Simulated Intestinal Fluids (SIF) (pH 7.4) media at 37°C. Data points are average values. Error bars indicate standard deviations (n=3).

It is important to notice that HA^{220}-*c*-Rfv 40/40 NHs were stable in physiological conditions while in the case of NHs previously prepared with HA-cholesterol derivatives aggregation occurred in few hours.[8] This property represents a significant advantage of the new polysaccharide-Rfv NHs for their potential use in the field of pharmaceutics and biomedicine.

In order to test the drug carrier properties of the new NHs developed, HA^{220}-*c*-Rfv 40/40 NHs were loaded with different hydrophobic model drugs. Piroxicam, a non-steroidal anti-inflammatory drug (NSAID), dexamethasone, a type of steroid medication, and paclitaxel, an anticancer drug, were chosen as model drugs. The autoclaving process was exploited allowing the formation of NHs and the loading of these drugs in one step.[32] This methodology allow the loading of hydrophobic drugs by the solvent-casting technique.

Dispersions of drugs-loaded NHs of HA^{220}-*c*-Rfv 40/40 prepared at polymer/drug ratio of 3/1 (feed loading concentration of 25%), resulted to be opalescent and homogeneous.
After purification, the NHs dispersions were analyzed in term of size by DLS measurement (Table 3).

Table 3. Z-average size of empty and drug-loaded NHs.

Z_{ave} ± SD*	Empty NHs	PIR-loaded NHs	DEX-loaded NHs	PTX-loaded NHs
HA^{220}-Prop-Rfv 4040	162 ± 10 nm	168 ± 22 nm	171 ± 9 nm	176 ± 8 nm

*(pol. Conc. 1mg/ml in H_20)

After removing the non-encapsulated drugs by mild centrifugation, the Encapsulation Efficiency (EE%) and Drug Loading (DL%) were calculated for all the drugs tested, indicating that HA^{220}-*c*-Rfv 40/40 NHs are suitable systems for loading and carrying hydrophobic drugs. In detail, as shown in Figure 7, for the HA^{220}-*c*-Rfv 40/40 based NHs, EE% values of 82 ± 8, 84 ± 6 and 42 ± 4 % were obtained for the PIR, DEX and PTX-loaded NHs respectively. The collected data in terms of DL% values resulted be 21 ± 1, 22 ± 2 and 12 ± 1 %, all relative to the 25% PIR, DEX and PTX respectively feed loading, confirming that these NHs act as solubility enhancers, increasing the solubility of poorly water soluble drugs, when loaded in such aggregated structures.

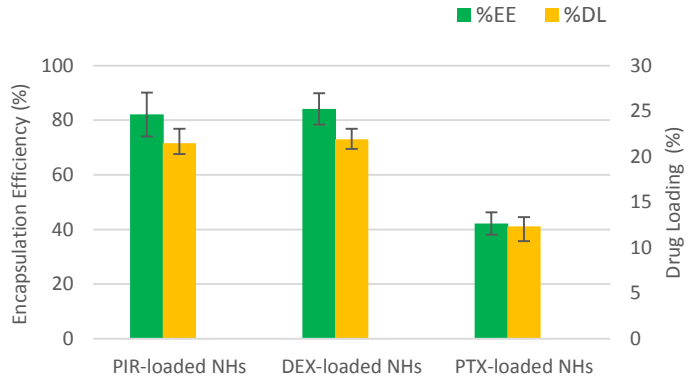

Figure 7. Encapsulation Efficiency (EE%) and Drug Loading (DL%) of Piroxicam, Dexamethasone and Paclitaxel -loaded NHs.

As reported in literature,[35] the water solubility values of the tested drugs are 23, 89 and 5.56 μg/ml for PIR, DEX and PTX respectively. Based on our analysis, the reached concentration of these drugs loaded into our NHs resulted be 274, 280

and 141 μg/ml, meaning an increase of the apparent water solubility of 12, 3 and 25-fold respectively.
Additionally, as shown in Figure 8, the storage at 4°C of these drug-loaded formulations resulted in stable formulation for at least two months.

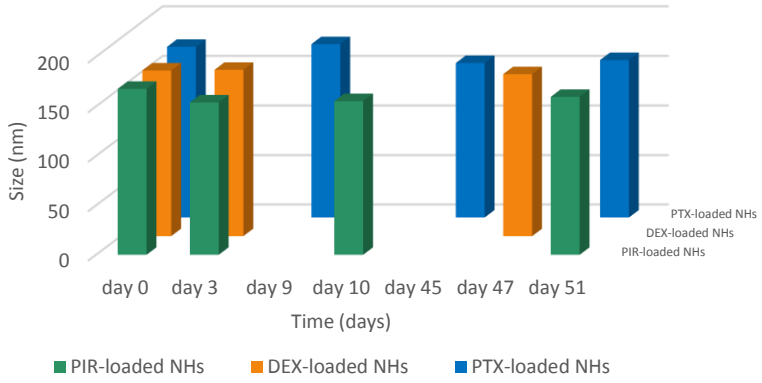

Figure 8. Average dimensions of PIR-loaded (in green), DEX-loaded (in orange) and PTX-loaded NHs (in blue) as function of the time, in water at 4 °C. Samples were analyzed in triplicate with standard deviation values lower than 10%.

Moreover, in order to obtain a long-life preparation of NHs, thus improving the industrial appeal of such systems, a cryoprotectant solution (1 % w/V dextrose) was added to the drug-loaded NHs, due to the fact that cryoprotection with sugars significantly enhanced the ability to re-suspend nanoparticles after freeze-drying without aggregation. The so formed sterile NHs were then freeze-dried and stored for several months. The Figure 9 shows that the drug-loaded systems developed in this work resulted to be stable at freeze-drying process and subsequent re-hydration.

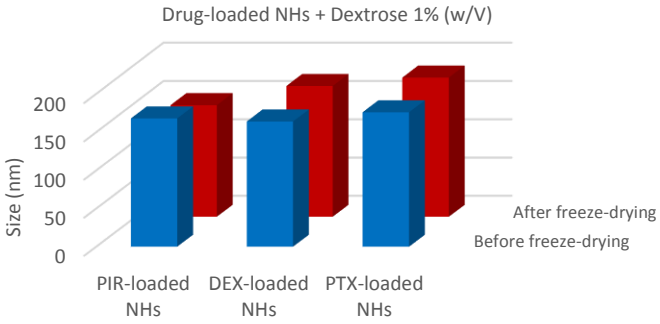

Figure 9. Average dimensions of drugs-loaded NHs as a function of time before (in blue) and after (in red) freeze-drying and re-hydratation. Samples were analyzed in triplicate with standard deviation values lower than 10%.

Finally, with the aim to have a prolonged blood circulation of these nanostructures, a PEG-HA^{220}-*c*-Rfv 60/40 product was synthetized as described in 2.10, from the previous derivative HA^{220}-*c*-Rfv 60/40 (60% of substitution degree with Prop moieties and 40% of Rfv coupling on it). This polymer presented less than 20% of propargylic moieties that we used to couple a PEG-N_3 *via* azide/alkyne click chemistry reaction.
NHs of the PEGylated derivative were obtained and analyzed in terms of size and ζ-potential.
PEG-HA^{220}-*c*-Rfv 60/40 based NHs (at concentration of 1 and 2 mg/ml) did not showed an increasing in term of size, compared to the HA^{220}-*c*-Rfv 60/40 based NHs. In fact, a size of 232 ± 5 nm was measured for the one prepared with the HA^{220}-*c*-Rfv 60/40, and of 239 ± 3 for the PEGylated polymers.
Nevertheless, a change in terms of ζ-potential was noticed (Figure 10).

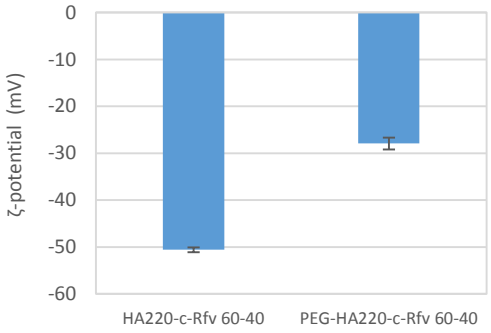

Figure 10. Average ζ-potential of the NHs obtained with the HA^{220}-c-Rfv 60/40 and its PEG-derivative at 1 mg/ml in water. Data points are average values. Error bars indicate standard deviations (n=3).

As expected, the NHs formed with the PEG-derivative polymer showed a less negative ζ-potential value (-27.9 ± 1.2 mV) that the ones formed with the HA^{220}-*c*-Rfv 60/40 polymer (-50.6 ± 0.5), suggesting that the click coupling of the azido-PEG was successful. Moreover, ^{1}H NMR spectra of the PEGylated polymer registered in D_2O confirmed the presence of the PEG showing its typical intense signal at 3.57 ppm. A correct quantification of the linked PEG was not possible due to the fact that this signal resulted more intense than the HA signals.

2.4 Conclusions

Amphiphilic HA-*c*-Rfv polymers were synthesized starting from HA with different M_w (57, 115, 220 and 280 kDa), that were previously modified with a propargylic portion, suitable for the coupling of the azido-derivative of riboflavin *via* click chemistry reaction. The obtained derivatives were characterized in terms of degree of substitution (DS) obtained with the Prop and $RfvN_3$ portions, and in terms of the ability to form self-assembled NHs. A new method to obtain NHs was tested, i.e. the autoclaving process, that generate in one-step spontaneously sterile NHs obtained by self-assembling of the polymer chains under thermal treatment. HA^{220}-*c*-Rfv derivatives were chosen for further investigations as NHs constituents for drug delivery applications. In particular, HA^{220}-*c*-Rfv 40-40 NHs suspensions showed a size of 162 ± 10 nm, a PDI of 0.2 ± 0.05 and a ζ-potential of about −50 mV. These formulation resulted be stable in water at 4°C for more than two months, whereas at 37°C in glycerol/Simulated Intestinal Fluids (SIF) (pH 7.4) media, NHs resulted stable for 48 hours. Piroxicam, dexamethasone and paclitaxel were chosen as model drugs tested for the encapsulation into such NHS, resulting in an increase of their apparent water solubility of 12, 3 and 25-fold respectively, confirming that these NHs indeed act as solubility enhancers. Moreover, the drug-loaded systems developed resulted to be stable for at least two months, and easily re-constituted after the freeze-drying process and subsequent re-hydration. Finally, HA^{220}-*c*-Rfv 60-40 derivative was subsequently conjugated with PEG-N_3 by Copper(I)-catalyzed Azide-Alkyne Cycloaddition (CuAAC), due to the fact that this derivative presented propargylic moieties still available for click coupling, thus potentially improving the blood circulation of these nanostructures. The click chemistry reaction was indeed a good synthetic strategy to easily modify the HA polymer chains, resulting in good yields, fast reaction and quantitative conversion of the $RfvN_3$ and PEG-N_3 grafted to the polymer backbone.

References

(1) C. Gonçalves, P. Pereira, M. Gama; Self-Assembled Hydrogel Nanoparticles for Drug Delivery Applications. *Materials* **2010**, 3: 1420-1460

(2) Z. Y. Qian, S. Z. Fu, S. S. Feng; Nanohydrogels as a prospective member of the nanomedicine family. *Nanomedicine* **2013**, 8: 161–164

(3) J.P. Plard, D. Bazile; Comparison of the safety profiles of PLA(50) and Me.PEG-PLA(50) nanoparticles after single dose intravenous administration to rat. *Colloids Surf. B*, **1999**, 16: 173–183

(4) M.T. Peracchia,E. Fattal, D. Desmaele, M. Besnard, J.P. Noel, J. M. Gomis, M. Appel, J. d'Angelo, P. Couvreur; Stealth PEGylated polycyanoacrylate nanoparticles for intravenous administration and splenic targeting. *J. Control. Release* **1999**, 60: 121–128

(5) K. Akiyoshi, S. Kobayashi, S. Shichibe et al.; Self-assembled hydrogel nanoparticle of cholesterol-bearing pullulan as a carrier of protein drugs: Complexation and stabilization of insulin. *J. Control. Release*, **1998**, 54: 313-320

(6) T. G. Shutava, Y. M. Lvov; Nano-engineered microcapsules of tannic acid and chitosan for protein encapsulation. *J. Nanosci. Nanotec.*, **2006**, 6: 1655-1661

(7) H. B. Patel, H. L. Patel, Z. H. Shah et al.; Review on hydrogel nanoparticles in drug delivery. *Am. J. Pharm. Tech. Res.*, **2011**, 1: 19-38

(8) E. Montanari, S. Capece, C. Di Meo et al.; Hyaluronic acid nanohydrogels as a useful tool for BSAO immobilization in the treatment of melanoma cancer cells. *Macromol. Biosci.*, **2013**, 13: 1185-1194

(9) T. Nakai, T. Hirakura, Y. Sakurai et al., Injectable hydrogel for sustained protein release by salt-induced association of hyaluronic acid nanogel. *Macromol. Biosci.*, **2012**, 12: 475-483

(10) K. Y. Choi, K. H. Min, H. Y. Yoon et al., PEGylation of hyaluronic acid nanoparticles improves tumor targetability in vivo. *Biomaterials*, **2011**, 32: 1880-1889

(11) S. Zhang, Emerging biological materials through molecular self-assembly. *Biotechnol. Adv.*, **2002**, 20: 321–339

(12) D. Jiang, J. Liang, P. W. Noble; Hyaluronan as an Immune Regulator in Human Diseases. *Physiol. Rev.*, **2011**, 91: 221-264

(13) H. J. Cho, H. Y. Yoon, H. Koo et al., Self-assembled nanoparticles based on hyaluronic acid-ceramide (HA-CE) and Pluronic® for tumor-targeted delivery of docetaxel. *Biomaterials*, **2011**, 32: 7181-7190

(14) L. Zhang, J. Yao, J. Zhou et al., Glycyrrhetinic acidgraft-hyaluronic acid conjugate as a carrier for synergistic targeted delivery of antitumor drugs. *Int. J. Pharm.*, **2013**, 441: 654-664

(15) N. Bextsinna, M. Solé. N. Taib, I. Bestel, Bioengineered riboflavin in nanotechnology. *Biomaterials*, **2016**; 80: 121-133

(16) H. J. Powers, Riboflavin (vitamin B-2) and health, *Am. J. Clin. Nutr*. **2003**; 77: 1352-1360

(17) H. C. Kolb, and K. B. Sharpless, The growing impact of click chemistry in drug discovery. *Drug Discovery Today*, **2003**; 8: 1128-1137

(18) H. C. Kolb, M. G. Finn, K. B. Sharpless, Click chemistry: diverse chemical function from a few good reaction. *Angew. Chem., Int. Ed.*, **2009**; 40: 2004-2021

(19) P. L. Golas, K. Matyjaszewsky, Marrying click chemistry with polymerization: Expanding of polymeric materials. *Chem. Soc. Rev.* **2010;** 39: 1338-1354

(20) M. Van Dijk, D. T. S. Rijkers, R. M. J. Liskamp, C. F. Van Nostrum, W. E. Hennink, Synthesis and application of biomedical and pharmaceutical polymers via click chemistry methodologies. *Bioconjugate Chem.*, **2009**; 20: 2001-2016

(21) C. Di Meo, E. Montanari, L. Manzi, C. Villani, T. Coviello, P. Matricardi, Highly versatile nanohydrogel platform based on riboflavin-polysaccharide derivatives useful in the development of intrinsically fluorescent and cytocompatible drug carriers. *Carbohydrate Polymers*, **2015**; 115: 502-509

(22) C. E. Schantéa, G. Zuber, C. Herlinb, T. F. Vandamme, Chemical modifications of hyaluronic acid for the synthesis of derivatives for a broad range of biomedical applications, *Carbohydr. Polym*., **2011**; 85: 469–489

(23) S. Singh, N. K.Mehra, N. K. Jain, Development and Characterization of the Paclitaxel loaded Riboflavin and Thiamine Conjugated Carbon Nanotubes for Cancer Treatment. *Pharm. Res.*, **2016**, 33: 1769–1781

(24) F. Danhiera, N. Lecouturiera, B. Vromana, C. Jérômeb, J. Marchand-Brynaertc, O. Ferond, V. Préata, Paclitaxel-loaded PEGylated PLGA-based nanoparticles: *In vitro* and *in vivo* evaluation. *J. Controlled Release*, **2009**; 133: 11–17

(25) T. Yang, M.K. Choi, Preparation and evaluation of Paclitaxel-loaded PEGylated immunoliposome. *J. Control. Release*, **2007**; 120: 169–177

(26) R. T. Liggins, H. M. Burt, Paclitaxel-loaded poly(l-lactic acid) microspheres 3: blending low and high molecular weight polymers to control morphology and drug release. *Int. J. Pharm.*, **2004**; 282: 61–71

(27) K. M. Huh, H. S. Min, S. Cheon Lee, H. J. Lee, S. Kim, K. Park A new hydrotopic block copolymer micelle system for aqueous solubilization of Paclitaxel. *J. Control. Release*, **2008**; 126: 122–129

(28) Z. Zhang, S.-S. Feng, The drug encapsulation efficiency, in vitro drug release, cellular uptake and cytotoxicity of Paclitaxel-loaded poly(lactide)-tocopheryl polyethylene glycol succinate nanoparticles. *Biomaterials*, **2006**; 27: 4025–4033

(29) X. Wei, T. H. Senanayake, G. Warren, and S. V. Vinogradov, Hyaluronic acid-based nanogel-drug conjugates with enhanced anticancer activity designed for targeting of CD44-positive and drug-resistant tumors. *Bioconjug Chem.*, **2013**; 24: 658–668

(30) E. Montanari, M. C. De Rugeriis, C. Di Meo, R. Censi, T. Coviello, F. Alhaique, P. Matricardi, One-step formation and sterilization of gellan and hyaluronan nanohydrogels using autoclave. *J Mater Sci: Mater Med*, **2015**; 26:32

(31) Z. Liu et al., Supramolecular Stacking of Doxorubicin on Carbon Nanotubes for In Vivo Cancer Therapy. *Angew. Chem. Int. Ed.*, **2009**; 48: 7668-7672

(32) G. D'Arrigo, G. Navarro, C. Di Meo, P. Matricardi, V. Torchilin, Gellan gum nanohydrogel containing anti-inflammatory and anti-cancer drugs: a multi-drug delivery system for a combination therapy in cancer treatment. *Eur. J. Pharm. Biopharm.*, **2014**; 87; 208-216

(33) T. Coviello, P. Matricardi, C. Marianecci, F. Alhaique, Polysaccharide hydrogels for modified release formulations. *J. Control. Release*, **2007**, 119: 5-24

(34) D. Steinhilber, M. Witting, X. Zhang, M. Staegemann, F. Paulus, W. Friess, S. Küchler, R Haag, Surfactant free preparation of biodegradable dendritic polyglycerol nanogels by inverse nanoprecipitation for encapsulation and release of pharmaceutical biomacromolecules. *J. Control. Release*, **2013**, 169: 289-295

(35) http://www.drugbank.ca/

(36) N. N. Sanders, S. C. De Smedt, S. H. Cheng, J. Demeester, Pegylated GL67 lipoplexes retain their gene transfection activity after exposure to components of CF mucus. *Gene Ther.,* **2002**; 9: 363-731

(37) M. Ogris, G. Walker, T. Blessing, R. Kircheis, M. Wolschek, E. Wagner, Tumor-targeted gene therapy: strategies for the preparation of ligand-polyethylene

glycolpolyethylenimine/DNA complexes. *Journal of Controlled Release*, **2003**; 91: 173–181

(38) M.C. Lenter, P. Garidel, J. Pelisek, et al., Stabilized nonviral formulations for the delivery of MCP-1 gene into cells of the vasculoendothelial system. *Pharmaceutical Research*, **2004**; 21: 683–691

(39) S. Mishra, P. Webster, M. E. Davis, PEGylation signifi cantly affects cellular uptake and intracellular traffi cking of non-viral gene delivery particles. *European Journal of Cell Biology*, **2004**; 83: 97–111

(40) S. H. Pun, F. Tack, N. C. Bellocq, et al., Targeted delivery of RNAcleaving DNA enzyme (DNAzyme) to tumor tissue by transferrin-modified, cyclodextrin-based particles. *Cancer Biology and Therapy*, **2004**; 3: 641–650

(41) X. Sun , R. Rossin , J. L. Turner , M. L. Becker , M. J. Joralemon , M. J. Welch , and K. L. Wooley, An Assessment of the Effects of Shell Cross-Linked Nanoparticle Size, Core Composition, and Surface PEGylation on in Vivo Biodistribution. *Biomacromolecules*, **2005**; 6: 2541–2554

(42) A. S. Zahr, M. de Villiers, M. V. Pishko, Encapsulation of drug nanoparticles in self-assembled macromolecular nanoshells. *Langmuir*, **2005**; 21: 403–410

Chapter 3

Synthesis and Characterization of Thermosensitive Polymeric Micelles with conjugated Riboflavin via Click Chemistry

G. Manzi [a,b], M. T. Hembury [b], M. Najafi [b], M. Pierini [a], C. Di Meo [a], P. Matricardi [a], W. E. Hennink [b], T. Vermonden [b]

[a] *Department of Drug Chemistry and Technology, ''Sapienza'' University of Rome, Rome, Italy*
[b] *Department of Pharmaceutics, Utrecht Institute for Pharmaceutical Sciences (UIPS), Utrecht University, Utrecht, The Netherlands*

ABSTRACT: Micellar nano-assemblies composed of thermosensitive amphiphilic block polymers are formed spontaneously above their CMC. For these types of polymers, the aqueous solubility properties depend on temperature, and micellar nanostructures are formed by self-assembly above their lower critical solution temperature (LCST) in aqueous media. For this purpose, poly *N*-isopropylacrylamide (pNIPAAm) block-copolymers were synthesized by free radical polymerization using a polyethylene glycol based macroinitiator. Upon dissolution in aqueous solvents and heating above the LCST, these polymers are able to form micelles. To stabilize these micelles, functional groups facilitating π-π stacking interactions were introduced into the polymers. For this purpose, riboflavin as aromatic moiety was coupled to the polymer backbone by azide-alkyne "click chemistry" reaction.

Two block-copolymers, methoxy poly(ethylene glycol)-*b*-(*N*-isopropylacrylamide)-*co*-(2-azidoethyl) methacrylate (mPEG-*b*-p(NIPAAm)-*co*-AzEMA) and the corresponding derivative methoxy poly(ethylene glycol)-*b*-(*N*-isopropylacrylamide)-*co*-(2-azidoethyl) methacrylate-riboflavin (mPEG-*b*-p(NIPAAm)-*co*-AzEMA-Rfv), were synthesized and compared in terms of physico-chemical properties, micelle size, drug retention and release. Micelles were formed by heating the polymeric aqueous solution from 0 to 50°C, and paclitaxel (PTX) was encapsulated by mixing a concentrated drug solution in ethanol with the polymer solution in phosphate buffer followed by heating. Three different feed PTX loadings (feed drug loading concentration of 5, 10 and 20%) were tested in micelles of both block-copolymers.

Upon introduction of riboflavin in the polymeric backbone, a lower critical micelle temperature was obtained by (26°C for mPEG-*b*-p(NIPAAm)-*co*-AzEMA and 24° C for the corresponding riboflavin containing polymer, respectively). An average size of ~50 nm for the mPEG-*b*-p(NIPAAm)-*co*-AzEMA and ~90 nm for the mPEG-*b*-p(NIPAAm)-*co*-AzEMA-Rfv micelles in water was observed respectively for empty micelles, which increased with ~20 nm in phosphate buffered saline. Drug loading resulted in an increase of the micelle size by approximately 10-20 nm (from 60 to 75 nm for mPEG-*b*-p(NIPAAm)-*co*-AzEMA based micelles, and from 150 to 170 nm for mPEG-*b*-p(NIPAAm)-*co*-AzEMA-Rfv based ones). Increased encapsulation efficiency (EE%) and drug loading (DL%) were obtained for micelles containing riboflavin; almost 100% encapsulation of PTX was found for a feed PTX loading of 5% . Nevertheless, drug release resulted be faster for the Rfv-derivative backbone based micelle, likely due to their lower polymer density.

Overall, this novel Rfv containing system is very promising in bringing advantages with regard to drug loading, warranting further investigations in tunability of drug release profiles for further application in stimuli-responsive anticancer therapy.

3.1 Introduction

Micellar nano-assemblies composed of amphiphilic block copolymers are formed spontaneously above their critical micelle concentration (CMC), which depends on the hydrophobicity/ hydrophilicity balance of the block copolymers, as well as their molecular weight, the length of the hydrophobic block, and chemical characteristics of the blocks (in terms of their chemical nature).[1, 2] The size of the polymeric micelles in general is between 10 and 200 nm depending on the molecular weight of the different blocks.[3]

In general, micellar structures in aqueous media consist of a hydrophobic core and hydrophilic corona (often composed of poly ethylene glycol (PEG)). The hydrophobic nature of the core give advantages on carrying hydrophobic molecules with ideally high loading capacity, and controlled release of encapsulated drug; the hydrophilic corona shields the hydrophobic cores, prevents particle precipitation in aqueous environment, and prolongs the blood circulation of these nanostructures.[4]

The use of polymeric micelles as carriers can benefit control over important biological characteristic such us pharmacokinetic profile, favorable biodistribution, extended circulation time of the drug.

For these kinds of polymeric systems, usually the CMC results be lower than, for example, the ones prepared with the conventional detergents, or compared to the lipid-core micelles,[1] resulting in higher stability and versatility of the developed systems.

In the last decade, thermosensitive polymers have received great interest for the preparation of micelles,[5,6] for which the aqueous solution properties are temperature dependent. Below their lower critical solution temperature (LCST), these polymers are in expanded state and fully dissolved because of the formation of hydrogen bonds between water and polymer molecules, while above their LCST, the polymeric chains are de-hydrated because of the disruption of the hydrogen bonds with water and consequently they collapse. If there is a good balance between the lengths of the hydrophobic and the hydrophilic blocks, the collapsed polymer forms nanostructures, whereas if the hydrophobic block is too long, the polymer precipitates in water in for example rods or lamellae-like morphology.[53]

Stimuli-responsive polymers, in particular systems based on poly(*N*-isopropylacrylamide) (pNIPAAm) have been extensively investigated for pharmaceutical and biomedical applications. pNIPAAm has a good aqueous solubility below its cloud point (CP), but above its CP it precipitates. This phase transition is reversible.[7-9] The strategy to use thermosensitive polymeric micelles propose to obtain temporal control of the release of the encapsulated drug: changing the temperature of the environment even only slightly above or below the CP can result in destabilization of the micelles and affect the release of the

encapsulated drug. In other words, the drug release could be temperature controlled.[20]

The CP of NIPAAm in water is 30-33°C, which can be tuned by copolymerization of NIPAAm with hydrophilic or hydrophobic monomers.[10, 11] AB block copolymers of pNIPAAM and a hydrophilic block (such as polyethylene glycol, PEG) forms micelles with NIPAAm as core and the hydrophilic corona of PEG above the CP. On the other hand, when pNIPAAm is polymerized with hydrophobic block, it can act as the shell of the formed micelles below its CP.[12] For both cases, micelles can be destabilized by hypo-hyperthermia in order to release an entrapped drug .

Unfortunately, many studies of drug-loaded micelles showed rapid drug release in the circulation, mostly due to a combination of extraction of the drug from the micelles and micellar destabilization.[13]

To stabilize such micelles, researchers have developed methods of covalent cross-linking of shells, interface or core. However, chemical conjugation methods are not always feasible, due the toxicity of some crosslinking agents and due some side reactions that can happen during the process that might affect the therapeutic properties of conjugated drugs. Alternatively, physical interactions, such as π–π stacking,[14-17] hydrogen bonding [18] or stereocomplex formation [19] have been investigated to improve the thermodynamic and kinetic stability of polymeric micelles.

Y. Shi et al.[51] synthesized thermosensitive amphiphilic block copolymers with novel aromatic monomers by free radical polymerization of *N*-(2-benzoyloxypropyl methacrylamide (HPMAm-Bz) or the corresponding naphthoyl analogue (HPMAm-Nt), with *N*-(2-hydroxypropyl) methacrylamide monolactate, using a polyethylene glycol based macroinitiator. Using these polymers, micelles were prepared with the aim to stabilize them by π–π interactions and thereby increase their loading capacity for chemotherapeutic drugs. They concluded that the π–π stacking effect introduced by aromatic groups indeed increased the stability and loading capacity of their polymeric micelles. Inspired by that work, in the present study we attempted to introduce Riboflavin as π–π stacking moiety, and hypothesized that such isoalloxazine compound might give rise to a stable micellar nanostructure.

Riboflavin (Rfv) or Vitamin B2 is an interesting molecule with attractive properties[21] such as biological activity as coenzyme for the flavoenzymes Flavin adenine dinucleotide (FAD) and Flavin mononucleotide (FMN) and their participation in a range of redox reactions,[22] light sensitivity originating from its isoalloxazine ring responsible for its UV absorption, fluorescence and photosensitivity. Due to these characteristics, Rfv attracted attention of multiple scientific studies in tissue and bio-electronic engineering,[23,24] targeted drug delivery and nanotechnology such as functionalized nanoparticles,[25-27] dendrimers,[28-30] polymers, biomacromolecules[31,32] and hydrogels. The isoalloxazine ring is well known to have a high propensity for forming charge-

transfer complexes with biologically aromatic compounds. Moreover, the π-bonding capability of the flavin ring, together with its hydrogen-bonding ability, significantly affects the physicochemical properties of crystalline riboflavin compounds.[33]

The aim of this study was to develop new thermosensitive amphiphilic block copolymers, making use of the beneficial properties of riboflavin that self-assemble into stable micelles at body temperature and exhibit high drug loading capacity and retention. For these purposes, methoxy poly(ethylene glycol)-*b*-(*N*-isopropylacrylamide)-*co*-(2-azidoethyl) methacrylate (mPEG-*b*-p(NIPAAm)-*co*-AzEMA) block copolymer was synthesized by free radical polymerization.[20] Subsequently, a propargyl derivative of riboflavin (Rfv-Prop) was synthesized and covalently coupled to the azide modified diblock copolymers mPEG-*b*-p(NIPAAm)-*co*-AzEMA by Copper(I)-catalyzed Azide-Alkyne Cycloaddition (CuAAC), due to the high efficacy and selectivity of this kind of reaction.[33-36]

The polymer mPEG-*b*-p(NIPAAm)-*co*-AzEMA, and its corresponding derivative methoxy poly(ethylene glycol)-*b*-(*N*-isopropylacrylamide)-*co*-(2-azidoethyl) methacrylate–riboflavin (mPEG-*b*-p(NIPAAm)-*co*-AzEMA-Rfv) were investigated and characterized in terms of coupling efficiency of Rfv, and were compared in terms of critical micellar temperature and concentration variation. Polymeric micelles were formed by heating the aqueous polymeric solutions and analyzed in terms of size/concentration dependent. Furthermore, those micelles with and without aromatic moieties in the hydrophobic core were used to loading the first-line anticancer drug Paclitaxel (PTX), in order to study the retention and the release profile of such a poorly water-soluble model compound.

Paclitaxel is a potent drug used extensively in breast, ovarian and lung cancer.[54] The hydrophobic nature of this drug is a serious hurdle in its efficient formulation and restricts its use in aqueous based solvent systems. In view to overcome these limitations, several PTX-loaded nanoformulations were already investigated and well described in literature.[37-42] These nanoscale drug formulations have demonstrated several merits, such as prolonged circulation time, better pharmacological profiles, decreased adverse effects and improved drug tolerance, over conventional clinical approaches. On this purpose, with this work we aimed to obtained advantages, such as in terms of loading of this drug in the lipophilic core (represented by riboflavin) of our micelle, exploiting hydrophobic interactions and the potential π-π stacking interactions that might exist between the aromatic rings of riboflavin and the drugs molecule (containing aromatic rings as well).

3.2 Materials and Methods

3.2.1 Materials

N-isopropylacrylamide (NIPAAm), poly(ethylene glycol) monomethyl ether (PEG, number-average molar mass Mn = 5000 g mol^{-1}), sodium azide (NaN_3), 2-bromoethanol, magnesium sulfate ($MgSO_4$), sodium bicarbonate ($NaHCO_3$), sodium chloride (NaCl), 1,8-diazabicyclo[5.4.0]undec-7-ene (DBU), propargyl bromide solution 80 wt. % in toluene, anhydrous sodium sulfate (Na_2SO_4), ethylenediaminetetraacetic acid disodium salt dihydrate (EDTA), copper(II) sulfate ($CuSO_4$) and L-ascorbic acid were purchased from Sigma-Aldrich (Zwijndrecht, The Netherlands). Riboflavin tetrabutyrate was purchased from TCI Europe. Phosphate buffered saline pH 7.4 (PBS, in 1000 ml: NaCl 8.2g, Na_2HPO_4 $12H_20$ 3.1g, NaH_2PO_4 $2H_2O$ 0.3g, water for injection) was obtained from B. Braun Melsungen AG (Melsungen, Germany). Paclitaxel (PTX) was purchased from LC Laboratories (MA, U.S.A.). Acetonitrile (ACN), dichloromethane (DCM), acetone, diethyl ether, ethyl acetate, hexane and *N,N*-dimethylformamide (DMF) were supplied by Biosolve Ltd. (Valkenswaard, The Netherlands).

3.2.2 Synthesis of methoxy poly(ethylene glycol)-4,4-azobis-(4-cyanopentanoic acid) macroinitiator (PEG_2-ABCPA)

Methoxy poly(ethylene glycol)- 4,4-azobis- (4-cyanopentanoic acid) ($mPEG_2$-ABCPA) macroinitiator (Mn of mPEG = 5000 g·mol^{-1}) was prepared as described previously.[43] In short, 2 g (0.4 mmol) of poly(ethylene glycol) monomethyl ether (PEG, number-average molar mass Mn = 5000 g mol^{-1}), 0.056 g (0.2 mmol) of 4,4-azobis- (4-cyanopentanoic acid) (ABCPA), 0.0189 g (0.06 mmol) of 4-(dimethylamino)pyridinium-4-toluenesulfonate (DPTS), and 0.125 g (0.6 mmol) of *N,N'*-dicyclohexylcarbodiimide (DCC) were dissolved in 1:1 mixture of DCM and dry DMF (final volume 30 ml). The mixture was stirred at room temperature for 24 h. After purification by extraction and precipitation, the product was obtained in a high yield (~ 80%) and characterized by ^{1}H NMR and gel permeation chromatography (GPC).

^{1}HNMR ($CDCl_3$) δ (ppm) 1.7 (C*H*$_3$, s), 2.4 (CH_2CH_2COOH, br), 3.6 ($CH_3OCH_2CH_2$, br, PEG).

Additionally, to confirm the substitution degree of the PEG, a few drops of trichloroacetyl isocyanate (TAIC) were added to the NMR tube and the sample was analyzed again in order to confirm the calculated degree of substitution, since TAIC induces a shift of the CH_2 protons adjacent to the OH-end groups to 4.37 ppm. GPC analysis was performed (two serial PLgel 5 μm MIXED-D column, PEGs

narrow molecular weights standards, DMF plus LiCl 10 mM eluent) to evaluate the molecular weight of the product, and the ratio between the bi-, mono- and non-functionalized products.

3.2.3 Synthesis of 2-azidoethanol

Following a slightly modified published procedure,[44] 2-azidoethanol was prepared. In short, NaN_3 (23.4 g, 360 mmol) and 2-bromoethanol (27.0 g, 216 mmol) were dissolved in a mixture of acetone (50 mL) and water (80 mL) and refluxed at 75 °C for 3 days. After removing acetone under vacuum, the product was 5 times extracted with 100 ml of ethyl acetate. The organic phase was dried using anhydrous $MgSO_4$ and the solvent was removed by evaporation, resulting in 10.4 g of a slightly yellow oil of product (Yield ~ 55%).

^{1}HNMR ($CDCl_3$) δ (ppm) 1.8 (O*H*, br), 3.4 (C*H*$_2$N$_3$, t), 3.8 (C*H*$_2$OH, t).

3.2.4 Synthesis of 2-azidoethyl methacrylate (AzEMA)

AzEMA monomer was prepared using a slightly modified published procedure.[45]
In brief, 2-azidoethanol (2.0 g, 23 mmol) and triethylamine (3.8 ml, 27 mmol) were dissolved in 40 ml dichloromethane and cooled in an ice bath. Next, methacryloyl chloride (2.6 g, 25 mmol) dissolved in 15 ml DCM was added dropwise for 20 min. The reaction was allowed to proceed for 2 h at room temperature. Next, 30 ml of saturated $NaHCO_3$ aqueous solution was added and the mixture was stirred for 30 min in an ice bath to deactivate excess methacryloyl chloride. The organic phase was washed with 30 ml of a saturated NaCl solution once, dried using anhydrous $MgSO_4$, and concentrated under reduced pressure. The crude product was purified by flash silica gel chromatography (Silica gel 60, 0.030-0.075 mm) with DCM as an eluent, resulting in 2.59 g of 2-azidoethyl methacrylate as slightly yellow oil (Yield ~ 73%).

^{1}H NMR ($CDCl_3$) δ (ppm) 1.89 ($CH_2C(CH_3)CO$, s), 3.43 (C*H*$_2$N$_3$, t), 4.25 (C*H*$_2$CH$_2$N$_3$, t), 5.55 and 6. 08 (C*H*$_2$C(CH$_3$)CO, s).

3.2.5 Synthesis of 3-propargyl-riboflavin tetrabutyrate (Rfv-Prop)

Riboflavin tetrabutyrate (1 g, 1.83 mmol) was dissolved in anhydrous DMF under Ar_2 atmosphere and heated to 55°C. Then DBU (3 eq, 837 mg, 5.5 mmol) and propargyl bromide (2 eq, 915 mg, 3.67 mmol) were added. After 48 h, the organic solvent was evaporated under reduced pressure. Water (100 ml) was added to the crude product, which was further extracted 3 times with diethyl ether (100 ml) and washed with brine (100 ml). Combined organic layers were dried over Na_2SO_4, filtered and the solvent was evaporated under reduced pressure. The crude product was purified using a silica column (ethyl acetate/hexane, 1/1 to 10/0, v/v) to yield 1.02 g of orange solid. (Yield ~ 94%).

^{1}H NMR ($CDCl_3$) δ (ppm) 8.02 (s, 1*H*), 7.56 (s, 1*H*), 5.67 (br s,1*H*), 5.43(m, 2*H*), 4.85 (s, 2*H*), 4.47 (d, 1*H*), 4.23 (dd, 1*H*), 4.09 (t, 2*H*), 2.54 (s, 3*H*), 2.42 (s, 3*H*), 2.28 (t, 2*H*), 2.03 (m, 1*H*), 1.87 (m, 3*H*), 1.74–1.67 (m, 10*H*), 1.65 (dd, 2*H*), 1.52–1.24 (m, 6*H*), 0.96 (q, 6*H*), 0.92(t, 3*H*), 0.59 (t, 3*H*).

FT-IR (KBr) 2964, 2936, 2874, 2100, 1745, 1663, 1550, 1158.

ESI–MS (+) m/z 695, 717 [M + Na]+.

3.2.6 Synthesis of methoxy poly(ethylene glycol)-*b*-(*N*-isopropylacrylamide)-*co*-(2-azidoethyl) methacrylate (mPEG-*b*-p(NIPAAm)-*co*-AzEMA)

$mPEG_{5000}$ –*b*-pNIPAAm block copolymer containing AzEMA monomers was synthesized by free radical polymerization using NIPAAm and AzEMA as monomers, and PEG_2-ABCPA as macroinitiator.[43]
In short, 150 mg of PEG_2-ABCPA, 569.5 mg of NIPAAm and 39.06 mg of AzEMA were dissolved in 10 ml of dry ACN under N_2 atmosphere for 20 minutes and then left to polymerize at 70 °C for 40 h under stirring. After cooling the mixture to room temperature, the formed polymer was precipitated in cold diethyl ether for 3 times, dried under high vacuum and collected as a white solid. (Yield ~ 93%)
^{1}H NMR ($CDCl_3$) δ (ppm) 1.11 ($CHC\mathit{H_3}C\mathit{H_3}$, s – NIPAAm), 3.62 ($CH_3OC\mathit{H_2}C\mathit{H_2}$, br, PEG), 3.97 ($C\mathit{H}CH_3CH_3$, s – NIPAAm), 4.20 ($C\mathit{H_2}CH_2N_3$, t, AzEMA)

3.2.7 Synthesis of methoxy poly(ethylene glycol)-*b*-(*N*-isopropylacrylamide)-*co*-(2-azidoethyl) methacrylate-riboflavin *via* Click Chemistry (mPEG-*b*-p(NIPAAm)-*co*-AzEMA-Rfv)

mPEG-*b*-p(NIPAAm)-*co*-AzEMA (300 mg, corresponding to 0.099 mmol AzEMA) and Rfv-Prop (62.53 mg, 0.099 mmol Rfv-Prop) were dissolved in 6 ml of DMF. Then $CuSO_4$ (57 mg, 1 eq to RfvProp) and Ascorbic Acid (63.36 mg, 1 eq to $CuSO_4$) were dissolved in 300 μl of H_20 and added to the mixture.
The reaction was carried out under N_2 atmosphere at 40°C for 48 h, and the product was then precipitated in an excess of diethyl ether, collected by centrifugation, dissolved in water and then dialyzed first against a EDTA solution 10 mM of for 3 h, and then against water for at least 24 h, and finally recovered by freeze-drying. (Yield ~ 87%)

^{1}H NMR ($CDCl_3$) δ (ppm) 1.11 (CHC*H*$_3$C*H*$_3$, s – NIPAAm), 3.62 ($CH_3OCH_2CH_2$, br, PEG), 3.98 (C*H*CH_3CH_3, s – NIPAAm), 7.55 (1*H*, s – Rfv), 7.87 (1*H*, s - triazolic ring), 7.97 (1*H*, s – Rfv).

3.2.8 Characterization of mPEG-*b*-p(NIPAAm)-*co*-AzEMA and mPEG-*b*-p(NIPAAm)-*co*-AzEMA-Rfv Block Polymers

The synthesized polymers were characterized by ^{1}H NMR and Gel Permeation Chromatography (GPC) analysis in order to obtain information about the number average molecular weight (M_n), weight average molecular weight (M_w) and polydispersity (PDI, equal M_w/M_n); information about the qualitative conversion of AzEMA monomer, and quantitative estimation of Rfv-functionalization.
FT-IR ATR analysis was performed in order to monitor the outcome of the click coupling reactions and of the purification process
^{1}H NMR spectra were recorded using Agilent 400 MHz spectrometer, using CD_3Cl as solvent (solvent signal at 7.26 ppm). The value of the signal of the mPEG at 3.62 ppm was normalized for 455 protons (average number of the protons per one mPEG chain M_n = 5000) and was used as reference signal. Based on this normalization, the signal of NIPAAm at 3.98 ppm was integrated to calculate the number of NIPAAm units per polymer. In addition, the signal at 1.12 ppm is related to the NIPAAm protons, and the calculation was confirmed for this peak as well.
GPC analysis was performed using two serial PLgel 5 μm MIXED-D columns and PEGs of narrow molecular weights as calibration standards. The eluent was DMF plus LiCl 10 mM, a flow rate of 1 ml/min was used at a column temperature of 60 °C. The GPC chromatograms were deconvoluted to calculate the weight ratio. The deconvolution was performed by Empower systems software produced by Waters Corporation (Milford, Massachusetts, USA).

FT-IR were measured using a Bio-Rad FTS6000 (BIO-RAD, Cambridge, Massachusetts, USA) in ATR mode. A spectral resolution of 4 cm^{-1} with 64 co-added scans was used for collection of reference spectra over a spectral range of 4000–600 cm^{-1}.

3.2.9 Cloud Point (CP)

The CPs of the block-co-polymers were measured by two different techniques: differential scanning calorimetry (Discovery DSC-TRIOS data analysis, TA instruments, New Castle, Delaware, USA) and light scattering at 550 nm by Jasco FP8300 Spectrofluorometer (Jasco Inc., Easton, Maryland, USA).
DSC analysis was performed to investigate the lower critical solution temperature (LCST) of the synthesized copolymers. All the samples were prepared by dissolving the block copolymers overnight at 4 °C at a concentration of 5 wt% in 0.1 M PBS buffer, pH 7.4. Into aluminum sample pans, 20 μL of these solutions were transferred and the pans were hermetically capped. Thermograms were recorded in triplicate from 0 to 80 °C, using a heating rate of 1 °C/min.
To confirm the data obtained from the DSC analysis, the following procedure was performed in order to determinate the cloud point of the block copolymers based on the intensity changes of scattered light from the polymers upon increasing temperature. The samples were prepared by dissolving the polymers overnight at 4 °C in a concentration of 10 mg/ml in 0.1 M PBS buffer, pH 7.4 and then diluted to a final concentration of 1 mg/ml. The samples were excited at 550 nm and the light scattering intensity values were registered from 5 to 55 °C, using a heating rate of 1 °C/min. The light scattering intensity was plotted against a temperature rate and the onset on the X-axis, obtained by the extrapolation of the Light Scattering Intensity-Temperatures curves to the baseline, was considered as the cloud point.

3.2.10 Preparation of Empty and Drug Loaded Micelles

Empty micelles were prepared by fast heating procedure.[48] In short, the polymers were dissolved in water or in PBS at 4 °C overnight at concentrations of 0.5, 1, 2 and 3 mg/ml. Subsequently, the polymer solutions were heated to 50 °C for 1 min in a water bath while stirring. The samples were then cooled down to 37 °C and analyzed in terms of size and polydispersity by DLS. DLS was performed using a Malvern CGS-3 multiangle goniometer with JDS Uniphase 22mW He-Ne laser operating at 632 nm, an optical fiber-based detector and a digital LV/LSE-5003 correlator (Langen, Germany). Autocorrelation functions were analyzed by the cumulants method (fitting a single exponential to the correlation function to obtain the mean size and the PDI) and the CONtIN routine (fitting multiple

exponential to the correlation function to obtain the distribution of the particle sizes). All the measurements were performed at 90 ° angle.
For paclitaxel loaded micelles, 20 μl of drug solutions in ethanol (drug feed loading concentration of 5, 10 and 20 % w/V) were added to 2 ml of ice cold polymer solutions in PBS (polymer concentration of 1 mg/ml) and then immediately heated at 50 °C for 1 min while shaking. Subsequently, the micellar dispersions were incubated overnight at 37 °C. Non-encapsulated drug was removed by centrifugation (5000 g, 37 °C, 10 min) and the micelles were analyzed in terms of size by DLS measurement. The PTX content in the micellar dispersion was quantify by HPLC method, as well aliquots at different time slots were taken and analyzed in order to follow the release profile of the drug.

3.2.11 Drug content assay and drug retention study

The concentration of the drug loaded in the micelles was evaluated by isocratic HPLC chromatography, using a C18 SunFire (5 μm, 4.6*150 mm) column and a mixture of ACN/water (60/40) and perchloric acid 0.1 % V/V, as eluent at flow rate 1 ml/min. The detection was performed by UV detector at 227 nm. Drug loaded micelles were diluted 9 times with ACN and subsequently vortexed to destabilize the micelles and dissolve the drug. Samples of drug in ACN in a concentration range of 0.2 to 100 μg/ml were used as standards for the calibration.
Encapsulation Efficiency (EE) and Drug Loading (DL) were calculated from the HPLC analysis data based on these equations:

$$\%EE = \frac{concentration\ of\ drug\ measured}{concentration\ of\ drug\ added}\ x\ 100$$

$$\%DL = \frac{concentration\ of\ drug\ measured}{concentration\ of\ (drug\ measured + polymer\ added)}\ x\ 100$$

Drug retention in the micelles at pH 7.4 in phosphate buffer at 37 °C was studied by measuring the remaining drug content in the micellar dispersion in time. For the release study, aliquots of PTX-loaded micelles prepared as described previously and incubated at 37 °C, were taken at different time points. Each aliquots was centrifuged (5000 g for 10 min at 37 °C) to spin down the released PTX crystallized because of its low water solubility (PTX water solubility 5.56 μg/ml). Subsequently, 9 parts of ACN were added at the aliquots, vortexed and injected to evaluate the amount of the residual drug retained in micelles (drug concentration was evaluated by HPLC method as described previously).

3.3 Results and Discussion

3.3.1 Synthesis of methoxy poly(ethylene glycol)-4,4-azobis-(4-cyanopentanoic acid) (PEG_2-ABCPA) macroinitiator

Monomethoxy-PEG substituted macroinitiator (PEG_2-ABPCA) was synthesized as shown in the following reaction scheme (Scheme 1)[43] in order to obtain AB block copolymers by free radical polymerization composed of PEG as block A.

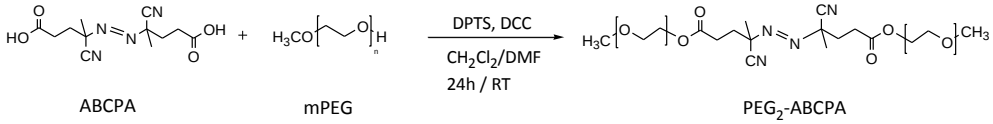

Scheme 1. Synthesis of PEG_2-ABPCA macroinitiator.

The product was obtained in a high yield (~ 80%), after precipitation in cold diethyl ether as white solid powder, and analyzed by ^{1}H NMR and GPC analysis.
To evaluate if the substitution of the PEG was successful and complete, an easy and fast analysis was performed based on ^{1}H NMR spectroscopy after addition of trichloroacetyl isocyanate (TAIC) to the NMR sample, suggested by R. De Vos et al.[40], used to test the end groups of a series of commercial PEG monomethyl ethers. TAIC was used as reagent to identify unreacted free hydroxyl groups by transforming them to trichloroacetyl urethane-end groups, which can be easily identified by ^{1}H NMR spectroscopy because the urethane derivative causes a shift (from 4.23 to 4.37 ppm) of the methylene protons in α-position of the OH end groups. The integrals of the two signals (4.23 ppm relative to the PEG-macroinitiator; 4.37 ppm relative to the PEG- trichloroacetyl urethane) are directly related to the relative amount of functionalized and non-functionalized PEG.

The functionalization degree determined was 76%. (Figure 1)

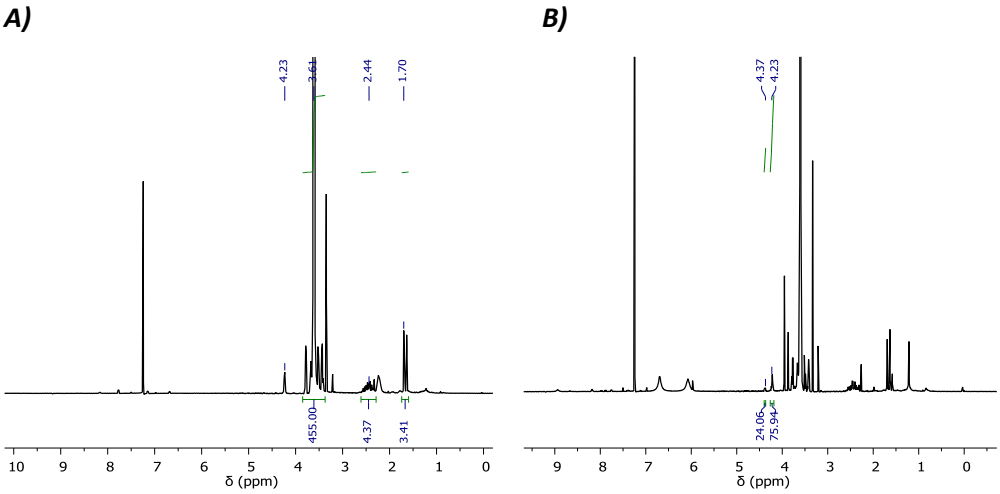

Figure 1. ^{1}H NMR spectra in $CDCl_3$ of **(A)** PEG-macroinitiator and **(B)** PEG-trichloroacetyl uretane.

GPC analysis was performed to evaluate the molecular weight of the product and the ratio between the bi and mono-functionalized products. The chromatogram (Figure 2) showed 2 peaks, peak A with a retention time of 14 min (Mn 10 kDa) and peak B with a retention time of 14.9 min (Mn 5 kDa). Based on calibration using PEGs of known molecular weight, peak A was assigned to the bi-functionalized product (PEG_2-ABPCA) and peak B is assigned to the mono-functionalized product (PEG-ABPCA) and non-functionalized PEG.

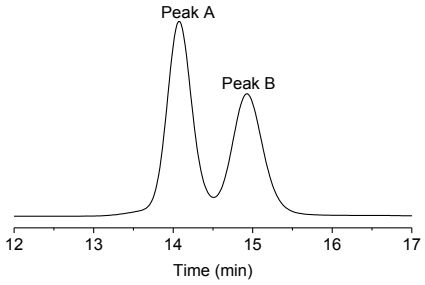

Figure 2. GPC chromatogram of PEG_2-ABPCA macroinitiator, which shows peak A (retention time 14 min) corresponding to the PEG_2-ABPCA product, and peak B (retention time 14.9 min) corresponding to PEG-ABPCA and non-functionalized PEG.

The areas under the curves of the two peaks give us the ratio of the two compounds. Accordingly, in this synthesized batch, the percentage of bi-functionalized PEG (PEG_2-ABPCA) resulted to be 57%, and 43% consisted of the mono-functionalized one (PEG-ABPCA) and non-functionalized PEG.

3.3.2 Synthesis of 2-azidoethyl methacrylate (AzEMA) monomer

AzEMA monomer was synthesized as shown in the following reaction scheme (Scheme 2), from a two-step synthesis by conversion of 2-bromoethanol to 2-azidoethanol by a nucleophilic substitution of the bromide with an azide group, and its subsequent methacrylation using methacryloyl chloride.

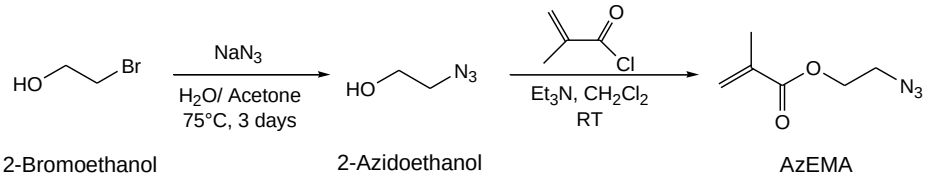

Scheme 2. Two-step synthesis of 2-azidoethyl methacrylate (AzEMA) by conversion of 2-bromoethanol to 2-azidoethanol and subsequent methacrylation using methacryloyl chloride.

From the first synthetic step, the compound 2-azidoethanol was collected in a yield of 55% after extraction, and its structure was confirmed by ^{1}H NMR analysis, which showed the shift of the methylene signals (-C*H*$_2$N$_3$) of the product from 3.4 ppm (-C*H*$_2$Br) to 3.3 ppm. (Spectra not shown)

Then, the alcoholic moiety of 2-azidoethanol was reacted with methacryloyl chloride to couple the methacrylic moiety necessary for the next step of polymerization. The 2-azidoethyl methacrylate product was obtained in a quite high yield (~ 73%) as yellowish oil and analyzed by ^{1}H NMR, which showed three additional signals at 6.10, 5.55 and 1.89 ppm of the protons corresponding to the methacrylate group. Moreover, the signal at 3.65 ppm (-C*H*$_2$OH) of the methyl protons adjacent to the hydroxyl group was shifted to 4.25 ppm, confirming the successful esterification.

Lastly, the infrared spectrum of the AzEMA compound showed the strong asymmetric vibration (N≡N asymmetric stretching absorption) at 2100 cm^{-1}. (Spectra not shown)

3.3.3 Synthesis of methoxy poly(ethylene glycol)-*b*-(*N*-isopropylacrylamide)-*co*-(2-azidoethyl) methacrylate (mPEG-*b*-p(NIPAAm)-*co*-AzEMA) block copolymer

The mPEG-*b*-p(NIPAAm)-*co*-AzEMA block copolymer was synthesized with a 5 mol% in content of AzEMA monomer (relative to the NIPAAm monomers) by free radical polymerization, using PEG_2-ABPCA as macroinitiator, NIPAAm and AzEMA as monomers. (Scheme 3)

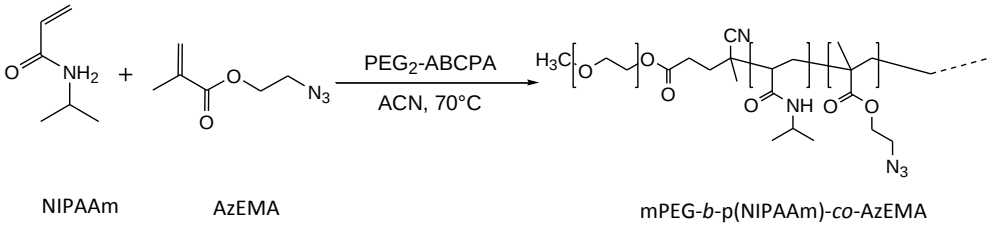

Scheme 3. Synthesis of mPEG-*b*-p(NIPAAm)-*co*-AzEMA block copolymer by free radical polymerization using PEG_2-ABPCA as macroinitiator, NIPAAm and AzEMA as monomers.

The polymer mPEG-*b*-p(NIPAAm)-*co*-AzEMA was obtained in a high yield of (88/90%) after purification by precipitation. Number average molecular weight (M_n), weight average molecular weight (M_w) and polydispersity (PDI, equal to M_w/M_n) were measured by GPC and ^{1}H NMR analysis.

^{1}H NMR analysis of the obtained mPEG-*b*-p(NIPAAm)-*co*-AzEMA block copolymer showed the mPEG signal at 3.62 ppm normalized for 455 protons and this peak was used as reference signal. (Figure 3)

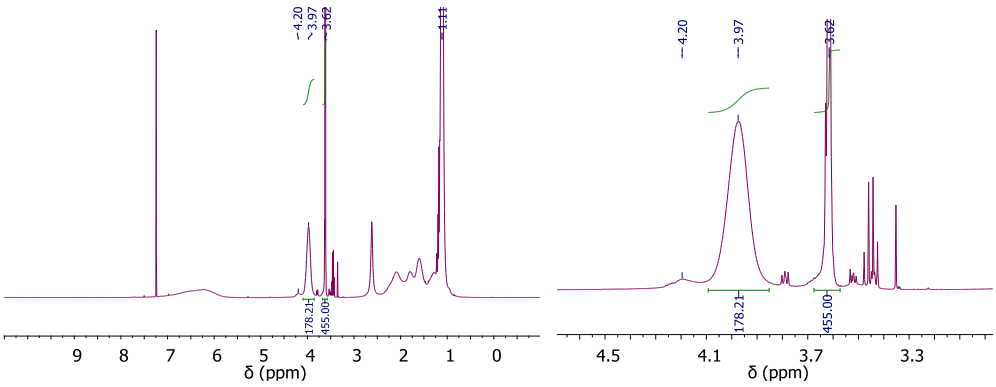

Figure 3. ^{1}H NMR spectra in $CDCl_3$ of mPEG-*b*-p(NIPAAm)-*co*-AzEMA block copolymer. Zoom-in on the region between 5 and 3 ppm where the PEG and NIPAAm signals can be observed. Peaks at 3.8, 3.5 and 3.4 ppm are related to residual solvent.

^{1}H NMR spectra also showed the unique signal of the AzEMA monomers at 4.20 ppm and the ratio between PEG and NIPAm signals indicated a good conversion with 178 NIPAm units per polymer corresponding to a Mn of 25.1 kDa. (Table 1)
GPC analysis was in line with ^{1}H NMR and showed an M_n of the polymer of 29.2 kDa (chromatogram not shown) with a PDI (M_w/M_n) of 2.5, which is acceptable for free radical polymerization techniques. (Table 1)
FT-IR analysis was performed by ATR method. The spectra clearly showed the strong asymmetric vibration (N≡N asymmetric stretching absorption) at 2100 cm^{-1} confirming the presence of the AzEMA monomer in the polymeric chains. (Spectra not shown) The feed ratio AzEMA : NIPAm was 5 : 95. Unfortunately, the exact determination of the obtained ratio was difficult to quantify exactly with these methods. Nevertheless, the presence of azide moieties was proven since they were clearly visible in both NMR and IR.

3.3.4 Synthesis of 3-propargyl-riboflavin tetrabutyrate (Rfv-Prop)

A propargyl derivative of riboflavin tetrabutyrate was synthesized as described in section 2.5, using DBU as base to deprotonate the nitrogen of the isoalloxazine ring that was afterwards alkylated using an excess of propargyl bromide (Scheme 4).

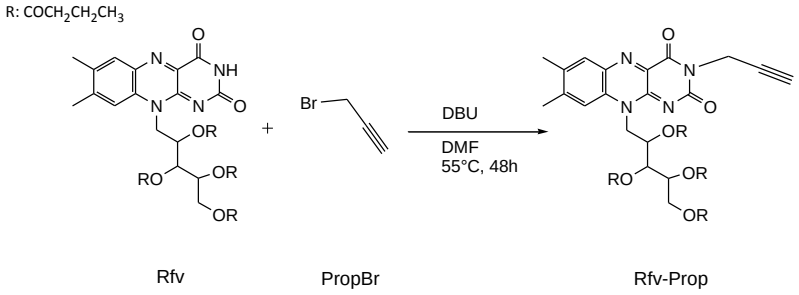

Scheme 4. Alkylation of riboflavin tetrabutyrate with propargyl bromide.

The pure product was obtained in high yield (~94%) after extraction and purification by column chromatography.
^{1}H NMR analysis confirmed the presence of the propargyl moiety in the product. The spectrum (Figure 4) clearly showed the signal at 4.85 ppm assigned to the 2 protons of the CH_2 group of the propargyl moiety (-C*H*$_2$C≡CH).

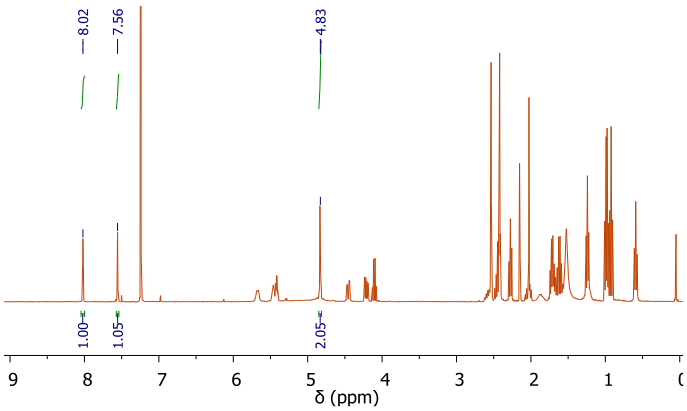

Figure 4. ^{1}H NMR spectrum of 3-propargyl-riboflavin tetrabutyrate (Rfv-Prop) in $CDCl_3$.

3.3.5 Coupling reaction of Rfv-Prop to mPEG-*b*-p(NIPAAm)-*co*-AzEMA *via* Click Chemistry

The coupling reaction of the Rfv-Prop derivative to mPEG-*b*-p(NIPAAm)-*co*-AzEMA polymer was carried out as explained in the following reaction scheme (Scheme 5), using $CuSO_4$/ascorbic acid as catalysts, and aiming to functionalize all azide containing monomers (ratio azide:alkyne 1:1).

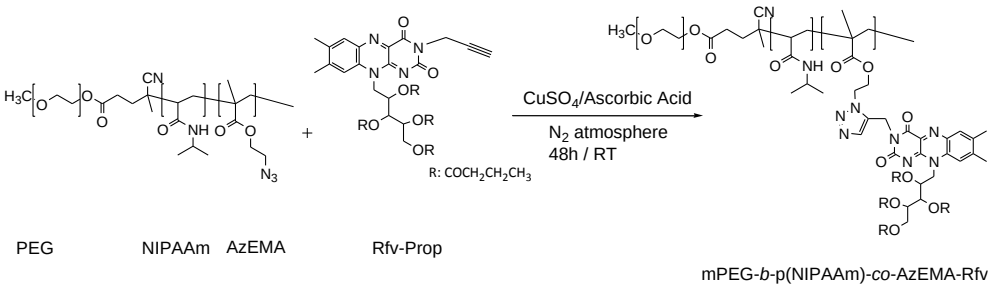

Scheme 5. Coupling reaction of Rfv-Prop to mPEG-*b*-p(NIPAAm)-*co*-AzEMA via Click Chemistry.

The polymer was collected after precipitation in cold diethyl ether, and then dialyzed against EDTA solution to purify the polymer from the Cu^+ ions. The obtained yellow polymer was analyzed by ^{1}H NMR and GPC analysis to determine M_n, M_w and PDI, and to quantify the amount of riboflavin moieties coupled to the polymer.

^{1}H NMR analysis of the block copolymer revealed the signal of PEG at 3.63 ppm (that was integrated and normalized for 455 protons, as described above); the signals of NIPAAm at 1.17 ppm (-CH(C*H*$_3$)$_2$) and 3.98 ppm (-C*H*(CH$_3$)$_2$), and the unique signal at 4.1 ppm of AzEMA. Moreover, signals of Riboflavin aromatic protons are shown at 7.97 (s, 1H) and 7.55 ppm (s, 1H) in Figure 7. The downfield region of the spectra showed an additional signal at 7.87 ppm (s, 1H), assigned to the proton of the triazolic ring formed after the click chemistry reaction. (Figure 5)

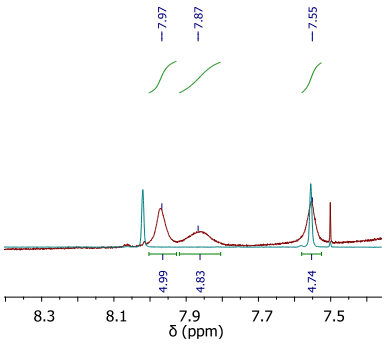

Figure 5. Zoom-in on the down field region of the overlap of the ^{1}H NMR spectra of mPEG-*b*-p(NIPAAm)-*co*-AzEMA-Rfv block copolymer (in red) and Rfv-Prop (in green) in $CDCl_3$.

From this analysis, it was possible to quantify the coupling efficiency of Rfv-Prop, using the integration values of the signals at 7.97 (s, 1H), 7.55 ppm (s, 1H) and 7.87 ppm (s, 1H), corresponding to the aromatic protons. The average integration value of these signals was 4.85, corresponding to almost 5 monomers containing Rfv moieties *per* polymer chain (and 178 NIPAm monomers, i.e. NIPAm : Rfv = 97.2 : 2.8). From the complete ^{1}H NMR spectrum it was possible to evaluate the M_n of the polymer (Table 1), based on the same considerations made for the previous block copolymer described in 3.2. The M_n was 25.1 kDa. GPC analysis performed in the same conditions as described in 2.4, gave 29.5 kDa as M_n value and a PDI of 6.2 (Table 1), which is very high value of polydispersity that can be attributed to the latent activity of the azido-groups. In fact, the azide group has been shown to form a highly reactive nitrene upon thermolysis or photolysis, which can then undergo a side reaction, resulting in crosslinking.[55-59]
These side reactions can likely be limited to a certain extent by using lower monomer concentrations during polymerization or decreasing the polymerization reaction time.
GPC analysis was performed using a refractive index detector (RI) to determinate the molecular weights and weight distributions of the polymer. UV dual detection (346 and 447 nm, corresponding to the characteristic wavelengths of Rfv absorptions) clearly indicated that nearly all riboflavin was covalently linked to the backbone (Figure 6).

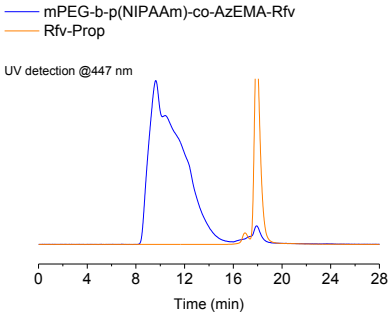

Figure 6. GPC chromatograms UV detection at a wavelength of 447 nm of free Rfv-Prop (in orange), and the click conjugate of mPEG-*b*-p(NIPAAm)-*co*-AzEMA with Rfv-Prop (in blue).

The overlapping chromatograms of the polymer mPEG-*b*-p(NIPAAm)-*co*-AzEMA-Rfv and of the free Rfv-Prop, at the same Rfv concentration, showed that at 447 nm the free Rfv-Prop eluted at 17.9 minutes, while the polymer obtained by click conjugation eluted at 9.6 minutes. The GPC analysis of the conjugated showed that the majority of the Rfv eluted at the same retention time of the polymer (RI detection, retention time of mPEG-*b*-p(NIPAAm)-*co*-AzEMA-Rfv 9.8 minutes, data not shown). A small peak was observed at the retention time of the free Rfv-Prop, residue from the purification process.

3.3.6 Cloud Point (CP)

The CPs of the block copolymers were measured by the intensity changes of scattered light from the polymers with increasing temperature. CPs of the synthetized polymers were obtained by measuring the light scattering intensity against the temperature rate and the onset on the X-axis was considered as the cloud point. For the mPEG-*b*-p(NIPAAm)-*co*-AzEMA block copolymer the CP found was 27 °C (in agreement with published data).[43] For the mPEG-*b*-p(NIPAAm)-*co*-AzEMA-Rfv polymer a CP 24 °C was found. As expected, the CP of the polymer with even only 2.8% of the monomers containing Rfv resulted be lower than the one without Rfv, which can be explained by the fact that Rfv contributes to increasing the hydrophobicity of the polymer chains.

The self-assembly behavior of polymers was indeed found to be a reversible process with an observed cooling hysteresis attributed to the restricted mobility of the phase separated polymer chains.

These data were confirmed by DSC analysis. In general, the characteristic phase separation temperatures have been defined as the onset of the transition endotherm (as the temperature at the peak of the thermogram).[47] From DSC analysis, the LCSTs of the mPEG-*b*-p(NIPAAm)-*co*-AzEMA block copolymer found were 26 °C and 24 °C for the mPEG-*b*-p(NIPAAm)-*co*-AzEMA-Rfv polymer.

The properties of both polymers obtained by ^{1}H-NMR, DSC and light scattering techniques are summarized in Table 1.

The enthalpy values obtained from the DSC analysis from the transition towards a dehydrated state of polymers was 1.59 J/g for the mPEG-*b*-p(NIPAAm)-*co*-AzEMA block copolymer, and 0.79 J/g for the mPEG-*b*-p(NIPAAm)-*co*-AzEMA-Rfv polymer, indicating that the polymer modified even with only 2.8% of Riboflavin containing monomers needs less energy to dehydrate.

Table 1. Summary of the characteristics of mPEG-*b*-p(NIPAAm)-*co*-AzEMA and mPEG-*b*-p(NIPAAm)-*co*-AzEMA-Rfv block copolymers.

	PEG:NIPAAm		%AzEMA		%Rfv	M_n (kDa)[a]	M_n (kDa)[b]	M_w/M_n [b]	LCST (°C)[c]	CP (°C [d]
	Feed	Obtained [a]	Feed	Obtained	Obtained [a]					
mPEG-*b*-p(NIPAAm)-*co*-AzEMA	1:168	1:178	5	ND	-	25.12	29.2	2.5	26	27
mPEG-*b*-p(NIPAAm)-*co*-AzEMA-Rfv					2.8	25.14	29.6	6.2	24	24

ND: not detected, [a] determined by ^{1}H NMR, [b] determined by GPC, [c] determined by DSC, [d] determined by light scattering.

3.3.7 Considerations about the contribution afforded by Riboflavin frameworks bound at the polymer backbone to the stability of the generated micellar core

In this study, we introduced a tetra esterified Riboflavin framework (Rfv) at the side chains of the outer blocks of the polymer backbone that are potentially able to establish effective supramolecular interactions with each other. Such interactions may significantly increase the stability of the final micellar nanostructure formed by this derivatized polymer.

Indeed, the isoalloxazine ring of Rfv is well known to have a high propensity for forming charge-transfer complexes based on π–π stacking, H-bond and electrostatic interactions with twin molecules, or other suitable aromatic molecular partners.[52] In general, the most stable dimeric adducts of Rfv are those displaying a parallel or T-shaped conformation of the aromatic planes, i.e. supramolecular species that are essentially isoenergetic and represent geometries of minimal energy.[52]

Hence, we performed some preliminary molecular modeling studies, based on semi-empirical calculations (functional AM1), aimed to elucidate the most favorable supramolecular geometries that can be formed by self-assembly of couples of Rfv frameworks. The obtained results are shown in Figure 7, and they pointed out that, in principle, several reciprocal 3D dispositions of the Rfv frameworks showed energetically favorable interactions that could potentially improve the stability of the micellar core.

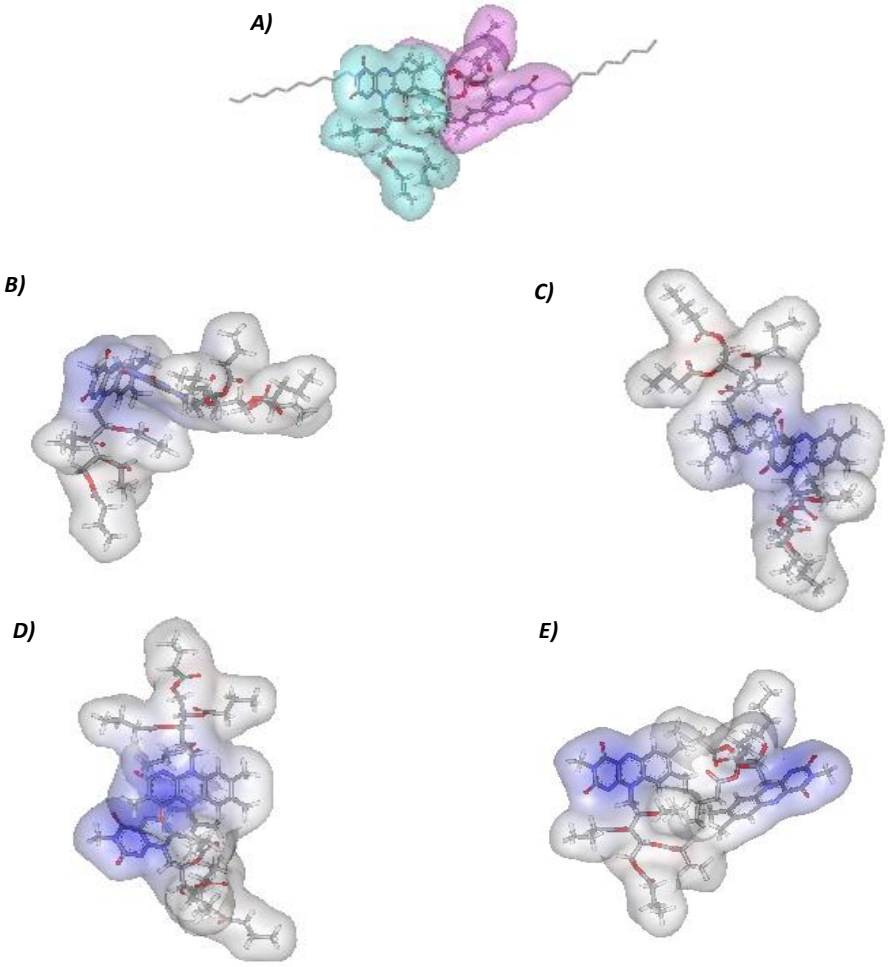

Figure 7. Minimum energy geometries of dimers of Riboflavin tetrabutyrate molecules optimized by molecular modeling calculations: **(A**) most stable adduct formed between two units of Rfv bonded to examples of polymeric chain: effective electrostatic interactions established between isoalloxazine ring and tetra-esterified ribose-moiety; **(B)** more stable "plane-to-edge" disposition of two units of Rfv; **(C)** more stable "plane-to-plane" disposition of two units of Rfv; **(D)** less stable "plane-to-plane" disposition of two units of Rfv; **(E)** less stable "plane-to-edge" disposition of two units of Rfv.

Among these, the most effective one displays a clear extensive involvement of the tetra-esterified ribose-moiety belonging to one of the two Rfv frameworks in the establishment of effective electrostatic interactions with the isoalloxazine ring belonging to the other supramolecular partner (Figure 7B). With respect to this dimeric geometry, the supramolecular association derived by the establishment of C-H... π interactions between the isoalloxazine rings of two units of Rfv, resulted be just a bit less effective, from an energetic point of view (~1.4 kcal×mol^{-1}). In such a supramolecular geometry, aligned according to a "plane-to-plane" disposition (Figure 7C), the flavins display their pyrimidine rings aligned and pointing along opposite direction. On the contrary, calculations also predicted that much less favorable C-H... π interactions (equal to approximately 12 kcal×mol^{-1}) can be established if the "plane-to-edge" aligned isoalloxazine rings point their pyrimidine rings in opposite directions (Figure 7E). Finally, although less effective (for about 3.6 kcal×mol^{-1}) than the first type of the above quoted C-H... π recognition, also the establishment of π…π interactions was assessed giving rise to an acceptable contribution able to improve the stability of the micellar core, providing that, in this case, the "plane-to-plane" aligned flavins point their pyrimidine rings in the same direction (Figure 7D).

However, overall, it is obvious that all the above analyzed molecular dockings, concerning dimers of Rfv, can only be considered as strongly simplified models of the possible interactions that may play a role in the generation of a very complex micellar core system, on which the tetra-esterified form of Rfv might occupy a large volume. This phenomenon can contribute to the less dense structure of the core of the obtained micelle. Moreover, in the core of the micelles a much greater number of Rfv units is present, which was not taken into account in this modelling experiment.

3.3.8 Empty and drug-loaded micelles preparation and characterization

In this work, due the thermosensitivity of the synthesized amphiphilic polymers, empty and drug-loaded micelles could be formed by a fast heating procedure, by heating the polymers solutions above their CPs. PTX was loaded by simply mixing of a small volume of concentrated PTX solution in ethanol with aqueous polymeric solutions at 4°C, subsequently heated to 50 °C in a water bath while stirring. Z-average hydrodynamic diameters of empty micelles prepared by this method at a concentration of 1 mg/ml in water and PBS was detected by DLS.
For the mPEG-*b*-p(NIPAAm)-*co*-AzEMA based micelles in water and in PBS, Z-average were 50 and 60 nm, respectively. For micelles based on mPEG-*b*-p(NIPAAm)-*co*-AzEMA-Rfv polymer, the mean diameters found were 90 and 150 nm in water and in PBS respectively. This noticeable increase in micelles size in PBS compared to water can be attributed to a salting-out effect of ions presents in the buffer.[48] For all the preparations, the polydispersity index was low (from 0.03 to 0.25). Micelles prepared starting from different polymer concentrations (0.5, 1, 2 and 3 mg/ml) in water and PBS were also analyzed in terms of size, polydispersity and count rate and for both the media. Remarkably the size of micelles based on mPEG-*b*-p(NIPAAm)-*co*-AzEMA-Rfv polymer resulted be concentration dependent, while the micelle size of mPEG-*b*-p(NIPAAm)-*co*-AzEMA was concentration independent (Figure 8). This phenomenon could be attributed to the fact the Rfv-derivatized polymer was partially cross-linked (as described in 3.5) and did not dissolve properly in the aqueous media, during the sample preparation for the further micelles formation.

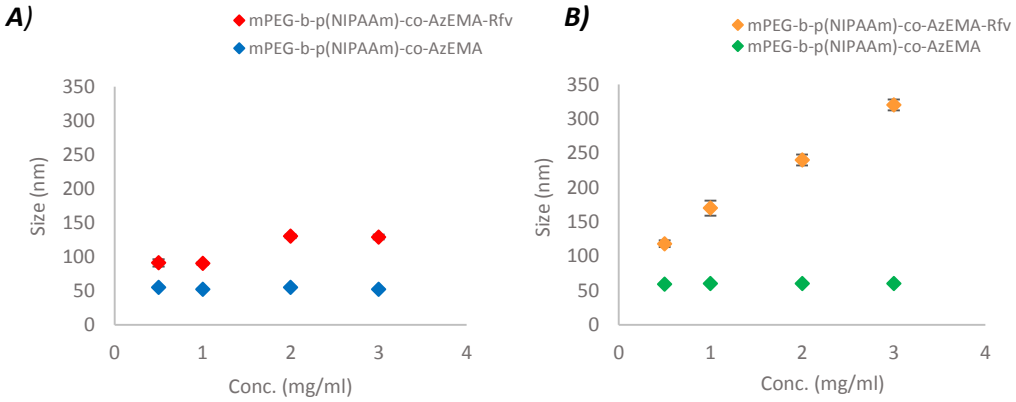

Figure 8. Z-Average hydrodynamic diameter of empty polymeric micelles in water **(A)** and PBS **(B)** media. Data points are average values. Error bars indicate standard deviations (n=3).

PTX loaded micelles were prepared as described in 3.2.10 and the micellar dispersions were analyzed in term of size by DLS measurements. (Table 2) Dispersions of PTX-loaded micelles of mPEG-*b*-p(NIPAAm)-*co*-AzEMA and mPEG-*b*-p(NIPAAm)-*co*-AzEMA-Rfv prepared at polymer/drug ratio of 2/1, were opalescent and homogeneous.

Table 2. Z-average size of empty and PTX-loaded micelles based on mPEG-*b*-p(NIPAAm)-*co*-AzEMA and mPEG-*b*-p(NIPAAm)-*co*- AzEMA-Rfv polymers. The size of the PTX-loaded micelles are relative to the feed drug loading concentration tested of 5, 10 and 20 % w/V (PTX5, PTX10 and PTX20 respectively).

Z_{ave} ± SD *	Empty micelle	PTX-loaded micelle (PTX5)	PTX-loaded micelle (PTX10)	PTX-loaded micelle (PTX20)
mPEG-*b*-p(NIPAAm) -*co*-AzEMA	60 ± 4 nm	71 ± 2nm	75 ± 3nm	76 ± 3 nm
mPEG-*b*-p(NIPAAm) -*co*-AzEMA-Rfv	150 ± 3 nm	168 ± 3nm	175 ± 5 nm	178 ± 3 nm

*(pol. conc. 1mg/ml in PBS)

After removing the precipitated non-encapsulated drug, the Encapsulation Efficiency (EE%) and Drug Loading (DL%) (for all the feed drug loadings tested) in mPEG-*b*-p(NIPAAm)-*co*-AzEMA-Rfv based micelles resulted be higher than in the mPEG-*b*-p(NIPAAm)-*co*-AzEMA based ones, indicating that micelles with aromatic groups are better capable to solubilize hydrophobic drugs such as PTX. (Figure 9)

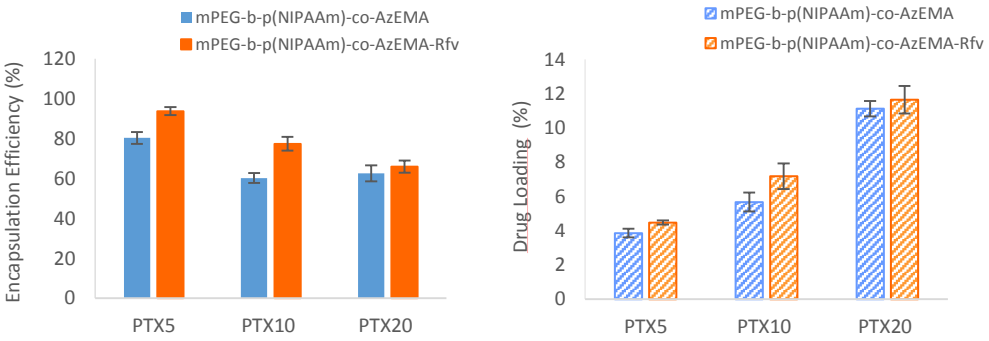

Figure 9. Encapsulation Efficiency (EE%) and Drug Loading (DL%) of PTX-loaded micelles relative to the feed drug loading concentration tested of 5, 10 and 20 % w/V (PTX5, PTX10 and PTX20 respectively). Data points are average values. Error bars indicate standard deviations (n=3).

In detail, EE% of 80.3 ± 3.8, 60.2 ± 5.7 and 62.6 ± 11.6 % were obtained for mPEG-*b*-p(NIPAAm)-*co*-AzEMA based micelles, for the 5, 10 and 20% feed PTX loadings respectively. For mPEG-*b*-p(NIPAAm)-*co*-AzEMA-Rfv based micelles, EE% values reached 93.7 ± 2, 77.4 ± 3.5 and 65.9 ± 3 for the three different feed PTX loadings, respectively. As expected, for all formulations, the encapsulation efficiency was

highest for the lowest feed drug loading, showing clearly that the EE% of PTX decreases when the feed concentration increased from 5 to 20%.
The overall drug loading % of mPEG-*b*-p(NIPAAm)-*co*-AzEMA based micelles with different drug feeds were 3.8 ± 0.25, 5.7 ± 0.55 and 11.1 ± 0.54 % , and 4.5 ± 0.12, 7.2 ± 0.75 and 11.6 ± 0.8 % for the mPEG-*b*-p(NIPAAm)-*co*-AzEMA-Rfv based micelles, showing again that a more efficient encapsulation was obtained for micelles based on the more hydrophobic polymer. Nevertheless, the highest DL% value related to the starting feed drug loading, was obtained for the mPEG-*b*-p(NIPAAm)-*co*-AzEMA-Rfv based micelle with a 5% of feed PTX loading.

3.3.9 *In vitro* drug release study

Drug release from the micelles at pH 7.4 in phosphate buffer at 37 °C was studied by measuring the residual drug concentration into micelles dispersion. (Figure 10) For each PTX-loaded micelle formulation, aliquots were taken at different time points (2, 4, 6, 8, 12 and 24 h), which were centrifuged to spin down the released PTX that crystallized because of its low water solubility (5.56 μg/ml). Then, for each aliquot the amount of the residue drug (in %) retained into micelles was evaluated (drug concentration was evaluated by HPCL method as described in 3.2.11).

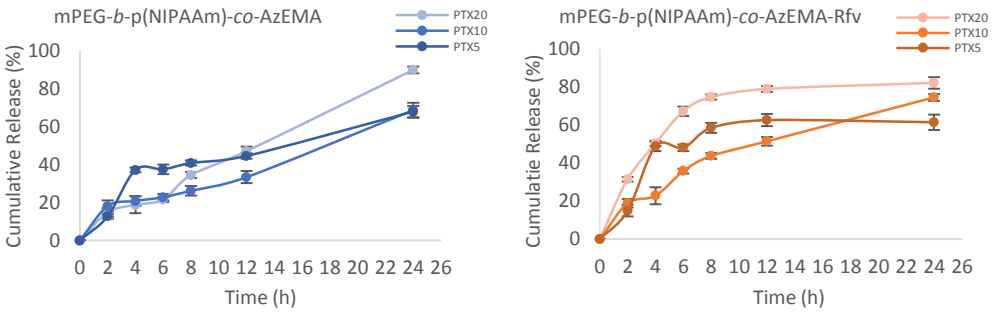

Figure 10. Cumulative release profile (%) of PTX from mPEG-*b*-p(NIPAAm)-*co*-AzEMA and mPEG-*b*-p(NIPAAm)-*co*-AzEMA-Rfv based micelles, prepared in PBS, pH 7.4, at 37 °C. Data points are average values. Error bars indicate standard deviations (n=3).

Unfortunately, PTX was not retained for long periods of time in both types of micelles with a complete release within 24h. In particular, the formulations of 20% feed drug loading were the most unstable and the drug was released fastest, while a lower drug feed loading resulted in a slightly slower release. Furthermore, the release was faster for mPEG-*b*-p(NIPAAm)-*co*-AzEMA-Rfv formulations (for all the feed drug loadings tested), which can be explained by the fact that these micelles were bigger, and therefore less dense than the mPEG-*b*-p(NIPAAm)-*co*-AzEMA based ones resulting in a faster diffusion of the drug.

3.4 Conclusions and Future Plans

A thermosensitive amphiphilic block polymer consisting of mPEG-*b*-p(NIPAAm)-*co*-AzEMA was synthetized having on average 5 AzEMA monomer per polymer. A propargyl derivative of Riboflavin (Rfv-Prop) was synthesized and covalently coupled to the azide modified diblock copolymers by Copper(I)-catalyzed Azide-Alkyne Cycloaddition (CuAAC). Both the obtained block-copolymers self-assembled into polymeric micelles above their characteristic CPs. The CP was affected by the coupling of Rfv resulting in a slightly lowered CP for the polymer with Riboflavin coupled to it, due to the increased hydrophobicity of the polymer. Also, micellar size was increased by the presence of Rfv, while the size increased slightly more upon loading of the poorly water-soluble anticancer drug Paclitaxel (PTX). Both types of micelles displayed a high Loading Efficiency, in particular higher for the mPEG-*b*-p(NIPAAm)-*co*-AzEMA-Rfv based micelle. The high drug loading of these micelles show their potentially interesting properties for controlled drug release applications. In this study, we observed that the drug release needs optimization, which may be obtained by increasing the Rfv amount conjugated to the backbone, meaning further increasing in hydrophobicity and possibly achieving better spatial arrangement of the flavin units as displayed in the modeling experiments. Therefore, before considering evaluation *in vivo*, a further optimized release profile needs to be obtained followed by *in vitro* cytotoxicity tests of these formulations.

References

(1) V. P. Torchilin, Micellar nanocarriers: Pharmaceutical perspectives. *Pharmaceutical research* **2007**; 24: 1-16

(2) S. Forsters; T. Plantenberg; From self-organizing polymers to nanohybrid and biomaterials. *Angewandte Chemie-International Edition* **2002**; 41: 689-714

(3) M. Talelli et al, Micelles based on HPMA copolymers. *Advanced Drug Delivery Reviews* **2010**; 62: 231-239

(4) K. Yasugi, Y. Nagasaki, M. Kato, K. Kataoka, Preparation and characterization of polymer micelles from poly(ethylene glycol)–poly(d,l-lactide) blockcopolymers as potential drug carrier. *J Controlled Release* **1999**; 62: 89–100

(5) H. Wei, X. Zhang, C. Cheng, S. X. Cheng, R. X. Zhuo, Self-assembled, thermosensitive micelles of a star block copolymer based on PMMA and PNIPAAm for controlled drug delivery. *Biomaterials* **2007;** 28: 99–107

(6) O. Soga, C. F. van Nostrum, W. E. Hennink, Thermosensitive and biodegradable polymeric micelles for paclitaxel delivery. *J. Controlled Release* **2005**; 101: 383–385

(7) S. Hirotsu, Y. Hirokawa, T. Tanaka, Volume-phase transition of ionised *N*-isopropylacrylamide gels. *J Chem Phys* **1987**; 87: 1392–5

(8) F. M. Winnik. Fluorescence studies of aqueous solutions of poly(*N*-isopropylacrylamide) below and above their LCST. *Macromolecules* **1990**; 23: 233–42

(9) C. K. Che, S. Rimme, I. Souta, L .Swanson. Fluorescence investigations of the thermally induced conformational transition of poly(N-isopropylacrylamide). *Polymer* **2001**; 42: 5079–87

(10) M. K. Yoo, Y. K. Sung, Y. M. Lee, C. S. Cho. Effect of polyelectrolyte on the lower critical solution temperature of poly(*N*-isopropylacrylamide) in the poly(NIPAAm-co-acrylic acid) hydrogel. *Polymer* **2000**; 41: 5713–9

(11) W. Xue, I. W. Hamley. Thermoreversible swelling behaviour of hydrogels based on *N*-isopropylacrylamide with a hydrophobic comonomer. *Polymer* **2002**; 43: 3069–77

(12) M. D. C. Topp, P. J. Dijkstr, H. Talsm, J. Feijen. Thermosensitive micelle-forming blockcopolymer s of poly(ethylene glycol) and poly(*N*-isopropylacrylamide). *Macromolecules* **1997**; 30: 8518–20

(13) C. J. Rijcken, C. J. Snel, R. M. Schiffelers, C. F. van Nostrum, W. E. Hennink. Hydrolysable core-crosslinked thermosensitive polymeric micelles: synthesis, characterisation and in vivo studies. *Biomaterials* **2007**; 28: 5581–5593

(14) K. M. Huh,H. S. Min, S. C. Lee, H. J. Lee, S. Kim, K. Park, Doxorubicin-loaded cholic acid-polyethyleneimine micelles for targeted delivery of antitumor drugs: synthesis, characterization, and evaluation of their in vitro cytotoxicity. *J. Controlled Release* **2008**; 126: 122–129

(15) H. Engelkamp, S. Middelbeek, JM, R. *Science* **1999**; 284: 785–788

(16) M. G. Carstens, P. H. de Jong, C. F. van Nostrum, J. Kemmink, R. Verrijk, L. G. J. de Leede, D. J. A. Crommelin, W. E. Hennink, The effect of core composition in biodegradable oligomeric micelles as taxane formulations. *Eur. J. Pharm. Biopharm*. **2008**; 68: 596–606

(17) M. G. Carstens,J. J. L. Bevernage, C. F. van Nostrum, M. J. van Steenbergen, F. M. Flesch, R. Verrijk, L. G. J. de Leede, D. J. A. Crommelin, W. E. Hennink, Photocytotoxicity of mTHPC (Temoporfin) Loaded Polymeric Micelles Mediated by Lipase Catalyzed Degradation. *Macromolecules* **2007**; 40: 116−122

(18) B. S. Kim, S. W. Park, P. T. Hammond, *ACS Nano* **2008**; 2: 386−392

(19) N. Kang, M. E. Perron, R. E. Prud'Homme, Y. Zhang, G. Gaucher, J. C. Leroux; Stereocomplex block copolymer micelles: core-shell nanostructures with enhanced stability. *Nano Lett*. **2005**; 5: 315−319

(20) H. Wei, S. X. Cheng, X. Z. Zhang, R. X. Zhuo, Thermo-sensitive polymeric micelles based on poly(*N*-isopropylacrylamide) as drug carriers. *Prog. in Poly. Science* **2009**; 34: 893**–**910

(21) N. Bextsinna, M. Solé. N. Taib, I. Bestel, Bioengineered riboflavin in nanotechnology. *Biomaterials*, **2016**; 80: 121-133

(22) H. J. Powers, Riboflavin (vitamin B-2) and health, *Am. J. Clin. Nutr*. **2003**; 77: 1352-1360

(23) M. E. Mertens, J. Frese, D. A. B€olükbas, L. Hrdlicka, S. Golombek, S. Koch, P. Mela, S. Jockenhovel, F. Kiessling, T. Lammers, FMN-coated fluorescent USPIO for cell labeling and non-invasive MR imaging in tissue engineering, *Theranostics* **2014;** 4: 1002-1013

(24) A. K. Nguyen, S. D. Gittard, A. Koroleva, S. Schlie, A. Gaidukeviciute, B. N. Chichkov, R. J. Narayan, Two-photon polymerization of polyethylene glycol

diacrylate scaffolds with riboflavin and triethanolamine used as a water-soluble photoinitiator*, Regen. Med*. **2013**; 8: 725-738

(25) J. Jayapaul, S. Arns, W. Lederle, T. Lammers, P. Comba, J. G€atjens, F. Kiessling, Riboflavin carrier protein-targeted fluorescent USPIO for the assessment of vascular metabolism in tumors, *Biomaterials* **2012**; 33: 8822-8829

(26) J. Jayapaul, M. Hodenius, S. Arns, W. Lederle, T. Lammers, P. Comba, F. Kiessling, J. Gaetjens, FMN-coated fluorescent iron oxide nanoparticles for RCP-mediated targeting and labeling of metabolically active cancer and endothelial cells, *Biomaterials* **2011;** 32: 5863-5871

(27) Y. Tsvetkova, N. Beztsinna, J. Jayapaul, M. Weiler, S. Arns, Y. Shi, T. Lammers, F. Kiessling, Refinement of adsorptive coatings for fluorescent riboflavin receptor-targeted iron oxide nanoparticles, *Contrast Media Mol. Imaging* **2016**; 11: 47-54

(28) A. B. Witte, C. M. Timmer, J. J. Gam, S. K. Choi, M. M. Banaszak Holl, B. G. Orr, J. R. Baker, K. Sinniah, Biophysical characterization of a riboflavin-conjugated dendrimer platform for targeted drug delivery, *Biomacromolecules* **2012**; 13: 507-516

(29) A. B. Witte, A. N. Leistra, P. T. Wong, S. Bharathi, K. Refior, P. Smith, O. Kaso, K. Sinniah, S. K. Choi, Atomic force microscopy probing of receptor-nanoparticle interactions for riboflavin receptor targeted gold dendrimer nanocomposites*, J. Phys. Chem. B* , **2014;** 118: 2872-2882

(30) T. P. Thomas, S. K. Choi, M. H. Li, A. Kotlyar, J. R. Baker, Design of riboflavinpresenting PAMAM dendrimers as a new nanoplatform for cancer-targeted delivery*, Bioorg. Med. Chem*. **2010**; 20: 5191-5194

(31) F. Marlin, P. Simon, S. Bonneau, P. Alberti, C. Cordier, C. Boix, L. Perrouault, A. Fossey, T. Saison-Behmoaras, M. Fontecave, C. Giovannangeli, Flavin conjugates for delivery of peptide nucleic acids, *ChemBioChem*, **2012**; 17: 2593-2598

(32) S. R. Holladay, Z. Yang, M. D. Kennedy, C. P. Leamon, R. J. Lee, M. Jayamani, T. Mason, P. S. Low, Riboflavin-mediated delivery of a macromolecule into cultured human cells, *Biochim. Biophys. Acta 1426*, **1999**; 1: 195-204

(33) M. Ebitani, Y. In, T. Ishida, K.-i. Sakaguchi, J. L. Flippen-Anderson, I. L. Karle, Structures of riboflavin tetraacetate and tetrabutyrate: molecular packing mode of riboflavin tetracarboxylate and its extensive stacking and hydrogen-bonding characteristics. *Acta Cryst.*, **1993**; B49: 136-144

(33) H. C. Kolb, and K. B. Sharpless, The growing impact of click chemistry in drug discovery. *Drug Discovery Today*, **2003**; 8: 1128-1137

(34) H. C. Kolb, M. G. Finn, K. B. Sharpless, Click chemistry: diverse chemical function from a few good reaction. *Angew. Chem., Int. Ed.*, **2009**; 40: 2004-2021

(35) P. L. Golas, K. Matyjaszewsky, Marrying click chemistry with polymerization: Expanding of polymeric materials. *Chem. Soc. Rev.* **2010;** 39: 1338-1354

(36) M. Van Dijk, D. T. S. Rijkers, R. M. J. Liskamp, C. F. Van Nostrum, W. E. Hennink, Synthesis and application of biomedical and pharmaceutical polymers via click chemistry methodologies, *Bioconjugate Chem.*, **2009**;20: 2001-2016

(37) S. Singh, N. K.Mehra, N. K. Jain, Development and Characterization of the Paclitaxel loaded Riboflavin and Thiamine Conjugated Carbon Nanotubes for Cancer Treatment. *Pharm. Res.*, **2016**, 33: 1769–1781

(38) F. Danhiera, N. Lecouturiera, B. Vromana, C. Jérômeb, J. Marchand-Brynaertc, O. Ferond, V. Préata, Paclitaxel-loaded PEGylated PLGA-based nanoparticles: *In vitro* and *in vivo* evaluation. *J. Controlled Release*, **2009**; 133: 11–17

(39) T. Yang, M.K. Choi, Preparation and evaluation of Paclitaxel-loaded PEGylated immunoliposome. *J. Control. Release*, **2007**; 120: 169–177

(40) R. T. Liggins, H. M. Burt, Paclitaxel-loaded poly(l-lactic acid) microspheres 3: blending low and high molecular weight polymers to control morphology and drug release. *Int. J. Pharm.*, **2004**; 282: 61–71

(41) K. M. Huh, H. S. Min, S. Cheon Lee, H. J. Lee, S. Kim, K. Park A new hydrotopic block copolymer micelle system for aqueous solubilization of Paclitaxel. *J. Control. Release*, **2008**; 126: 122–129

(42) Z. Zhang, S.-S. Feng, The drug encapsulation efficiency, in vitro drug release, cellular uptake and cytotoxicity of Paclitaxel-loaded poly(lactide)-tocopheryl polyethylene glycol succinate nanoparticles. *Biomaterials*, **2006**; 27: 4025–4033

(43) D. Neradovic, C. F. van Nostrum, and W. E. Hennink, Thermoresponsive Polymeric Micelles with Controlled Instability Based on Hydrolytically Sensitive *N*-Isopropylacrylamide Copolymers, *Macromolecules* **2001**; 34: 7589-7591

(44) M. Talelli, K. Morita, C. J. F. Rijcken, R. W. M. Aben, T. Lammers, H. W. Scheeren, C. F. van Nostrum, G. Storm, and W. E. Hennink, Synthesis and Characterization of Biodegradable and Thermosensitive Polymeric Micelles with Covalently Bound Doxorubicin-Glucuronide Prodrug via Click Chemistry, *Bioconjugate Chem.*, **2011**; 22: 2519–2530

(45) Y. Zhang, H. He, C. Gao and J. Wu, Covalent Layer-by-Layer Functionalization of Multiwalled Carbon Nanotubes by Click Chemistry. *Langmuir* **2009**; 25: 5814–5824

(46) R. De Vos, E. J. Goethals, End group analysis of commercial poly(ethylene glycol) monomethyl ether's. *Polymer Bulletin* **1986**; 15: 547-549

(47) C. Boutris, E. G. Chatzi and C. Kiparissides., Characterization of the LCST behaviour of aqueous poly(*N*-isopropylacrylamide) solutions by thermal and cloud point techniques. *Polymer* **1997**; 38: 2567-2570

(48) D. Neradovic, O. Soga, C. F. Van Nostrum, W. E. Hennink, The effect of the processing and formulation parameters on the size of nanoparticles based on block copolymers of poly(ethylene glycol) and poly(*N*-isopropylacrylamide) with and without hydrolytically sensitive groups. *Biomaterials* **2004;** 25: 2409-2418

(49) G. Kwon, M. Naito, M. Yokoyama, T. Okano, Y. Sakurai, K. Kataoka, Block copolymer micelles for drug delivery: Loading and release of doxorubicin. *J. Controlled Release* **1997**; 48: 195−201

(50) A. L. Z. Lee, S. Venkataraman, S. Sirat, S. Gao, J. L. Hedrick, Y. Y. Yang. The use of cholesterol-containing biodegradable block copolymers to exploit hydrophobic interactions for the delivery of anticancer drugs. *Biomaterials* **2011;** 33: 1921−1928

(51) Y. Shi, M. J. van Steenbergen, E. A. Teunissen, L. Novo, S. Gradmann, M. Baldus, C. F. van Nostrum, W. E. Hennink. Π−Π Stacking Increases the Stability and Loading Capacity of Thermosensitive Polymeric Micelles for Chemotherapeutic Drugs. *Biomacromolecules* **2013**; 14: 1826-1837

(52) H. Suzuki, R. Inoue, S. Kawamorita, N. Komiya, Y. Imada, and T. Naota; Highly Fluorescent Flavins: Rational Molecular Design for Quenching Protection Based on Repulsive and Attractive Control of Molecular Alignment. *Chem. Eur. J.* **2015**; 21: 9171 – 9178

(53) L. Zhang and A. Eisenberg. Multiple morphologies of crew-cut aggregates of polystyrene-b-poly(acrylic acid) block copolymers. *Science,* **1995***,* 268: 1728-1731

(54) J. H. Kim, J. O. Lee, N. Kim, H. J. Lee, Y. W. Lee, H. I. Kim, et al, Paclitaxel suppresses the viability of breast tumor MCF7 cells through the regulation of EF1α and FOXO3a by AMPK signaling. *Int J Oncol*., **2015**; 47: 1874-80

(55) Y. Li, J. Yang, B. C. Benicewicz, Well-Controlled Polymerization of 2-Azidoethyl Methacrylate at Near Room Temperature and Click Functionalization. *J. of Pol. Sc.: Part A: Pol. Chem.*, **2007**, 45: 4300–4308

(56) J. Bang, J. Bae, P. Löwenhielm, C. Spiessberger, S. A. Given-Beck, T. P. Russell, and C. J. Hawker, Facile Routes to Patterned Surface Neutralization Layers for Block Copolymer Lithography. *Adv. Mater.,* **2007**, 19: 4552–4557

(57) M. G.-Burgos, A. Alegría, A. Arbe, J. Colmeneroa, and J. A. Pomposo, An unexpected route to aldehyde-decorated single-chain nanoparticles from azides. *Polym. Chem*., **2016**, 7: 6570

(58) D. Hua , W. Bai , J. Xiao , R. Bai , W. Lu , and C. Pan, A Strategy for Synthesis of Azide Polymers via Controlled/Living Free Radical Copolymerization of Allyl Azide under ^{60}Co γ-ray Irradiation. *Chem. Mater.,* **2005**, 17: 4574–4576

(59) K. Schuh, O. Prucker, and J. Ru¨he, Surface Attached Polymer Networks through Thermally Induced Cross-Linking of Sulfonyl Azide Group Containing Polymers. *Macromolecules* **2008**, 41: 9284-9289

Chapter 4

Summary and Perspectives

4.1 Summary

The research described in this thesis is focused on the design of two kinds of self-assembled nanocarriers for the delivery of hydrophobic drugs: nanohydrogels and micelles that both contain a hydrophobic internal domain and a surrounding hydrophilic shell. The development of Nano Drug Delivery Systems (NDDS) is a promising approach for promoting intelligent therapeutic systems to bring significant advances in the diagnosis and treatment of diseases, with the challenges to maximize therapeutic activity and to minimize undesirable side effects.

Nanogels or nanohydrogels (NHs) are hydrophilic 3D polymer networks on the nanoscale with a tendency to swell in water when placed in an aqueous environment. NHs were first defined by Kabanov and Vinogradov to describe cross-linked bifunctional networks of a polyion and a non-ionic polymer.[1, 2] Later, Akiyoshi et al. described the phenomenon of physical cross-linking (self-assembly) of cholesterol-modified polysaccharides which resulted in formation of swollen hydrogels at nanoscale size.[3] Since then, NHs development as functional smart materials for biotechnological and biomedical applications have been exhaustively described in literature.[4-6]

Polymeric micelles are self-assembling nanosized colloidal particles with a hydrophobic core and hydrophilic shell, and they are currently successfully used as pharmaceutical carriers.[7] Micelles are formed from amphiphilic block or graft copolymers when dissolved in selective solvent (in a concentration above their CMC), phenomenon first observed by Merret in 1954.[8] Then, since Ringsdorf et al. publication,[9] micelles where proposed and investigated for the last three decades as promising drug delivery systems for a broad variety of applications, especially in biomedical field. [7, 10, 11]

Typical advantages from the use of these self-assembled nanostructures in the nanomedicine field, are the possibility to obtain an elevated degree of encapsulation without chemical reactions of many macromolecule types, and their ability to reach the smallest capillary vessels and penetrate the tissues either through the paracellular or the transcellular pathways.[12-15]

In this thesis, data from studies done on Hyaluronan based nanohydrogel and pNIPAAm based micelles are reported with emphasis on the synthetic strategies for polymers modification (in particular exploit by azido-alkyne *click chemistry* reaction) and their extensive characterization, nanostructures formulation and subsequent drugs loading capacity investigation.

Chapter 1 of the thesis provide a general introduction on the development of Nano Drug Delivery Systems (NDDS) such as polysaccharide based NHs and polymeric micelles, and their promising approach for developing intelligent therapeutic systems. In particular, Hyaluronan based NHs and thermosensitive poly(NIPAAm) based micelle were introduced. Moreover, riboflavin 2',3',4',5'-tetrabutyrate was introduced and used in this work, in order to provide the needed amphiphilic character of the chosen polymers necessary to provide the aimed self-assembled nanostructures. The use of Rfv in nanomedicine field indeed represent a promising alternative, due to its biocompatibility, low cost, versatile chemistry and specific transporter systems overexpressed in metabolically active cells. To the end, Copper(I)-catalyzed Azide-Alkyne Cycloaddition (CuAAC) reaction, well known as azido-alkyne *click chemistry* reaction, was mentioned as synthetic strategy used for the polymers modification. Generally, click chemistry reactions are modular, wide in scope, high yielding, create only inoffensive by-products, stereospecific, simple to perform and that require benign or easily removed solvent.[16] Finally, the aims of the thesis were outlined.

Nowadays, polysaccharide-based nanoparticles have been proposed for innovative NDDSs due to their unique multi-functional groups in addition to their physicochemical properties, in particular their marked biocompatibility and biodegradability.[17] Among polysaccharides, hyaluronic acid (HA) seems to be one of the most interesting material for the development of biocompatible drug carriers. In **Chapter 2**, hyaluronan was chosen as representative of anionic polysaccharide, from which an amphiphilic polymer was obtained after conjugation of riboflavin tetrabutyrate (Rfv) as hydrophobic moiety, to form NHs by self-assembly. Different M_w of hyaluronan were first modified with a propargylic portion (Prop) suitable for the coupling on it of the azido-derivative of riboflavin ($RfvN_3$) *via* azide-alkyne click chemistry reaction. In the chapter, all the synthetic strategies and the characterization techniques, in terms of degree of substitution (DS) obtained with the Prop and $RfvN_3$ portions and in terms of the ability to form self-assembled NHs, are described and discussed. In particular, HA derivatization with propargylic portion was always a good strategy to easily modify the polymer chains and obtain a derivative in high yield and with a good derivatization degree.

The coupling with $RfvN_3$ by click chemistry, as expected, resulted in quantitative derivatization, due to the high efficacy and selectivity of this kind of reaction. Next, the HA-*c*-Rfv derivatives were tested with a new method to obtain NHs, i.e. the autoclaving process, to generate in one-step spontaneously sterile NHs by self-assembling of the polymer chains under thermal treatment.[18] HA-*c*-Rfv NHs showed a good average size (depending on the M_w of HA derivative used and its DS with Prop and Rfv), low PDI and high stability in aqueous suspensions. Then, the nano-carrier ability to load by physical interaction hydrophobic model drugs was successfully tested. These NHs indeed have been used to solubilize piroxicam,

dexamethasone and paclitaxel resulting in an increase of their water solubility of 12, 3 and 25-fold respectively. Moreover, in order to obtain a long-life preparation of NHs, a cryoprotectant solution (1 % w/V dextrose) was added to the drug-loaded NHs before their storage for several months after freeze-drying, due to the fact that cryoprotection with sugars significantly enhanced the ability to re-suspend nanoparticles after freeze-drying without aggregation. Lastly, with the aim to have a prolonged blood circulation of these nanostructures, a PEG-HA-*c*-Rfv product was synthetized from HA-*c*-Rfv derivative that presented free propargylic moieties available for the *click* coupling of a PEG-N_3, because PEGylation has recently been shown to dramatically improve particle transport through biological obstacles.

For polymeric micelles, a promising strategy to be successful in field of drug delivery the drug should be released only after it accumulates at the targeted tissue in a controlled manner by using i.e. stimulus responsive systems. Stimulation by either a physiological or an external trigger then results in the destabilization of micelles. An important class of stimuli-responsive micelles are those comprising polymers with thermosensitive behavior, of which the aqueous solution properties are temperature dependent.[19] In **chapter 3**, thermosensitive polymeric micelles based on poly(*N*-isopropylacrylamide) (pNIPAAm) have been investigated. In particular, mPEG-*b*-p(NIPAAm)-*co*-AzEMA AB block-copolymer was synthesized by free radical polymerization using a polyethylene glycol based macroinitiator. Subsequently, a propargylic derivative of riboflavin tetratubutyrate (RfvProp) was conjugated by azido-alkyne *click reaction* as functional groups facilitating π-π stacking interactions to stabilize these micelles. The mPEG block is hydrophilic, while the p(NIPAAm) block is thermosensitive, and therefore when aqueous solutions of this polymer were heated from 4°C to above the LCST of the thermosensitive block, micelles were formed consisting in mPEG corona and p(NIPAAm)-AzEMA or p(NIPAAm)-AzEMA-Rfv core, respectively.
Noteworthy, Rfv contributed to an increase of the hydrophobicity of the polymer, resulting in reduction of the cloud point of the thermosensitive block (from 27°C for mPEG-*b*-p(NIPAAm)-*co*-AzEMA to 24°C for mPEG-*b*-p(NIPAAm)-*co*-AzEMA-Rfv), and in less energy needed to dehydrate for the polymers during micelle formation. The possibility of the Rfv framework to establish effective supramolecular interactions with each other via its aromatic moieties was investigated by molecular modeling. In general, the most stable dimeric adducts of Rfv are those displaying a parallel or T-shaped conformation of the aromatic planes.[20] Based on the modeling experiments, some possible interactions were identified that may play a role in the generation of a complex micellar core system in which the tetra-esterified form of Rfv occupies a relatively large volume, resulting, in less dense structure of the core of the obtained micelle. In addition, the high value of polydispersity obtained for the mPEG-*b*-p(NIPAAm)-*co*-AzEMA-Rfv derivative, can be attributed to the latent activity of the azido-groups, which

might suggest partial crosslinking of the polymer chains. Importantly, the poorly water-soluble anticancer drug paclitaxel (PTX) was successfully encapsulated into the micelles formed by these two synthesized polymers with a high loading efficiency, in particular higher for the mPEG-*b*-p(NIPAAm)-*co*-AzEMA-Rfv based micelle. PTX was however not retained for long periods of time in both types of micelles with a complete release within 24h.

4.2 Perspectives

The development of two kinds of self-assembled nanocarriers, i.e. nanohydrogel and micelles, is presented in this thesis, and the shown results are promising for their application in nanomedicine therapies. Nevertheless, further optimization and research is necessary to take their development to reach clinical trials. Before the clinical application, detailed pharmacokinetic and biodistribution studies need to be performed as well as efficacy studies. Moreover, improvement and more sophisticated chemical modification strategies for the polymers synthesis may enhance the preparation of well-defined polymers.

4.2.1 Polymer design

In this thesis, the main synthetic strategy used for polymers modification was 1,3-dipolar azide-alkyne cycloaddition reaction carried out under mild conditions using Cu(I) as the catalyst. Although copper catalysis has been widely employed to activate terminal alkynes in click chemistry, this may be incompatible with living systems due to toxicity of copper. Even though, in both the reaction strategies described in this thesis Cu^{+} ions were removed by work up of the products by ethylenediaminetetraacetic acid disodium salt dihydrate (EDTA) solution, enabling its chelating properties to coordinate the metal ions, that might bring, in our case, pure non-cytotoxic products . Moreover, recently severe cleavage of polysaccharide backbone have been reported after their derivatization by CuAAC reaction.[21] The observed depolymerizaion was rationalized as being mediated by ROS agents formed from the oxidation of Cu(I) to Cu(II) by atmospheric oxygen. In this respect, in the presented strategies, the Cu(I) catalyst was prepared *in situ* by reducing copper(II) salts, such as $CuSO_4$ $5H_2O$, with a reducing agent, such as sodium ascorbate. This used method suppressed the formation of undesired byproducts associated with the use of Cu(I) and had the advantage of not requiring inert conditions to prevent the oxidation of Cu(I) to Cu(II) by atmospheric oxygen.
However, a valid alternative may be the employment of highly strained cyclic alkynes that readily and selectively react with azides at ambient temperature and pressure, and do not need use of catalysts. In this way, the click chemistry products do not present apparent cytotoxicity.

This copper-free click chemistry reaction proposed by Codelli et al., presented a rate of the reaction comparable to that of the Cu(I)-catalyzed reaction, validating the potential of this strategy.[22] In addition, Mock and co-workers established that the rate and regioselectivity of the azide-acetylene cycloaddition can be dramatically enhanced by sequestering the two components inside a host structure (i.e. enzymes), confirming the possibility of click chemistry *in situ* as further alternative to the Hüisgen reaction.[23, 24]

In addition, in order to develop systems for clinical evaluation, the materials used need to be well defined and pharmaceutically acceptable. The polymer described in chapter 3, mPEG-*b*-p(NIPAAm)-*co*-AzEMA, was synthetized by free radical polymerization. The main disadvantage of this polymerization strategy are the low control on the molecular weight and a broad molecular weight distribution as results of the strategy. ATRP (atom transfer radical polymerization) and RAFT (reversible addition-fragmentation chain transfer) polymerizations are most attractive in that sense, resulting in more control over polydispersity of the obtained products.[25, 26] Moreover, azido-groups of the mPEG-*b*-p(NIPAAm)-*co*-AzEMA-Rfv chains showed latent activity. In fact, other scientist reported that the azide group is able to form a highly reactive nitrene upon thermolysis or photolysis, which can then undergo a side reaction, resulting in crosslinking.[27] These side reactions can likely be limited to a certain extent by using lower monomer concentrations during polymerization or decreasing the polymerization reaction time.

In conclusion, improvement of the chemical modification strategies may result in well-defined polymers, which may result in monodisperse, smaller and more efficient nanocarriers.

4.2.2 Biomedical application

The studies described in this thesis are mainly focused on the polymers design, characterization and nanostructures formulation. However, great progress can still be made in further developing these nanoparticles for biomedical application. As shown in the thesis, the use of natural molecules and polymers, such as riboflavin and hyaluronan, formed promising nanohydrogels that are expected to be biocompatible. However, before considering evaluation *in vivo*, *in vitro* cytotoxicity tests of both the developed systems need to confirm their biocompatibility. Moreover, due to the fluorescence properties of riboflavin, may facilitate the quantification of the amount of Rfv derivatives in the nanocarrier, and these NHs and micelles may be easily detected in biodistribution studies and may be applied for image guided drug delivery, which would allow following the destiny of the drug loaded nanocarriers in a real time and non-invasive manner. On this respect, preliminary studies of the fluorescence profile of riboflavin were carried out, even though its fluorescence quantum is dependent from solvent

polarity due to particular interactions between the molecule and the medium that can easily result in fluorescence quenching. Nevertheless, as already reported in literature,[28] improvement of the experimental conditions related to the medium choice and appropriate concentration of the samples, may solve Rfv quenching phenomenon, reaching the goal of the mentioned study.

Moreover, overexpression of RCP (Riboflavin Carrier Protein) was found in tumor tissues, in particular in the cases of breast, prostate and hepatocellular carcinoma. For this purpose, it may be interesting to improve the design these nanocarriers, i.e. by attaching Rfv on the outside as targeting ligand for specific delivery of anticancer therapeutics to such tumors, even though the interactions between Rfv and cancer cells is quite complex and the regulative mechanisms is not well clarified yet. Last but not least, to simplify the core structure of the micelle developed in chapter 3, a non-esterified form of Rfv may be used in order to preserve the isoalloxazine ring to act as stabilizer of the micelle dispersion by π-π stacking interactions, that may occupy less volume and may result in a more dense structure.

Finally, both the developed nanosystems have been shown that are likely suitable to load drugs that are characterized by an high hydrophobicity and have aromatic groups. Piroxicam and dexamethasone loaded-NHs may potentially benefit for arthritis treatment. Paclitaxel loaded-NHs and micelle may result a good strategy for cancer therapy. On one hand, it would be possible to load multiple hydrophobic drugs/compounds to achieve synergistic effect.

4.3 Conclusions

In conclusion, this thesis describes the development of two kinds of promising Nano Drug Delivery Systems: polysaccharide NHs and polymeric micelles, which both can be obtained by chemical tailoring of the composition and architecture of amphiphilic polymers. Their pharmaceutical formulations resulted be easy and occurred in nano-sizes carriers with long-term stability, that can potentially reach the smallest capillary vessels and penetrate the tissues. Moreover, the adopted physical entrapment of drugs in such nanocarriers might result in preservation of their activity and integrity to reach the desired area for a maximized therapeutic activity and minimized undesirable side effects. The mentioned aspects indeed encourage further investigations for their improved therapeutic performance.

References

(1) S. V. Vinogradov, E. V. Batrakova, A.V. Kabanov, Poly(ethylene glycol)-polyethyleneimine NanoGel(TM) particles: Novel drug delivery systems for antisense oligonucleotides. *Coll. Surf. B: Biointerfaces.,* **1999**; 16: 291–304

(2) P. Lemieux, S. V. Vinogradov, C. L. Gebhart, N. Guérin, G. Paradis, H. K. Nguyen, B. Ochietti, A. V. Kabanov, et al, Block and graft copolymers and NanoGel copolymer networks for DNA delivery into cell. *J Drug Target.*, **2000**; 8: 91-105

(3) K. Akiyoshi, S. Deguchi, N. Moriguchi, S. Yamaguchi, J. Sunamoto, Self-aggregates of hydrophobized polysaccharides in water. Formation and characteristics of nanoparticles. *Macromolecules*, **1993**, 26: 3062–3068

(4) Z. Y. Qian, S. Z. Fu and S. S. Feng, Nanohydrogels as a prospective member of the nanomedicine family. *Nanomedicine*, **2013**, 8: 161–164

(5) C. Gonçalves, P. Pereira and M. Gama, Self-Assembled Hydrogel Nanoparticles for Drug Delivery Applications. *Materials*, **2010**, 3: 1420-1460

(6) D. A Ossipov, Nanostructured hyaluronic acid-based materials for active delivery to cancer. *Expert Opin. Drug Deliv.*, **2010**, 7: 681-703

(7) V. P. Torchilin, Micellar Nanocarriers: Pharmaceutical Perspectives. *Pharmaceutical Research*, **2007**, 24

(8) F. M. Merrett, The interaction of polymerizing systems with rubber and its homologues: part 2. –Interaction of the rubber in the polymerization of methyl methacrylate and of styrene. *Transactions of the Faraday society*, **1954**, 50: 759-767

(9) H. Bader, H. Ringsdorf, B. Schmidt, Watersoluble polymers in medicine. *Die Angewandte Makromolekulare Chemie*, **1984**, 123: 457–485

(10) H. M. Aliabadi & A. Lavasanifar, Polymeric micelles for drug delivery. *Expert Opinion on Drug Delivery*, **2006**, 3: 139-162

(11) G. S. Kwon, M. Naito, K. Kataoka, M. Yokoyama, Y. Sakurai, T. Okano, Block copolymer micelles as vehicles for hydrophobic drugs. *Colloids and Surfaces B: Biointerfaces*, **1994**, 2: 429-434

(12) F. Sultana, Manirujjaman, Md. Imran-Ul-Haque, M. Arafat, S. Sharmin, An Overview of Nanogel Drug Delivery System. J*. of App. Pharma. Sc.*, **2013**, 3: 95-105

(13) S. Rigogliuso, M. A. Sabatino, G. Adamo, N. Grimaldi, C. Dispenza and G. Ghersia, Polymeric Nanogels: Nanocarriers For Drug Delivery Application. *Chem. Eng. Transactions*, **2012**, 27

(14) C. Gonçalves, P. Pereira and Mi. Gama, Self- Assembled Hydrogel Nanoparticles for Drug Delivery Applications. *Materials*, **2010**, 3: 1420-1460

(15) K. A. Wilk, K. Zieliñska, J. Pietkiewicz, J. Saczko, Loaded nanoparticles with cyanine-tipe photosensizers: preparation, characterization and encapsulation. *Chem. Eng. Transactions*, **2009**, 17: 987-992

(16) H. C. Kolb, M. G. Finn and K. B. Sharpless, Click Chemistry: Diverse Chemical Function from a Few Good Reactions. *Angew Chem Int Ed Engl.,* **2001**; 40: 2004-2021

(17) B. Kang, T. Opatz, K. Landfester, F.R. Wurm, Carbohydrate nanocarriers in biomedical applications: functionalization and construction. *Chem. Soc. Rev.,* **2015**, 44: 8301–8325

(18) E. Montanari, M. C. De Rugeriis, C. Di Meo, R. Censi, T. Coviello, F. Alhaique, P. Matricardi, One-step formation and sterilization of gellan and hyaluronan nanohydrogels using autoclave. *J Mater Sci: Mater Med*, **2015**; 26: 32

(19) P. Shao, B. Wang, Y. Wang, J. Li, and Y. Zhang, The Application of Thermosensitive Nanocarriers in Controlled Drug Delivery. *J. of Nanomaterials,* **2011**

(20) H. Suzuki, R. Inoue, S. Kawamorita, N. Komiya, Y. Imada, and T. Naota; Highly Fluorescent Flavins: Rational Molecular Design for Quenching Protection Based on Repulsive and Attractive Control of Molecular Alignment. *Chem. Eur. J.* **2015**; 21: 9171 – 9178

(21) E. Lallana, E. Fernandez-Megia, and R. Riguera, Surpassing the Use of Copper in the Click Functionalization of Polymeric Nanostructures: A Strain-Promoted Approach. *J. Am. Chem. Soc.*, **2009**, 1311: 5748–5750

(22) J. A. Codelli, J. M. Baskin, N. J. Agard, et al. Second-generation difluorinated cyclooctynes for copper-free click chemistry. *J Am Chem Soc*, **2008**; 130: 11486

(23) W. L. Mock, T. A. Irra, J. P. Wepsiec, T. L. Manimaran, Cycloaddition induced by cucurbituril. A case of Pauling principle catalysis. *J. Org. Chem.*, **1983**, 48, 3619–3620

(24) W. G. Lewis, L. G. Green, F. Grynszpan, Z. Radic, P. R. Carlier, P. Taylor, M. G. Finn, and K. Barry Sharpless, Click Chemistry In Situ: Acetylcholinesterase as a Reaction Vessel for the Selective Assemblym of a Femtomolar Inhibitor from an Array of Building Blocks*. Angew. Chem. Int. Ed.*, **2002**, 41: 1053-1057

(25) G. Moad, E. Rizzardo, S. H. Thang, Living radical polymerization by the RAFT process-A firs update. *Australian Journal of Chemistry*, **2006**, 59: 669-692

(26) K. Matyjaszewski, J. Xia, Atom transfer radical polymerization. *Chem. Rev.*, **2001**, 101: 2921-2990

(27) Y. Li, J. Yang, B. C. Benicewicz, Well-Controlled Polymerization of 2-Azidoethyl Methacrylate at Near Room Temperature and Click Functionalization. *J. of Pol. Sc.: Part A: Pol. Chem.*, **2007**, 45: 4300–4308

(28) P. F. Heelis, The photophysical and photochemical properties of flavins (isoalloxazines). *Chem. Soc. Rev.*, **1982**, 11: 15-39

Acknowledgment

First, I would like to thank my advisors Dr. Pietro Matricardi and Dr. Chiara Di Meo for offering me the possibility to work in their group and guide me in this research. It is my pleasure to express my gratitude to Prof. Tommasina Coviello and Prof. Franco Alhaique for their special help, support and wide knowledge.

I would like to thanks once again Prof. Marco Pierini for his support and precious (scientific and non) suggestions…again, anyway.

I express my gratitude to Prof. Wim Hennink and Dr. Tina Vermonden for providing me with the opportunity to spend the last 18 months of my PhD at the Utrecht University as external PhD visiting.

My deeper gratitude is obviously extended to my family and my friends.